JOÃO ANDRÉ TRAILA AREZES

THE ROLE OF HEPCIDIN IN HOST DEFENSE AGAINST *Vibrio vulnificus* INFECTION

Tese de Candidatura ao grau de Doutor em Biologia Básica e Aplicada submetida ao Instituto de Ciências Biomédicas Abel Salazar da Universidade do Porto.

Orientador – Doutora Elizabeta Nemeth
Categoria – Full Professor
Afiliação – University of California, Los Angeles

Co-orientador – Doutor Tomas Ganz
Categoria – Distinguished Professor
Afiliação – University of California, Los Angeles

Co-orientador – Doutora Maria da Graça Beça Gonçalves Porto
Categoria –Professora Catedrática
Afiliação – Instituto de Ciências Biomédicas Abel Salazar

Os seguintes artigos foram publicados no âmbito desta tese, tendo servido de base para a sua escrita:

Arezes, J., Jung G., Gabayan, V., Valore E., Ruchala, P., Gulig P.A., Ganz, T., Nemeth, E. and Bulut, Y., 2015, *Hepcidin-Induced Hypoferremia Is a Critical Host-Defense Mechanism against the Siderophilic Bacterium Vibrio vulnificus*, Cell Host Microbe, **17**(1): p.47-57

Arezes, J. and Nemeth, E., 2015, *Hepcidin and iron disorders: new biology and clinical approaches*, Int J Lab Hematol, **37** Suppl 1: -92-98

Aos meus pais

Any truth is better than indefinite doubt.

Arthur Conan Doyle

ACKNOWLEDGEMENTS

Although a doctoral thesis is recognized as the work of one individual, my experience as a PhD student taught me that this is not a solitary journey, and that it goes beyond the scope of laboratory research. I have met several people, colleagues, and friends, who contributed, in one way or another, to shape this dissertation. For that reason, I dedicate the following paragraphs to them.

First of all, a huge thanks to Tomas Ganz and Elizabeta Nemeth, who are the best mentors I could hope for. Besides being fantastic scientists, they are also wonderful people, who helped me in every single obstacle I encountered, even the ones not related to my work. I thank them for accepting me in their lab, for guiding me when I needed guidance, and for giving me the liberty to pursue my own path. Being able to get to know them was truly a privilege.

I thank Graça Porto for receiving me with open arms once I came back to Porto, for accepting me as her student, and for giving me the tools I needed to finish my thesis. I also thank her for all the discussions and knowledge shared throughout the years, even before I started my PhD stage.

Because the work presented here results from the effort of several people, I acknowledge my colleagues at the Center for Iron Disorders at UCLA who were involved in this project - Yonca, Victoria, Grace, Erika, Piotr and Debbie - for their help throughout every stage of my project from the experimental design to the publication of our results. Also, thanks to my labmates: Kristine, Rose, Mark, Airie, Eileen, Diana, Bo and JoAnne and to my friends from across the corridor, George and Min, for their support and friendship. To all the lab helpers, for making my job easier and more efficient. A special thanks to Léon, my European fellow who was always available to help me from the very first moment I arrived and for the meticulous discussions about experimental procedures, data analysis, football (the real one) and American culture. Another special thanks to Sharraya for her friendship, help, honesty and patience during the good and bad moments.

Some of the work presented here was only possible with the help of research facilities which aided me in various experiments, and for that I thank the people from the Clinical Microarray Core, the Translational Pathology Core Laboratory, and the Division of Laboratory Animal Medicine, all from UCLA. Thanks also to Drs Paul A. Gulig and Joon Haeng Rhee for providing us with material and for scientific discussions. Because all this work requires funding, I thank "Fundação para a Ciência e a Tecnologia", the National Institutes of Health, the Stein Oppenheimer Endowment Awards Program and the UCLA Clinical and Translational Science Institute.

Back to my Portuguese "home", many thanks to the BCRIBs - Tiago, Mónica, Inês, Ana, Sílvia, Andreia, and Eugénia - with whom I shared the lab while writing my thesis. Thanks for keeping such a nice and friendly environment, which made it easier to come to work every day.

Acknowledgements

Obviously an enormous thanks to the GABBA program, which started this all by giving me the privilege to do the PhD that I wanted, where I wanted. I thank the current and former directors Drs. Alexandre do Carmo and António Amorim. A special thanks to Professor Maria de Sousa, for providing instrumental input throughout the several discussion we had, for sharing her knowledge and for challenging me to make a difference with my work.

My experience as a PhD student was immensely enhanced by getting to know my fellow GABBAs 15th: Gonçalo, Diana, Joana, Mafalda, Inês, João Neto, Dário, António, Ana Lima, Danica and Ana Maria, who rapidly became very good friends, making the GABBA annual meeting one of the events I look most forward to attend every year.

Obrigado à minha família, em especial aos meus pais, pelo carinho e apoio constante e incondicional, e por me deixarem seguir os meus sonhos, ainda que isso envolva estar a um continente e um oceano de distância. Apesar de aparentemente não terem tido um papel evidente no desenvolvimento desta tese, tenho a certeza que aquilo que alcancei nunca seria possível sem o seu esforço durante todos estes anos.

Finally, a very special thanks to Jorge Pinto, who was by my side since the first time I stepped into a lab, for believing in me, and for the shared scientific journey. Even though his life was cut short too soon, his work will persist in the form of his scientific contributions, and through the work of the students he mentored, which I am grateful to be a part of.

ABSTRACT

Hepcidin is a peptide hormone that regulates iron homeostasis, acting by preventing iron export from cells, and therefore promoting a decrease in the blood iron concentration. Insufficient hepcidin production promotes increased dietary iron absorption and increased release of iron from the tissues (mostly the spleen and liver), leading to iron overload. Excess iron is deposited in the parenchyma, causing tissue damage. This is commonly observed in patients with hereditary hemochromatosis (HH), an iron overload disease caused by deficient production of the hormone hepcidin. HH, as well as other disorders, is known to be a risk condition for lethal infections by siderophilic bacteria, whose growth and virulence are enhanced by iron. For example, *Vibrio vulnificus* (*V. vulnificus*), a Gram-negative siderophilic bacterium, may cause fulminant and deadly sepsis in patients with severe HH, while healthy people resist the infection and only develop mild symptoms. The work presented here aims to elucidate the mechanisms of susceptibility to *V. vulnificus* infection, focusing on the hypoferremic response triggered by hepcidin. Additionally, based on our findings we sought to develop a strategy to mitigate the infection in susceptible mice.

We infected wild-type (WT) and hepcidin-deficient (*Hamp1*$^{-/-}$) mice with *V. vulnificus* and found that hepcidin deficiency resulted in increased bacteremia and decreased survival of infected mice, which could be partially ameliorated by dietary iron depletion. WT mice responded to the infection by acutely increasing hepcidin production after inflammatory stimuli triggered by interleukin 6 (IL-6) and activin B, leading to a decrease in serum iron. This response was critical to prevent rapid bacterial growth and consequent septic shock. Disruption of this response in *Hamp1*$^{-/-}$ mice accounted for the development of severe infection and lethality.

Based on our findings, we attempted to elicit a protective response in the highly susceptible *Hamp1*$^{-/-}$ mice. For that purpose, we administered minihepcidins (synthetic hepcidin agonists) to infected mice before or a few hours after infection. Minihepcidins induced hypoferremia, which resulted in decreased bacterial loads and decreased mortality, regardless of initial iron levels. The effect of minihepcidins on bacterial growth was a consequence of the hypoferremic response rather than a direct bactericidal effect.

To investigate the role of iron in *V. vulnificus* virulence, we studied bacterial growth *ex vivo.* We observed that high iron sera from hepcidin-deficient mice supported extraordinarily rapid bacterial growth and that growth was inhibited in hypoferremic sera. Furthermore, the presence of non-transferrin-bound iron (NTBI), particularly Fe (III), was critical to trigger *V. vulnificus* growth in serum and plasma, which can partially explain the severe infection observed in iron-overloaded individuals. *V. vulnificus* was previously shown to respond to iron concentrations through the Ferric Uptake Regulator (Fur) system. However, infection with a Fur deletion mutant caused the same mortality as WT *V. vulnificus*. Alternative candidates involved in iron-induced growth and virulence were found by RNA sequencing of *V. vulnificus*, grown in the presence or absence of NTBI.

In summary, the work presented in this thesis demonstrates that hepcidin-mediated hypoferremia is a critical host defense mechanism against *V. vulnificus* infection, and offers an explanation for the poor prognosis of this condition in severely iron overloaded individuals. The removal of NTBI from circulation is essential to prevent rapid bacterial growth and septic shock. This can be accomplished by administration of minihepcidins, which were shown to mitigate infections by siderophilic bacteria in susceptible mice. Therefore, minihepcidins constitute a promising strategy to treat siderophilic infections in susceptible patients, including those with iron overload disorders such as hereditary hemochromatosis or thalassemia.

RESUMO

A hepcidina é a hormona que regula a homeostasia do ferro, actuando de forma a prevenir a exportação de ferro das células. Assim, a ação da hepcidina provoca uma diminuição da concentração de ferro no sangue. A produção insuficiente de hepcidina resulta num aumento da absorção de ferro proveniente da dieta, bem como um aumento da libertação de ferro dos tecidos (principalmente o baço e o fígado), o que leva à sobrecarga de ferro. O ferro em excesso é depositado no parênquima e resulta no desenvolvimento de lesões nos tecidos. Este fenómeno é observado em doentes com hemocromatose hereditária (HH), uma doença de sobrecarga de ferro causada pela produção insuficiente da hormona hepcidina. A HH, assim como outras doenças, é um factor de risco para o desenvolvimento de infeções letais causadas por bactérias siderofílicas, cujo crescimento e virulência são exacerbados na presença de ferro. Por exemplo, a *Vibrio vulnificus* (*V. vulnificus*) é uma bactéria siderofílica e Gram-negativa, que pode causar sepsis fulminante e letal em pacientes com HH grave. Contudo, pessoas saudáveis são resistentes a esta infeção e apenas manifestam sintomas ligeiros. O trabalho apresentado nesta tese tem o objetivo de elucidar os mecanismos que explicam a suscetibilidade a infeções causadas por *V. vulnificus*, focando-se na resposta de diminuição de ferro no sangue pela ação da hepcidina. Adicionalmente, pretendemos desenvolver uma estratégia para combater a infeção em murganhos altamentes suscetíveis a esta infecção.

Murganhos do tipo selvagem (WT) ou deficientes na produção de hepcidina (*Hamp1*$^{-/-}$) foram infetados com *V. vulnificus*, tendo-se verificado que a deficiência em hepcidina resulta num aumento do número de bactérias no hospedeiro e a uma diminuição na taxa de sobrevivência após infeção. Ambos os aspetos foram parcialmente melhorados através da utilização de uma dieta pobre em ferro. Murganhos WT responderam à infeção através de um rápido aumento da produção de hepcidina em reposta ao estímulo inflamatório causado pela interleucina 6 (IL-6) e pela ativina B, o que levou a uma diminuição dos níveis de ferro no soro. Esta resposta foi fundamental na prevenção do rápido crescimento das bactérias e no desenvolvimento de choque séptico. A ausência desta resposta em murganhos *Hamp1*$^{-/-}$ explica o desenvolvimento de infeção grave e morte dos animais infectados.

Com base nos resultados descritos, tentamos desencadear uma resposta protetora em murganhos *Hamp1*$^{-/-}$, através de tratamentos com minihepcidinas (péptidos sintéticos com ação semelhante à hepcidina), antes ou depois da infeção. Estes tratamentos induziram uma diminuição de ferro no soro, resultando num decréscimo do número de bactérias no hospedeiro e diminuição da taxa de mortalidade dos animais, independentemento dos níveis iniciais de ferro. O efeito das minihepcidinas no crescimento bacteriano foi uma consequência da diminuição do ferro no soro e não devido a um efeito bactericida.

De forma a investigar o papel do ferro na virulência de *V. vulnificus,* estudamos o crescimento das bactérias *ex vivo*. As bactérias cresceram muito rapidamente em soro rico em ferro proveniente de murganhos *Hamp1*$^{-/-}$, enquanto o crescimento foi inibido em soro pobre em ferro. Além disso, a presença de ferro não ligado à transferrina (NTBI), particularmente Fe (III), foi fundamental para o crescimento em soro e plasma, o que poderá explicar em parte o desenvolvimento de infeções graves em doentes com sobrecarga de ferro. A resposta ao estímulo do ferro por *V. vulnificus* ocorre através do sistema *Ferric Uptake Regulator* (FUR). Contudo, infecções com uma bactéria mutante que não possui a proteína Fur causaram a mesma taxa de mortalidade que a estirpe selvagem. Procuramos então candidatos alternativos envolvidos no aumento do crescimento e virulência induzidos pelo ferro, através da sequenciação de RNA de bactérias incubadas com ou sem NTBI.

Em suma, o trabalho apresentado nesta tese demonstra que a diminuição de ferro no soro através da hepcidina é fundamental para a proteção contra infeções por *V. vulnificus*. A remoção de NTBI da circulação é essencial para prevenir o crescimento bacteriano e o desenvolvimento de choque séptico. Isto pode ser conseguido através da administração minihepcidinas, um tratamento eficaz na melhoria das infeções por bactérias siderofílicas em murganhos susceptíveis a este tipo de infeções. Dessa forma, as minihepcidinas são uma estratégia promissora no tratamento de infeções siderofílicas em pacientes suscetíveis, incluindo aqueles com doenças de sobrecarga de ferro tais como a hemocromatose hereditária ou talassemia.

LIST OF ABBREVIATIONS

ALAS2	Aminolevulinate synthase 2
BMP	Bone Morphogenetic Protein
C strain	Clinical strain
cAMP	Cyclic adenosine monophosphate
CDC	Centers for Disease Control and Prevention
cDNA	Complementary DNA
CFU	Colony-forming units
CKD	Chronic kidney disease
CPDA-1	Citrate phosphate dextrose-adenine 1
CPS	Capsule Polysaccharide
CRP	C-reactive protein
DcytB	Duodenal cytochrome B
DMT1	Divalent Metal Transporter 1
DNA	Deoxyribinucleic acid
E strain	Environmental strain
ELISA	Enzyme-linked immunosorbent assay
ERFE	Erythroferrone
FAC	Ferric ammonium citrate
FAS	Ferrous ammonium sulfate
Fpn	Ferroportin
Ft	Ferritin
FU	Fluorescence units
Fur	Ferric uptake regulator
GDF15	Growth differentiation factor 15
GNPAT	Glyceronephosphate O-acyltransferase
GPI	Glycosylphosphatidylinositol
Hamp1$^{-/-}$	Hepcidin knockout
HFE	Hemochromatosis gene
HH	Hereditary hemochromatosis
HJV	Hemojuvelin
HO-1	Heme Oxygenase 1
Hph	Haephastin
IFN-γ	Interferon γ
IL	Interleukin

IRE	Iron-responsive element
IRIDA	Iron refractory iron deficiency anemia
IRP	Iron-responsive protein
JAK	Janus kinase
KC/GRO	Keratinocyte chemoattractant / growth-regulated oncogene
LB	Luria-Bertani
LB-N	Luria-Bertani, NaCl
LB-NAC	Luria-Bertani broth, NaCl, arabinose and cloramphenicol
LD-50	Median lethal dose
LIP	Labile iron pool
LPI	Labile plasma iron
LPS	Lipopolysacharide
MALDI-MS	Matrix-Assisted Laser Desorption Ionization - Mass
Spectrometry	
MAPK	Mitogen-activated protein kinases
MARTX	Multifunctional Autoprocessing Repeats-in-Toxin
mRNA	Messenger RNA
NF-κB	Nuclear factor-kappa B
NTBI	Non-transferrin-bound iron
OD	Optical density
PBS	Phosphate-buffered saline
PCBP	Poly r(C)-Binding Protein
PCR	Polymerase chain reaction
PG	Protegrin
ppm	parts per million
qRT-PCR	Quantitative reverse transcriptase - polymerase chain reaction
RNA	Ribonucleic acid
ROS	Reactive oxygen species
RP-HPLC	Reversed-phase high-performance liquid chromatography
rpm	Revolutions per minute
s.c.	Subcutaneous
SD	Standard Deviation
sHJV	Soluble hemojuvelin
SMAD	Mothers against decapentaplegic homolog

STAT	Signal Transducer and Activator of Transcription
STEAP3	Six transmembrane epithelial antigen of the prostate 3
TBI	Transferrin-bound iron
Tf	Transferrin
TfR1	Transferrin receptor 1
TfR2	Transferrin receptor 2
TIBC	Total iron binding capacity
TLR	Toll-like receptor
TMPRSS6	Transmembrane protease, serine 6
TNF-α	Tumor necrosis factor α
TWSG1	Twisted gastrulation protein homolog 1
UIBC	Unsaturated iron binding capacity
UTR	Untranslated region
V. vulnificus	*Vibrio vulnificus*
WT	Wild-type
ZIP14	Zrt/Irt-like protein 14

TABLE OF CONTENTS

CHAPTER I

General Introduction

Section 1

Mammalian Iron Metabolism

Section 1 - Mammalian Iron Metabolism

From being produced in the core of massive stars to playing essential roles at the cellular level, iron has taken center stage in the history of the universe and in the biology of nearly all living creatures. Its exceptional capacity to act both as an electron donor and acceptor rendered it a privileged co-factor for enzymes involved in various metabolic pathways, such as oxygen sensing and transport, mitochondrial respiration, cell proliferation as well as host defense [1]. However, this capacity for transferring electrons also makes iron a highly reactive and toxic element. Iron catalyzes the formation of reactive oxygen species (ROS) through the Haber-Weiss and Fenton reactions, causing damage to DNA, proteins, and organelles, and ultimately leading to organ dysfunction [2]. For this reason, iron levels must be tightly regulated to fulfill the metabolic demand while avoiding excess iron, both at the cellular and systemic levels. Iron toxicity is also avoided through coupling the metal ion with prosthetic groups and proteins, both in the intra- and extracellular space. Several molecules involved in the intricate network of mammalian iron metabolism have been discovered in recent decades and will be summarized in this section (Figure 1), with emphasis on the iron-regulatory hormone hepcidin.

1.1 - Iron distribution and recycling

The average adult human contains ~4 grams (g) of iron, from which ~2-3 g are found in hemoglobin from erythroid precursors and mature erythrocytes [1]. Other iron-rich tissues include the liver and the spleen (containing 0.5-1 g of iron), where the iron is mainly stored in hepatocytes and macrophages, and is readily available if necessary. The daily iron requirement for erythrocyte synthesis is 20-25 mg. However, only 1-2 mg are absorbed through dietary consumption by the enterocytes, mostly to compensate for iron losses through shedding of intestinal epithelial cells, desquamation of skin, blood losses and sweat [3]. Most of the iron is supplied by a highly efficient recycling mechanism, by which senescent or damaged erythrocytes are phagocytosed by reticuloendothelial macrophages and iron is recovered and delivered back into circulation [4]. This recycling loop assures that erythropoiesis is not compromised by the natural variability of dietary

iron content, its poor solubility and bioavailability and its inefficient intestinal absorption. The enterocytes (absorption) and the macrophages (recycling) are therefore two main determinants of iron homeostasis due to their ability to deliver iron into blood circulation. The third piece in this puzzle is the hepatocyte, a specialized iron storage cell that produces of a plethora of iron-related proteins [5].

1.2 - Iron absorption and traffic

Due to the absence of a regulated mechanism of iron excretion, the maintenance of appropriate levels of iron in the body relies on the control of dietary iron absorption. Dietary iron is found predominantly in its oxidized Fe (III) form or associated with heme groups, and is absorbed at the brush border of duodenal enterocytes. The mechanism for heme-iron absorption has not been elucidated, and it appears to be independent from inorganic iron uptake. The absorption of inorganic Fe (III) requires its reduction to Fe (II) partially by the membrane-associated ferrireductase DcytB (Cybrd1) at the apical membrane of enterocytes [6]. Other ferrireductases may be involved in this process since DcytB knockout mice present normal iron metabolism [7] except when they are stressed by hypoxia [8]. Fe (II) is then transported to the cytosol via the Divalent Metal Transporter I (DMT1 / solute carrier family 11, member 2 SLC11A2), a proton/divalent transporter [9, 10]. DMT1 is strongly induced by iron deficiency, further supporting its important role in iron metabolism [9]. Once in the cytosol, iron that is not used for cellular processes is exported into the bloodstream by the basolateral transporter ferroportin, the sole known cellular iron exporter [11, 12]. Coupled to its export, Fe (II) undergoes oxidation to Fe (III) catalyzed by hephaestin, a multicopper oxidase homolog of liver ceruloplasmin, to allow iron to be loaded onto the iron transport molecule transferrin (Tf) as a mono- or diferric molecule and delivered to distant tissues [13].

Transferrin is a glycoprotein with two high-affinity binding sites for Fe (III) [14]. This iron transporter ensures efficient delivery of iron to target tissues (mostly the bone marrow), while maintaining it in a chemically inert form, thus preventing the formation of damaging toxic radicals. Transferrin-bound iron (TBI) is delivered to the cells by interaction with the Transferrin Receptor 1 (TfR1) and subsequent

endocytosis of the TBI-TfR1 complex [15, 16]. The low pH in the endosomes causes iron to be released, followed by reduction to Fe (II) by the metalloreductase Six Transmembrane Epithelial Antigen of the Prostate 3 (STEAP3) [17] and transported to the cytosol by DMT1 [18]. If required for cellular processes, iron enters the Labile Iron Pool (LIP), a metabolically active and regulatory form of iron [19, 20]. Excess iron can be stored in ferritin, a protein "cage" that can accommodate up to 4500 iron atoms [21]. The delivery of iron into ferritin is carried out by Human poly (rC)-binding proteins (PCBPs), cytosolic iron chaperones [22]. Tf-TfR1 is cycled back to the cell membrane and the neutral pH promotes the dissociation of transferrin back into circulation, while TfR1 stays in the membrane ready for the next endocytic cycle.

In normal conditions, iron concentration in plasma ranges from 10 to 30 μM, which corresponds to ~30% of transferrin saturation [23]. In iron overload disorders, such as hereditary hemochromatosis (HH) and β-thalassemia, iron exceeds transferrin binding capacity. In this situation, excess iron binds to low-molecular weight compounds, such as citrate and acetate, and also albumin, forming complexes collectively known as non-transferrin-bound iron (NTBI) [24, 25]. NTBI is avidly taken up by the liver (and at to a lesser extent by the heart and pancreas), possibly decreasing the circulation of highly reactive iron species in the blood and more widespread toxic damage. However, iron deposition can seriously damage parenchymal cells and cause organ dysfunction [26, 27]. The mechanism of NTBI uptake by the liver has not been fully clarifeid yet. A candidate for NTBI transport is the Zrt-Irt-like protein 14 (Zip14 / SLC39A14), although its relevance *in vivo* has still to be demonstrated [28].

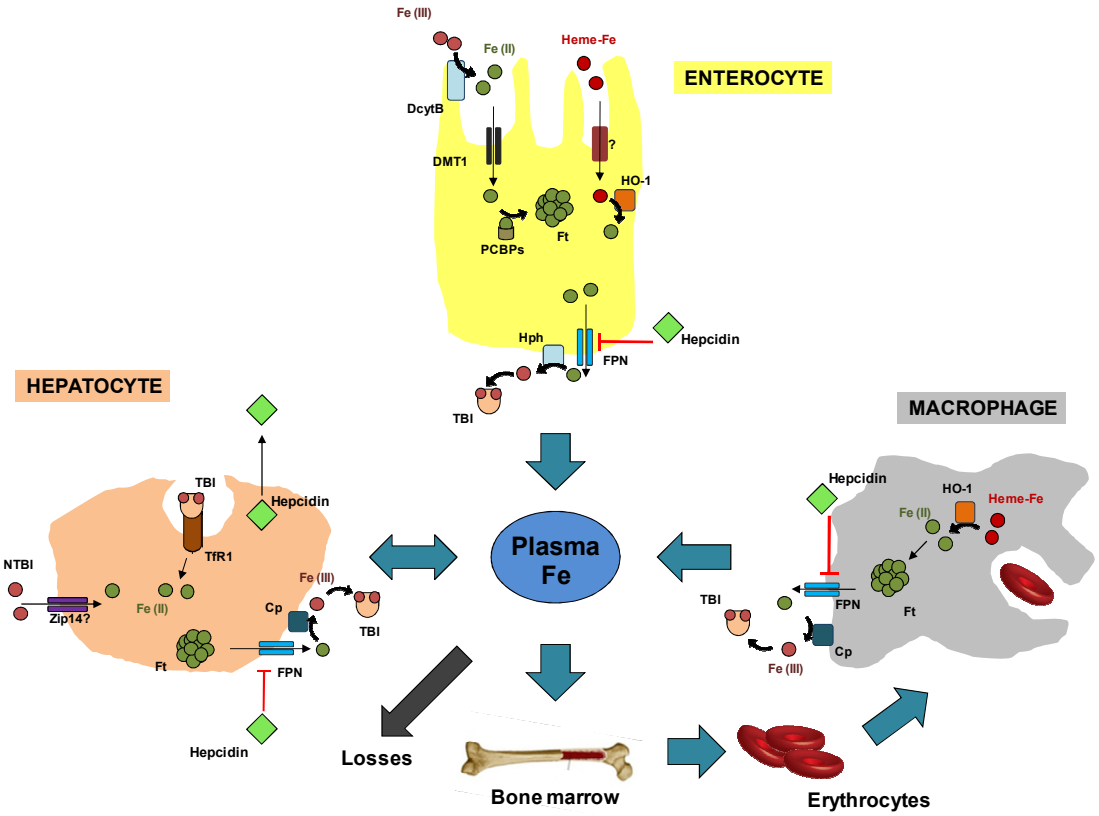

Figure 1. Overview of iron metabolism. Enterocyte: dietary iron is absorbed in duodenal enterocytes. The low amount of iron absorbed (1-2 mg) is mostly used to compensate for small daily losses. Dietary Fe (III) is reduced at the apical membrane by the Duodenal cytochrome B (Dcytb) and enters the enterocytes via the Divalent Metal Transporter 1 (DMT1). Iron contained in heme groups is transported across the apical cell membrane through an unknown mechanism and converted to Fe (II) by Heme Oxygenase 1 (HO-1). Intracellular iron is then used for cellular processes, delivered to ferritin (Ft) by Poly(rC)-binding proteins (PCBPs) complexes or released via ferroportin (Fpn), followed by oxidation to Fe (III) by haephastin (Hph). Fe (III) in the bloodstream binds to transferrin (TBI) and is delivered to various tissues, including the bone marrow, where it is incorporated in heme groups during erythropoiesis. **Hepatocyte:** hepatocytes are the primary storages of iron in the organism. Besides TBI, these cells are able to take up non-transferrin bound iron (NTBI), via an unknown mechanism, although evidence support that the ZRT/IRT-like protein 14 (ZIP14) may be the NTBI transporter. Similarly to enterocytes, iron can be used, stored within ferritin or released via ferroportin. Hepatocytes are also the primary producers of hepcidin, therefore acting as important regulators of iron homeostasis. Hepcidin promotes the degradation of ferroportin in various cell types which results in higher intracellular iron retention and lower systemic iron levels, due to the inhibition of iron absorption from enterocytes and iron release by other cells. **Macrophage:** Macrophages in the spleen and liver are responsible for the phagocytosis of senescent or damaged erythrocytes, ensuring that heme-iron is recycled through the action of HO-1 and released into the bloodstream through Fpn, maintaining a daily systemic iron flux of 20-25 mg that is required for erythropoiesis.

1.3 - Regulation of cellular iron - The IRE/IRP system

Cellular iron levels must be tightly regulated so that the appropriate amount is available for metabolic functions, while avoiding toxic damage through the formation of ROS. The best characterized model for cellular iron regulation is the IRE/IRP system, a post-transcriptional regulatory mechanism that ensures that proteins involved in iron uptake, usage, storage and export are coordinately regulated according to the intracellular iron levels [29, 30]. This system involves the iron regulatory proteins 1 and 2 (IRP-1 and IRP-2) and the conserved iron-responsive elements (IRE) present in the untranslated regions (UTR) of various iron-regulated transcripts. Regulatory IRE can be located in the 3' or 5' regions of the UTR and their location dictates the fate of the transcript. Transcripts harboring 3' IRE are stabilized after binding to IRP, increasing their levels, while 5' IRE blocks the translation initiation process [31]. In iron-restricted conditions, IRP is recruited to bind IRE located in the 3' IRE of proteins involved in iron uptake (TfR1 and DMT1) mRNA, stabilizing the transcripts, and to the IREs in the 5' UTR of iron storage (ferritin), usage (aminolevulinic acid synthetase 2 - ALAS2) and export (ferroportin), inhibiting the translation of these mRNAs. The net result is higher iron uptake via TfR1 and less iron stored in ferritin complexes and exported via ferroportin, leading to higher iron availability. Conversely, in iron-replete cells IRP fail to bind IRE, inhibiting iron uptake and promoting the storage and export of excess iron. Combined disruption of IRP-1 and IRP-2 results in early embryonic lethality in mice, demonstrating the importance of this regulatory system [32]. Disruption of only one of the IRPs is compatible with life but results in distinct phenotypes depending on the protein mutated: IRP-1 disruption causes polycythemia and pulmonary hypertension [33]; IRP-2 deletion results in microcytic anemia, iron overload and neurological defects [34]. These phenotypes support the idea that the two IRPs have both overlapping and specialized functions.

1.4 - Regulation of systemic iron - Hepcidin

In vertebrates, the regulation of systemic iron levels is orchestrated by hepcidin, a 25 amino acid peptide hormone synthesized by the liver [35-37]. Hepcidin is released in the circulation to control the efflux of iron into plasma from the three main iron sources: absorption of dietary iron in the duodenum, release of recycled iron from macrophages in the spleen, and release of stored iron from hepatocytes. While hepatocytes constitute the major source of circulating hepcidin, other cells, such as macrophage, lymphocytes and adipocytes, have been found to express hepcidin mRNA, although at much lower levels [38-40]. The pathophysiological role of the extrahepatic sources of hepcidin is still unclear.

Hepcidin inhibits iron release into the plasma by decreasing the amount of ferroportin, the only known cellular iron exporter [41]. In mammals, ferroportin is abundant in iron-exporting cells - enterocytes, hepatocytes and macrophages - and present at lower levels in other organs possibly to prevent iron toxicity (heart [42]) or for yet unknown functions (e.g. erythrocyte precursors [43], and the lungs [44]). Hepcidin binds to ferroportin and triggers its ubiquitination, presumably by inducing a conformational change [45]. This results in endocytosis, subsequent lysosomal degradation of the hepcidin-ferroportin complex, and decreased cellular iron export. Therefore, the hepcidin-ferroportin interaction decreases iron flux into the bloodstream, promoting hypoferremia. Aberrant expression or interaction of hepcidin and ferroportin causes or contributes to a large spectrum of iron disorders, from iron overload diseases to iron-restricted anemias [46]. Hepcidin production is tightly regulated by three main stimuli: iron, erythropoiesis and inflammation (Figure 2).

1.4.1 Regulation of hepcidin expression

Regulation by iron: the control of iron homeostasis by hepcidin represents a classical endocrine regulatory system. Hepcidin regulates iron and in turn, hepcidin production is regulated by iron in circulation and in liver stores: when iron is abundant, hepcidin production is increased to limit dietary iron absorption and release from the stores; when iron is required, a decrease in hepcidin production allows iron to enter the bloodstream to meet the iron requirements of erythropoiesis and metabolic functions [47]. The lack of IRE motifs in hepcidin

mRNA precludes its regulation through the IRE/IRP system. Therefore other regulatory mechanism have to come into play. The sensing of extracellular iron occurs through an intricate mechanism that effectively senses the iron-bound form of transferrin, holotransferrin, via receptors TfR1 and TfR2, together with the membrane protein HFE which is able to interact with both receptors [48]. It has been proposed that HFE binding to TfR1 is competitively inhibited by holotransferrin, causing the displacement of HFE and its subsequent binding to TfR2. The HFE-TfR2 binding is further stabilized by holotransferrin and this complex stimulates hepcidin expression possibly through bone morphogenic proteins (BMP) and/or mitogen-activated protein kinases (MAPK) signaling pathways [49].

The involvement of the BMP/mothers against decapentaplegic homolog (SMAD) pathways in transcriptional regulation of hepcidin is strongly supported by the development of hepcidin deficiency and iron overload in BMP6-deficient mice [50, 51] and the loss of hepcidin expression when SMAD4 is disrupted in the liver [52]. Interaction of BMPs with their membrane receptors promotes intracellular phosphorilation of SMAD1/5/8 which bind to SMAD4 promoting its migration to the nucleus, where it binds to the hepcidin promoter to increase hepcidin expression [53]. Activation of BMP signaling requires the GPI-linked protein hemojuvelin (HJV), which acts as a BMP co-receptor [54]. Disruption of HJV results in a severe and early-onset form of hemochromatosis. A soluble form of this protein (sHJV) is produced through cleavage of HJV by the pro-hormone convertase furin [55] and the transmembrane protein serine 6 (TMPRSS6, also known as matriptase 2), and acts as a negative regulator of hepcidin expression [56]. Neogenin, a ubiquitously expressed membrane protein, was found to interact with HJV and TMPRSS6, regulating BMP signaling and HJV cleavage [57, 58]. There is evidence that intracellular iron stores in the liver also stimulate hepcidin production, in part by increasing BMP6 concentrations [59], but the mechanism of intracellular iron sensing to control hepcidin expression has not been elucidated.

Regulation by erythropoiesis; The production of erythrocytes is strictly dependent on the availability of iron to be incorporated in heme groups and hemoglobin. Accordingly, the supply of iron for erythropoiesis must be increased when erythropoiesis is stimulated. The long sought "erythroid factor" that inhibits

hepcidin expression in response to the erythropoietic drive was recently found and named erythroferrone (ERFE) [60]. This peptide hormone is produced by erythropoietin-stimulated erythroblasts and suppresses hepcidin synthesis to allow the mobilization of iron to the bone marrow. ERFE-deficient mice fail to decrease hepcidin in response to hemorrhage or erythropoietin administration, which results in a delayed recovery from anemia. The receptor and signaling pathways involved in ERFE signaling are still unknown. Other mediators, including the growth differentiation factor 15 (GDF15) [61] and the twisted gastrulation protein homolog 1 (TWSG1) [62], may also be implicated in this response.

Regulation by inflammation: Hepcidin production is increased during inflammation, a response that may have evolved as a host defense mechanism to reduce iron availability to invading extracellular pathogens [63, 64]. In support of this idea, patients with iron overload disorders, such as hereditary hemochromatosis and β-thalassemia are highly susceptible to infection by certain extracellular microbes such as *Vibrio vulnificus* and *Yersinia enterocolitica* [65]. However, the efficacy of this mechanism remains to be shown *in vivo*. During inflammation, hepcidin expression is increased mainly through interleukin 6 (IL-6) [66] and possibly other mediators such as Activin B [67]. Binding of IL-6 to its receptor triggers a signaling pathway mediated by Janus kinase (JAK) and activation of the signal transduction and activator of transcription (STAT) 3 to increase hepcidin transcription [68]. Activin B signals through the BMP/SMAD pathway and may act synergistically with the JAK/STAT3 pathway to increase hepcidin expression in response to inflammation [67]. During chronic inflammation, the sustained stimulation of hepcidin production may result in anemia of inflammation (also known as anemia of chronic disease) due to the inadequate supply of iron for erythropoiesis [69].

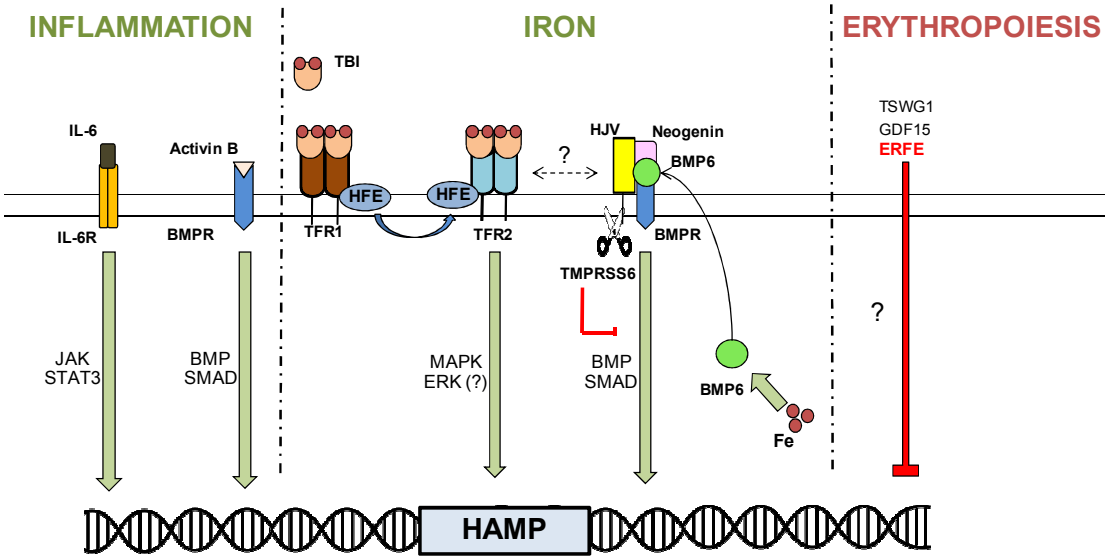

Figure 2. Signaling pathways involved in hepcidin regulation. Inflammation: Hepcidin (*HAMP*) expression is regulated in response to various stimuli, such as inflammation, iron levels, and erythropoiesis. Inflammation-mediated hepcidin up-regulation is controlled by several cytokines, but IL-6 seems to be the most prominent stimulus. By binding to the IL-6 receptor (IL-6R), IL-6 activates the JAK/STAT3 pathway. Activin B can also positively regulate hepcidin in inflammatory conditions through the BMP-SMAD pathway. **Iron:** The proposed model for hepcidin regulation in response to extracellular iron involves transferrin-bound iron (TBI) binding to TfR1, releasing HFE which becomes available to bind TfR2. This interaction increases *HAMP* expression, by promoting the SMAD signaling and possibly also via the MAPK/ERK1-2 pathway. Intracellular iron was shown to increase the expression of Bone Morphogenic Protein 6 (BMP6) which can in turn increase *HAMP* expression through the BMP/SMAD pathway. This mechanism also involves the BMP co-receptor hemojuvelin (HJV) and neogenin, which is thought to stabilize the signaling complex. In low iron conditions, TMPRSS6 (matriptase 2) acts as a negative regulator of this pathway by cleaving HJV. **Erythropoiesis:** Erythropoiesis is a strong negative regulator of hepcidin production, leading to increased iron availability for the production of red blood cells. This response is mediated by erythroferrone (ERFE), via a still unknown signaling pathway. Other mediators may be involved in this response, such as the growth differentiation factor 15 (GDF15) and the twisted gastrulation protein homolog 1 (TWSG1).

1.4.2 - Diseases of hepcidin deficiency / hepcidin resistance

In hereditary hemochromatosis, a genetic iron overload disease, patients have deficient hepcidin production leading to an iron-overload phenotype: ferroportin is highly expressed on the cell membrane, which results in hyperabsorption of dietary iron by the duodenal enterocytes, increased release of iron from recycling macrophages and subsequent increase in plasma iron concentrations, transferrin saturation and appearance of NTBI [70]. Since there is no regulated iron excretion mechanism in humans and animals, excess iron is deposited in the tissues that have active uptake transporters for NTBI (mainly the liver, but also heart, pancreas and other endocrine glands). Excessive and prolonged uptake of NTBI can result in organ damage and failure. Inadequate hepcidin production in response to iron loading is most commonly due to mutations in genes encoding iron sensors or signaling pathways that regulate hepcidin production. The severity of the disease appears to be proportional to the degree of hepcidin deficiency. Autosomal recessive mutations in the hemochromatosis gene (HFE) are the most frequent cause of genetic iron overload (Type 1), particularly homozygous HFE C282Y mutations and occasionally compound heterozygote C282Y/H63D mutations. This form of the disease is incompletely penetrant, and clinically-important iron overload usually develops only in the presence of modifying factors that further decrease hepcidin production (e.g. alcohol [71], or additional genetic variations as in GNPAT gene [72]). More penetrant and severe forms of hereditary hemochromatosis are fortunately rare and originate from mutations in transferrin receptor 2 (Type 3) which cause a disease of intermediate severity and mutations in HJV (Type 2A) and the hepcidin gene itself (Type 2B). Mutations in HJV or hepcidin lead to an early onset and severe form of the disease called juvenile hemochromatosis. Another rare form of hemochromatosis is due to autosomal dominant mutations in the hepcidin receptor ferroportin (Type 4). These mutations (such as C326S) lead to ferroportin's resistance to hepcidin, so that iron is absorbed and exported to the circulation despite the presence of hepcidin [73].

Currently, phlebotomy is the treatment of choice to reverse iron overload in hereditary hemochromatosis. The loss of each 1 ml of packed erythrocytes removes 1 mg of iron and promotes mobilization of iron from iron-loaded tissues and into the bone marrow for restorative erythropoiesis. This treatment is highly

effective, inexpensive, and has very few side effects, although some patients require frequent treatments.

Low hepcidin is also an important feature of iron-loading anemias, such as β-thalassemia [74]. Iron overload is the major cause of morbidity and mortality associated with this disease, both in non-transfusion-dependent and transfusion-dependent thalassemia. Defective β-globin production during erythropoiesis results in the precipitation of excess α-chains and apoptosis of the erythroid precursors during their maturation, causing anemia. In an attempt to compensate for the lack of mature red blood cells, erythropoietin production is increased causing a massive expansion of the erythroid compartment but this fails to generate sufficient mature red cells. In the absence of transfusions, iron overload develops due to hyperabsorption of dietary iron secondary to low hepcidin. Hepcidin decrease is a result of overproduction of suppressive factors, possibly erythroferrone [8] and GDF15 [17], by developing erythroblasts. Treatment by transfusion partially corrects the anemia and hepcidin suppression, but it supplies very high amounts of iron in the form of red blood cell hemoglobin which is eventually degraded and its iron released when these cells are phagocytosed by macrophages. Iron overload in β-thalassemia is treated with iron chelators. However, adverse effects frequently experienced by patients treated with chelators emphasize the need for new therapies, which are currently under development [75, 76].

1.4.3 - Diseases of hepcidin excess / ferroportin deficiency

Elevated hepcidin results in hypoferremia and insufficient supply of iron for erythropoiesis, leading to several types of anemia [77]. The underlying causes of hepcidin elevation in iron-restricted anemias are varied. An example of a genetic cause of hepcidin increase is the familial iron-refractory iron deficient anemia (IRIDA), an autosomal recessive disorder caused by a mutation in TMPRSS6 (matriptase-2) [78]. IRIDA patients are not able to suppress hepcidin production in iron-deficient conditions, resulting in abnormally increased hepcidin production.

Inflammation is a frequent cause of hepcidin overproduction, and chronic inflammatory disorders, such as inflammatory bowel disease and rheumatologic disorders are associated with elevated hepcidin, hypoferremia and anemia. Although anemia of inflammation results not only from hepcidin overproduction but also from direct effect of cytokines on erythroid production and lifespan, therapeutic targeting of hepcidin is a rational approach as indicated by animal models of anemia of inflammation in which ablation of hepcidin is sufficient by itself to lessen anemia and accelerate recovery of hemoglobin [79].

Anemia is also ubiquitous among patients with chronic kidney disease (CKD). Current treatment for this condition involves administration of high doses of erythropoiesis-stimulating agents. Studies have shown that the effects of erythropoiesis-stimulating agents are potentiated by the administration of parenteral iron, suggesting that an iron-restrictive component contributes to the pathogenesis of the anemia. CKD patients have increased hepcidin levels that likely result from a combination of inflammation and inadequate hepcidin clearance by the kidney [80].

Anemia of cancer is a feature of some malignancies and correlates with disease burden, and the intensity of chemotherapy and radiation exposure of the bone marrow. Several factors may be involved in the development of anemia: blood loss, malnutrition, infiltration of the bone marrow by tumor, and cytotoxic injury to bone marrow precursors. However, in some cases, the anemia is also accompanied by an increase in hepcidin and cytokine production, resembling anemia of inflammation [81].

Finally, anemia is a common trait in the elderly population, affecting ~10% of men and women over the age of 65. The causes for the anemia may result from nutrition deficiencies, blood loss, chronic inflammation, renal disease, or myelodysplastic syndrome among other causes. In a recent study, plasma hepcidin was found to be increased in elderly subjects presenting with anemia of inflammation, anemia of kidney disease, and unexplained anemias when compared with participants without anemia [82].

Section 2

Biology and Virulence of Vibrio vulnificus

Section 2 - Biology and Virulence of *Vibrio vulnificus*

Vibrio vulnificus (*V. vulnificus*) is a Gram-negative bacterium highly lethal in patients with certain underlying disorders, such as chronic liver disease, diabetes, immunosuppressive disorders, and iron overload conditions, namely hereditary hemochromatosis. Several studies have shown that *V. vulnificus* virulence is highly enhanced when iron is abundant, turning this otherwise mild infection into a lethal condition in patients with iron overload, causing fulminant sepsis that often culminates in the host's death. The state of the art in the biology, epidemiology, and mechanisms of virulence of *V. vulnificus* will be described in this section. The goal of this project is to elucidate the relationship between iron and *V. vulnificus* infection, and to use this knowledge to improve the treatment of the disease.

2.1 - Epidemiology of *V. vulnificus*

V. vulnificus is a halophilic microbe ubiquitous in coastal waters, living mainly in shellfish such as oysters [83]. The bacteria are more plentiful in seafood during the summer months, when most oysters are positive for *V. vulnificus* [84]. In fact, infections by *V. vulnificus* are more commonly reported during summer and through ingestion of raw or undercooked oysters [85]. While this form of transmission is the most common, infection can also occur through exposure of open wounds to waters or sea creatures contaminated with *V. vulnificus* [86]. Although the number of reported infections is relatively low (900 cases reported by the Centers for Disease Control and Prevention [CDC] between 1988 and 2006), *V. vulnificus* is the leading cause of seafood related deaths in the USA, and has the highest case-fatality rate among foodborne pathogens, exceeding 50% [87, 88]. In addition, the number of reported *V. vulnificus* infections registered a 78% increase between 1996 and 2006, with cases described in an ever growing geographical region, a phenomenon facilitated by global warming [85]. The incidence of infection by this pathogen is expected to increase in the next years, and for this reason expanding the knowledge on *V. vulnificus* infection is crucial to tackle this disease.

The relative rarity of reported disease compared with the abundance of *V. vulnificus* in coastal waters have two main explanations: 1) not all *V. vulnificus* strains are pathogenic; 2) severe infection affects patients with underlying conditions, while healthy subjects very rarely develop grave symptoms. These aspects will be discussed below.

2.2 - *V. vulnificus* biotypes and strains

V. vulnificus strains are classified into biotypes according to their biochemical and serological properties [89]. Biotype 1 is associated with human disease and it is further categorized into clinical (C) or environmental (E) strains, according to different genetic signatures [90]. C strains are highly virulent and possess a genomic island (*vcg*) important for virulence in other pathogens. E strains are enriched in genes associated with metabolic functions. The low percentage of C strains in oysters (15.6 C vs. 84.4 E) contributes for the low incidence of the disease [90]. Biotype 2 is an eel pathogen, although some studies suggest that it may also be an opportunistic human pathogen [91] . Biotype 3 was described during a *V. vulnificus* outbreak in Israel and is associated with wound infection after handling of contaminated fish [92]. C and E strains were identified in biotype 2, while only C strains were detected for biotype 3. All the information discussed henceforth refers to the clinical strain of biotype 1.

2.3 - Risk groups for *V. vulnificus* infection

V. vulnificus is highly virulent and lethal in humans affected by underlying disorders such as chronic liver disease, diabetes, immunosuppression, kidney disease, and iron overload disorders, namely hereditary hemochromatosis [88, 93, 94]. In addition, this infection affects mostly males (89%), possibly due to a protective effect by estrogen in females as shown in rat studies [95]. Most of these risk groups present several characteristics that impair the response to infection, such as decreased complement levels or reduced phagocytic and chemotaxis capacity [94]. The reason why patients with hereditary hemochromatosis are so susceptible to infection has not been clearly elucidated, but it has been

hypothesized that it may have to do with the increased virulence of *V. vulnificus* in an iron-rich environment. This hypothesis will be addressed in ensuing chapters of this dissertation with an approach to elucidate the molecular mechanism involved in that response.

2.4 - Clinical features of *V. vulnificus* infection

V. vulnificus infection develops into three possible outcomes, depending on the route of transmission: severe and fulminant primary septicemia, gastro-intestinal (GI) tract-limited infection (both caused by ingestion of raw/undercooked contaminated seafood), or development of necrotizing wound infections after contact of open wounds with contaminated water or sea creatures [96]. The incubation time is extremely short, with an average of 26 hours (h) after ingestion or 16 h after contact with open wounds [97]. Symptoms include fevers, chills, nausea, abdominal pain and secondary skin lesion in the limbs of patients [94]. Less common symptoms include meningitis, peritonitis, urinary tract infection, osteomyelitis, corneal ulcers and rhabdomyolysis. Since the infection develops so fast, early treatment is decisive to prevent mortality. In fact, the median duration from patient admission to death is 2 days and there is 100% mortality if not treated by 3 days [97]. Although the data on the usefulness of antibiotics is limited, treatment includes doxycycline and ceftazidime administration. A recent study demonstrated that a combination of ciprofloxacin and cefotaxime was more effective in clearing the infection in mice [98]. Amputation of the affected limbs is obligatory if there is a necrotizing wound. The development of effective and fast-acting alternative treatments for the disease is essential to improve the outcome of this infection.

2.5 - Virulence factors

The fulminant course of this infection has been intensively studied and two hypotheses to explain this phenomenon have been proposed: rapid evasion of the immune system and rapid growth rate associated with iron abundance (Figure 3). As a foodborne pathogen, *V. vulnificus* has to cope with the acidic gastric environment. Acid tolerance is achieved through a lysin/cadaverin antiporter and a lysin decarboxylase, both encoded by the *cadBA* operon [99]. Mutations in this operon lead to a decrease in acid resistance. After passing this first barrier, *V. vulnificus* evades complement opsonization and macrophagic phagocytosis by expressing a capsular polysaccharide (CPS) [100]. CPS also masks immunogenic structures to avoid recognition by non-specific immune responses and it is absolutely required for pathogenicity. Compared to experimentally-designed non-capsulated strains, encapsulated *V. vulnificus* are more slowly cleared from the bloodstream, more invasive in subcutaneous tissue and more lethal [101]. Interestingly, *V. vulnificus* experience a phase-variable expression of the capsule whose function is still unknown, but it may be more important for environmental survival rather than causing human infection [102]. Several other virulence factors have been discovered and characterized. *V. vulnificus* is able to cause cellular damage and toxicity through hemolytic factors. The extracellular hemolysin VvhA was shown to increase vascular permeability, promote apoptosis of endothelial cells and stimulate the inducible nitric oxide synthase *in vitro* [103, 104]. Injection of purified VvhA into mice reproduced several characteristic effects of this infection including tissue necrosis and lethality [105]. However, infection with a VvhA-inactivated strain did not reveal a difference in tissue necrosis and LD50 in iron loaded mice, when compared with the wild-type strain [106]. Similar results were obtained in experiments involving the non-specific extracellular protease VvpE, in which the purified enzyme caused tissue necrosis [107], but VvpE-depletion did not have a significant impact mouse survival when compared to bacteria able to synthesize this protease [108, 109]. Furthermore, the VvhA/VvpE double-mutant strain remained highly cytotoxic [110]. Another virulence factor, the multifunctional-autoprocessing repeats-in-toxin (MARTX), was found through random mutagenesis experiments [111]. This molecule, a homolog of *Vibrio cholerae* RtxA, consists of repeated structural subunits able to form pores in cellular

membranes. The importance of MARTX for *V. vulnificus* virulence was demonstrated both *in vitro* and *in vivo* [111]. MARTX is increased upon cell-to-cell contact and lyses host cells [111]. Mutations in the *rtx* operons resulted in a decreased of cellular damage, bacterial spread to the liver, and mice lethality [111, 112]. In addition, monoclonal antibodies against *V. vulnificus* MARTX reduced lethality in infected mice [113]. Taken together, these data suggests that MARTX is a primary virulence factor, while VvhA and VvpE have auxiliary or negligible roles in human infection. Other virulence factors include pili, flagella, outer membrane proteins, lipopolysaccharide (LPS) and the metalloprotease VvpM, but the specific roles of these are still under investigation. The fulminant septic shock observed during infection is a consequence of cytokine hyper-activation [114]. A surface lipoprotein IlpA stimulates the production of IL-6 and TNF-α through binding to TLR2 [115]. TLR2 knock-out mice showed increased resistance to infection with *V. vulnificus* [116]. TLR5 can also be activated upon binding to *V. vulnificus* flagellin (FlaB) and induces NF-kappaB and IL-8 [117]. Several *V. vulnificus* virulence factors are under the control of global regulators. The cyclic adenosine monophosphate (cAMP) - cAMP receptor protein (CRP) system controls the expression of hemolysin, metalloprotease and iron-acquisition proteins [118-121]. A homolog of *V. cholerae* AphB, a transcriptional regulator that controls virulence factors, was also discovered in *V. vulnificus* [122, 123]. Mutations in either of these global regulators caused a decreased in the LD50 in mice, demonstrating their importance for the infection [121, 123]. Interestingly, AphB regulates several genes involved in nutrient acquisition and metabolism, which may be important for bacterial growth. More recently, another regulator named HlyU was found to bind a region upstream of the rtx operon and act as a positive regulator of MARTX [124].

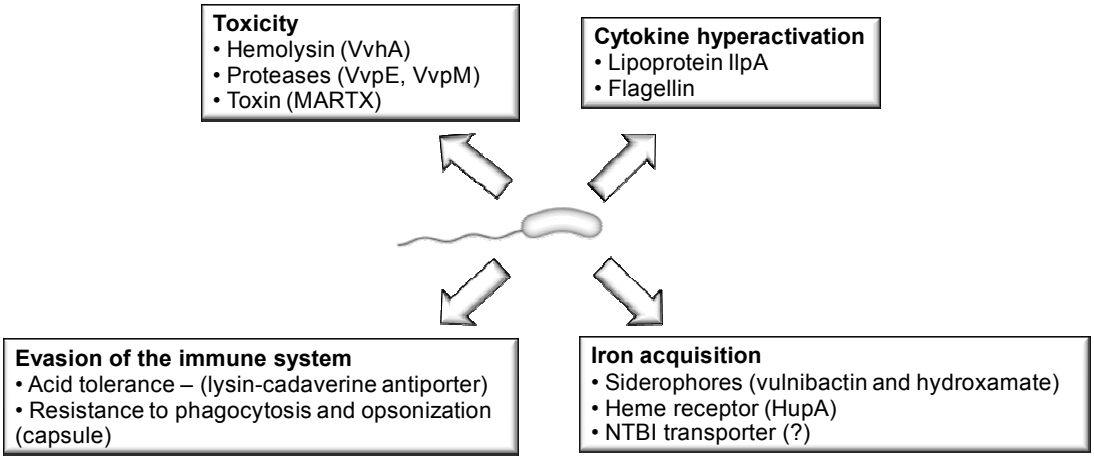

Figure 3. Virulence factors involved in *V. vulnificus* infection. Different strategies applied by *V. vulnificus* in the during an infection, including toxic molecules, hyperactivation of the host's immune system, evasion of the immune system, and iron acquisition from the host.

2.6 - Iron hunt and usage by *V. vulnificus*

Several evidence have demonstrated that iron is an important nutrient during *V. vulnificus* infection. The bacteria grow vigorously when iron is abundant in mammalian hosts [125]. Interestingly, this bacterium usually resides in oysters, which rank among the foods richest in iron. Many severe cases of *V. vulnificus* have been associated with patients suffering from the iron overload disorder hereditary hemochromatosis although the exact mechanism that explains this high susceptibility has yet to be explained [126]. Infection in hereditary hemochromatosis patients is almost exclusively associated with septicemia, even though some wound infection cases have been reported [127]. Mortality after *V. vulnificus* infection was directly correlated to serum iron levels [128]. Several mechanism for iron acquisition within the host have been reported. These include the production of siderophores (secreted molecules that possess high affinity for iron) and a mechanism for iron-uptake from heme. *V. vulnificus* produces two types of siderophores: vulnibactin (a catechol-like siderophore), and an unnamed hydroxamate [129]. Vulnibactin is required to scavenge iron bound to the iron transporter transferrin [130]. Mutations in vulnibactin-associated genes (*vuuA*, *venB*, *vvsA*, and *vvsB*) lead to a decrease in virulence [131-133], although these strains are still infectious, suggesting that the bacterium has other ways to acquire

iron. The role of hydroxamate is still unclear. *V. vulnificus* also expresses receptors for exogenous siderophores produced by other bacteria, such as deferoxamine and aerobactin [134, 135]. The uptake of iron from red blood cells is facilitated by lysing red blood cell through the hemolysin VvhA, thus releasing hemoglobin that is taken up by the membrane heme receptor HupA [136]. Vulnibactin, HupA and VvhA production is regulated by the Ferric Uptake Regulator (FUR) system, a transcriptional repressor ubiquitous in prokaryotes that uses iron as signaling stimulus [136-139]. Although several studies have demonstrated that transferrin-bound iron is essential for *V. vulnificus* growth during infection, Kim *et al* reported that the initiation of growth leading to infection requires the presence of non-transferrin-bound iron *in vitro* (NTBI) [140]. However, the transporter for these iron species is still elusive. Given the pivotal role of iron during human infection, understanding the reasons for the high susceptibility of HH patients to *V. vulnificus* infection is therefore essential in order to prevent and treat this infection.

Section 3

Background and Research Aims

Section 3 - Background and Research Aims

Although the hypoferremic response has been accepted as a host defense mechanism to keep iron out of the pathogens' reach, the molecular players involved in this response were unclear for a long time. The discovery of iron-regulatory peptide hepcidin prompted research groups to address if this peptide was the critical player in mounting the hypoferremic response. Hepcidin mRNA was found to be increased in response to inflammatory stimulus, both *in vitro* and *in vivo*, as well as in patients with anemia of inflammation [66, 141, 142]. However, the physiological relevance of the hepcidin-induced hypoferremic response has never been formally demonstrated in the context of an animal infection. We decided to address this question by using as an infection model *V. vulnificus*, a Gram-negative siderophilic bacterium highly lethal in patients with hereditary hemochromatosis, in a host mouse model lacking hepcidin. The absence of this peptide enables the study of the possible critical role of hepcidin for the host defense. The main objectives of the work presented here are the following.

1) Characterize the hypoferremic response in the context of *V. vulnificus* infection and its dependence on hepcidin **(Chapter III)**

2) Address the potential usefulness of hepcidin agonists in the prevention/treatment of *V. vulnificus* infection **(Chapter IV)**

3) Characterize the mechanism of iron-induced *V. vulnificus* growth **(Chapter V)**

The findings observed in response to each of these objectives will be integrated and discussed on **Chapter VI.** We expect that the significant advances made on understanding hepcidin as a component of the host response may be applied in the future for the management of *V. vulnificus* infection.

CHAPTER II

Materials and Methods

Preparation of bacteria

Vibrio vulnificus CMCP6 strain (provided by Dr. Paul A. Gulig, University of Florida) and ΔFur mutant CMCP6 strain (provided by Dr. Joon Haeng Rhee, Chonnam National University) were grown in LB-N medium - Luria-Bertani broth (BD Difco) containing 0.85% NaCl (Fisher Scientific). Bacterial stocks were stored at -80°C in LB-N with 35% glycerol. The day before the experiment, 50 µl of *V. vulnificus* stock was diluted 1:1000 in LB-N and grown at room temperature overnight. On the day of the experiment, the culture was diluted 1:30 in LB-N and shaken (300 rpm) at 37°C until the optical density at 600nm reached 0.3. Bacteria were then harvested by centrifugation (13800g for 10 min at 4°C) and suspended in 0.9% sodium chloride injection solution (Hospira) at the required concentrations for infections. For *in vitro* growth analysis, bacteria were suspended in LB-N, serum or plasma, as described in later sections.

Animal studies

All experiments involving animals were approved by the University of California, Los Angeles (UCLA) Office of Animal Research Oversight. C57BL/6 wild-type (WT) mice were obtained from Charles River Laboratories. Hepcidin-1 knockout (*Hamp1*$^{-/-}$) mice (originally provided by Dr. Sophie Vaulont [143] and backcrossed by us onto the C57BL/6 background using marker—assisted accelerated backcrossing [144]) were bred in our vivaria. Only 8-12 weeks old male mice were used. WT and *Hamp1*$^{-/-}$ mice were iron-depleted or iron-loaded using dietary manipulations. Starting at 6 weeks of age, WT mice were fed an iron-poor (4 ppm Fe) or iron-rich (10000 ppm Fe) diet (Harlan) for 2 weeks. Starting at 4-5 weeks of age, *Hamp1*$^{-/-}$ mice were fed an iron-poor (4 ppm Fe) or standard diet (270 ppm Fe) for 4-6 weeks before the infection. The earlier start and longer regime of low-iron diet in *Hamp1*$^{-/-}$ mice was necessary to achieve substantial iron depletion because these mice are already iron-overloaded at a young age.

All bacterial infections were performed by subcutaneous (s.c.) injection (100 µl) in the interscapular area with $1x10^3$-$1x10^7$ CFU of *V. vulnificus* suspended in 0.9% sodium chloride (Hospira). Control mice received equivalent injections of saline. For survival experiments, mice were observed for 4 days after infection or were euthanized earlier by isofluorane inhalation (Clipper) if they became moribund. For

tissue and blood collection, WT and *Hamp1*$^{-/-}$ mice were infected with 300 CFU (and 1x10^5 CFU only in WT mice) and control animals received saline injections. Mice were euthanized 16-18h after infection, were exsanguinated by cardiac puncture, and their livers were harvested. For histopathology analysis, *Hamp1*$^{-/-}$ mice were injected with 1x10^3 CFU of *V. vulnificus* or saline, euthanized 10-12h after infection and a piece of the liver and the injection site (skin) were collected into tubes containing 4% formalin (Medical Chemical Corporation).

To analyze early changes in iron, hepcidin and pro-inflammatory cytokines after infection, WT mice (fed an iron-poor or iron-rich diet for 2 weeks) were injected with 1x10^5 CFU of *V. vulnificus* or saline and animals were euthanized at 3, 6 or 10 h after infection to harvest blood and tissues.

To test the therapeutic effects of minihepcidin, mice were injected intraperitoneally with 100 nmol of minihepcidin PR73 dissolved in 100 µl of SL220 [144, 145] (a PEG-phospholipid based solubilizer, NOF Corp.), whereas control groups were injected with the same amount of solvent. For minihepcidin pretreatment studies, animals were injected 24 h and 3 h before infection. For treatment studies, animals received minihepcidin or solvent injection 3 h after the infection. Mice were euthanized 16-18 h after infection, were exsanguinated by cardiac puncture, and their livers were harvested for iron and CFU quantification. In survival experiments, surviving animals received additional minihepcidin or solvent injections, 24 h and 48 h after infection.

Iron measurements: serum, plasma, liver and unsaturated iron binding capacity

Mouse blood was collected in serum separator tubes (BD) and allowed to clot at room temperature for 30 min followed by centrifugation for 5 min, at 4500 rpm and 4^{o}C. The serum was transferred to new tubes for serum iron quantification using the colorimetric Iron-SL assay (Sekisui Diagnostics) following the manufacturer's instructions. Human plasma samples were centrifuged at 8000g for 10 minutes and the supernatants were used for iron quantification using the same assay. Unsaturated iron binding capacity (UIBC) in human plasma was measured using the colorimetric Unsaturated Iron Binding Capacity assay (Sekisui Diagnostics) following the manufacturer's instructions. For liver iron measurements, the tissue

was homogenized and a 75 µl sample was added to 1125 µl of protein precipitation solution (0.53M HCl and 5.3% trichloroacetic acid, Fisher Scientific). The samples were heated at 100 °C for 1 hour, centrifuged for 10 minutes (13000 rpm at 4°C), and the supernatant was used for the Iron-SL assay (Sekisui Diagnostics), measuring the absorbance at 595 nm relative to Iron AA Standard (Ricca Chemical Company). Results are expressed as µg Fe per gram of wet liver weight.

Bacterial growth analysis

To measure iron-dependent growth, bacteria were incubated in 100 µl of LB-N or heat-inactivated serum (30 min at 56^{o}C) from iron-depleted or iron-loaded mice, at a concentration of 1x10^{4} CFU/ml, supplemented with Ferric Ammonium Citrate (FAC, Sigma, added to a final concentration of 100 µM), the iron chelator deferiprone (Sigma, 150 µM), or protegrin (Bioworld, 0.4 mg/ml), using a 96-well plate (Costar 3604) at 37^{o}C with shaking (300 rpm). Bacterial growth was measured by plating 6 µl of serial dilutions of each condition (in triplicate) on LB-N plates containing 1.5% agar. Plates were incubated at 37°C until colonies were visible for enumeration.

To address the effect of different forms of iron in *V. vulnificus* growth, bacteria were incubated in 250 µl of LB-N or heat-inactivated human plasma (30 min at 56 ^{o}C, followed by centrifugation of 8000g for 15 min to remove debris). Plasma samples were obtained from the blood of healthy volunteers at the Ronald Reagan UCLA Medical Center after treatment with citrate phosphate dextrose adenine (CPDA-1). *V. vulnificus* was added at a concentration of 1x10^{3} or 1x10^{4} CFU/ml in a 96-well plate (Costar 3604), and supplemented with various concentrations of FAC, Holo-Transferrin (Serologicals Corporation), Apo-Transferrin (Celliance), ferric ammonium sulfate (FAS, Sigma), a combination of FAC and Apo/Holo-transferrin, or deferiprone (150 µM). Bacterial growth was monitored using a Gemini XS microplate reader (Molecular Devices), by measuring the optical density at 600nm, each 15 min for 10h, at 37^{o}C with shaking 800 sec before each read.

Bacterial CFU quantification in blood and liver

Blood was collected by cardiac puncture into 1.5 ml tubes containing 1 unit of heparin (Elkin Sinns Inc.), mixed vigorously and used directly for CFU quantification. A piece of liver (~100mg) was mixed with 250 µl of sterile H_2O, homogenized, centrifuged at 2000 rpm for 5 min and the supernatant collected for CFU quantification. Serial 1:5 dilutions (as well as 1:100 and 1:1000) were prepared in saline and 6 µl of each sample was plated on LB-N agar plates (1.5% agar) and incubated at 37^{o}C until colonies were visible for counting.

Histopathology analysis

Liver and skin sections were fixed in 4% formalin for 12 h, imbedded in paraffin, cut in 5-micron sections and stained with hematoxylin and eosin at the UCLA Translational Pathology Core Laboratory. Skin sections were also stained using the Gram Stain for Tissue kit (Sigma) following the manufacturer's instructions. Microscopic images were acquired on a Nikon Eclipse E600 microscope using Nikon Plan Fluor 4x/0.13, Plan Apo 10×/0.45, Plan Apo 40×/0.95 and Plan Fluor 100x/1.30 objectives with a Spot RT3 2MP Slider camera and Spot 5.0 software. Pictures were assembled using Adobe Photoshop CS5.

Labile plasma iron quantification

Labile plasma iron (LPI), a redox-active form of non-transferrin bound iron [146], was measured using the FeROS eLPI kit (aFerrix) according to the manufacturer's instruction. Briefly, 20 µl of mouse serum was plated in duplicate in 96-well plates and treated with 100 µl of LPI reagent containing buffered 2,3-dihydrorhodamine and ascorbate, in the presence or absence of an iron chelator. Fluorescence resulting from oxidation of 2,3-dihydrorhodamine after exposure to reactive oxygen species was measured in a Gemini XS microplate reader (Molecular Devices) using 495 nm for excitation and 525 for emission. A kinetic measurement was performed every 2 minutes for 40 minutes. The ΔFU/min for each sample, with or without the iron chelator, was converted to LPI units by comparing it with the standard values obtained in the same test. Values higher than 0.2 were considered indicative for the presence of NTBI.

Gene expression analysis

RNA from mouse liver was extracted by TRIzol Reagent (life technologies), and cDNA was synthesized using the iScript cDNA Synthesis Kit (Bio-Rad) following manufacturer's instructions. Real-time quantification of transcripts was performed in duplicates in a CFX96 Touch Real-Time PCR Detection System (Bio-Rad) using Sso Advance SYBR Green Supermix (Bio-Rad) and specific primers for *Hamp1* (fwd: TTGCGATACCAATGCAGAAGA; rev: GATGTGGCTCTAGGCTATGTT), *Inhbb* (fwd: CTCCGAGATCAT CAGCTTTGC, rev: GGAGCAGTTTCAGGTACAGCC), *Saa1* (fwd: AGTCTGGGCTGCTGAGAAAA; rev: ATGTCTGTTGGCTTCCTGTG) and *Actb* (fwd: ACCCACACTGTGCCCATCTA; rev: CACGCTCGGTCAGGATCTTC). Data were normalized to the expression of β-actin.

Serum hepcidin assay

Mouse hepcidin ELISA was performed as previously described [147]. Mouse hepcidin-1 monoclonal antibodies, Ab2B10 (capture) and AB2H4-HRP (detection), as well as synthetic mouse hepcidin-25, were a generous gift from Amgen. High binding 96-well EIA plates (Corning Costar) were coated overnight at room temperature with 50 µl/well of 3.6 µg/ml Ab2B10 in 0.2 M carbonate-bicarbonate buffer pH 9.4 (Pierce - Thermo Scientific). Plates were washed two times with wash buffer - Phosphate Buffered Saline (PBS, Life Tech) + 0.5% Tween-20 (Fisher Scientific) - and then blocked for 45 minutes with 200 µl/well blocking buffer - PBS, 1% Bovine Serum Albumin (BSA, Sigma), 1% goat serum (Sigma), 0.5% Tween-20. Serum samples (previously diluted in blocking buffer at 1:10000 for iron-loaded mice or 1:1000 for iron-depleted mice) and standards were incubated for one hour at room temperature (50 µl/well), washed four times with wash buffer, incubated for one hour with 50 µl/well of 130 ng/ml Ab2H4-HRP, washed 4 times and then developed with 100 µl/well Ultra-TMB substrate (Thermo Scientific) for 15 min in the dark at room temperature. The reaction was stopped by adding 50 µl 2M sulfuric acid, and the absorbance was measured at 450 nm using a 96-well plate reader (Molecular Devices).

Quantification of inflammatory cytokines in serum

Inflammatory cytokines (IFN-γ, IL-1β, IL-2, IL-4, IL-5, IL-6, KC/GRO, IL-10, IL-12p70 and TNF-α) were measured in mouse serum using the Proinflammatory Panel 1 (mouse) kit (Meso Scale Discovery) following the manufacturer's instructions. Briefly, 50 µl of standards and 2-fold diluted samples were added to a 10-spot multiplex plate pre-coated with capture antibodies, and the plate was incubated at room temperature with shaking for 2 hours. After washing 3 times with wash buffer (PBS supplemented with 0.05% Tween-20), 25 µl of detection antibody was added to each well and incubated for 2 hours, washed 3 times and incubated with 150 µl of 2X read buffer (provided with the kit). The plate was read in a chemiluminescence reader (SECTOR Imager 2400, Meso Scale Discovery), and data were analyzed using the MSD Discovery workbench software (Meso Scale Discovery).

Minihepcidin synthesis

Minihepcidin PR73 was synthesized as a C-terminal amide using standard solid-phase Fmoc chemistry and was purified by preparative reverse-phase high performance liquid chromatography (RP-HPLC). Its purity was evaluated by matrix-assisted laser desorption ionization spectrometry (MALDI-MS) as well as analytical Reversed-phase high performance-liquid chromatography (RP-HPLC). From N- to C-terminus the primary sequence of PR73 was: iminodiacetic acid, L-threonine, L-histidine, L-3,3-diphenylalanine, L-β-homoproline, L-arginine, L-cysteine, L-arginine, L-β-homophenylalanine, 6-aminohexanoic acid, iminodiacetic acid palmitylamide (Ida-Thr-His-Dpa-bhPro-Arg-Cys-Arg-bhPhe-Ahx-Ida(NHPal)-CONH2).

Analysis of minihepcidin and hepcidin-25 bactericidal activity *in vitro*

V. vulnificus were incubated in 12 µl of LB-N broth at a concentration of $1x10^3$ CFU/ml, supplemented with various concentrations (0, 0.9, 2.7, 9.1, 27 and 91 µM) of human hepcidin-25 (Peptides International) or minihepcidin PR73, or 4mg/ml of protegrin, for 3 h at 37^{o}C with shaking (300 rpm). Bacterial growth was measured by CFU quantification as described above.

Analysis of the bactericidal and bacteriostatic effects of minihepcidin on *V. vulnificus*

To analyze the mode of action of minihepcidin PR73 in mouse serum, we used *V. vulnificus* CMCP6 containing pGTR905, a marker plasmid that confers resistance to chloramphenicol, as described in Starks *et al* [148] (Figure 1). The plasmid replicates only in the presence of arabinose, which is not found in mouse tissues. Thus, the loss of plasmid from the bacterial population during growth in mouse serum is a measure of bactericidal activity. The principle is graphically illustrated in Gulig *et al* [149] and in Figure 6, Chapter 4. The plasmid-containing bacterial inoculum was first grown in LB-NAC - LB-N broth supplemented with 1% L-arabinose (Sigma) and 5 µg/ml chloramphenicol (Sigma) - to enable and select for plasmid replication. The bacteria were then washed, suspended in LB-N at $1x10^5$ CFU/ml and 10 µl added to 40 µl of mouse serum in 96-well plates. Serial 5-fold dilutions were performed in serum. Serum samples were obtained from *Hamp1*$^{-/-}$ mice kept on an iron-poor or standard diet for 4-6 weeks and injected 24 h and 3 h before blood collection with 100 nmol PR73 in SL220 or with SL220 only (5 mice per group). Sera were also collected from WT mice kept on iron-poor or iron-rich diet for 2 weeks (5 mice per group). For each mouse group, sera was pooled and used for *in vitro* experiments. 96-well plates with bacteria were incubated for 2 h at 37 C with shaking (300 rpm), using triplicates for each condition. Five µl from each well was plated on LB-N and LB-NAC plates (containing 1.5% agar) and CFU were counted for each plate as described above.

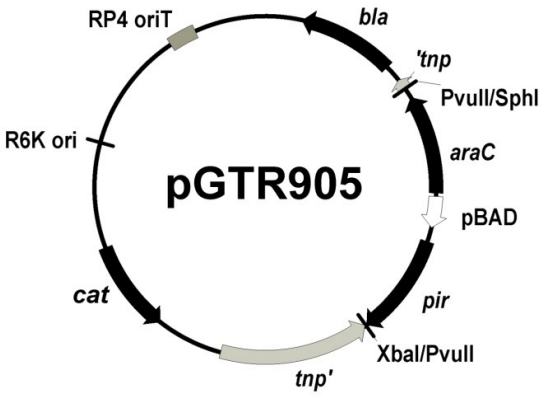

Figure 1. Genetic and physical map of marker plasmid pGTR905. The marker plasmid pGTR905 was constructed by the insertion of the pir gene, under the control of the tightly regulated araC, pBAD promoter system, into the suicide plasmid pUTmini-Tn5Tag9 at a unique PvuII site within the Tn5 transposase gene (tnp) forming the tnp' and 'tnp gene fragments. Also shown are the β-lactamase gene (bla), chloramphenicol-resistance gene (cat), RP4 origin of transfer (oriT), and R6K origin of replication (R6K ori).

V. vulnificus RNA isolation for sequencing

V. vulnificus CMCP6 were incubated in 250 µl of heat-inactivated human plasma (30 min at 56^{o}C, followed by centrifugation at 8000g for 15 min to remove debris), supplemented with 50 µM of FAC to allow growth initiation, in two full 96-well plates (Costar 3635). The use of 96-well plates allowed us to follow bacterial growth in real time by continually measuring the optical density during the course of the experiment. Bacterial growth was monitored using a Gemini XS microplate reader (Molecular Devices), by measuring the optical density at 600nm, each 15 min, at 37^{o}C with shaking 800 sec before each read. At early exponential phase (time-point T1, when the average OD600>0.010), one plate was used for bacterial RNA isolation using TRIzol reagent (life technologies) following the manufacturer's instructions, and bacteria in the remaining plate were pooled, centrifuged and re-suspended in fresh plasma supplemented with 50 µM FAC or non-supplemented fresh plasma and re-incubated in the same conditions. After 5 hours (time-point T2), bacteria in each condition (0 µM and 50 µM) were pooled and RNA was extracted. RNA integrity and quality was evaluated using the Agilent 2100 Bioanalyzer (Agilent technologies) at the UCLA Clinical Microarray Core, and samples were selected for sequencing if the RNA integrity number was 9.5-10. Samples were obtained from 3 independent experiments (total of 9 samples).

RNA sequencing

Libraries were prepared with KAPA stranded RNA-seq library preparation kit (Kapa Byosystems). The workflow consists of double-stranded cDNA generation using random priming, fragmentation of double stranded cDNA, end repair to generate blunt ends, A-tailing, adaptor ligation and PCR amplification. Different adaptors were used for multiplexing samples in one lane. Sequencing was performed on Illumina Hiseq2000 (Illumina) for a single read 50 run. Data quality check was done on Illumina SAV. Demultiplexing was performed with Illumina CASAVA 1.8.2. The reads were first mapped to the *V. vulnificus* transcript set using Bowtie2 version 2.1.0 [150] and the gene expression level was estimated using RSEM v1.2.15 [151]. TPM (transcript per million) was used to normalized the gene expression. Differentially expressed genes were identified using the DeSeq program. Genes showing altered expression with $p<0.05$ and more than 1.5 fold changes were considered differentially expressed.

Statistical analysis

The statistical significance of differences between groups was evaluated using Student *t* test if data were normally distributed or Mann-Whitney *U* test if this condition was not met. Survival differences were analyzed using Kaplan-Meier survival curves and Log-Rank test. All statistics were done using Sigmaplot 12.5 (Systat Software).

CHAPTER III

Hepcidin-induced hypoferremia in V. vulnificus infection

Specific aims

Hypoferremia (decrease in blood iron) during infections has been proposed as a host defense mechanism that evolved to restrict iron availability for extracellular pathogens but specific support for this hypothesis has been lacking. Infections by siderophilic (iron-loving) bacteria, such as *Vibrio vulnificus*, are severe and often lethal in patients with hereditary hemochromatosis (HH), while healthy individuals only experience mild symptoms. Since HH patients develop iron overload as a consequence of hepcidin deficiency, we hypothesized that hepcidin plays a critical role in host defense against *V. vulnificus* infections. To address this hypothesis, we pursued the following aims:

a. compare the susceptibility to infection between wild-type and hepcidin deficient (*Hamp1*$^{-/-}$) mice

b. investigate which forms of iron are relevant to the development of infection (serum iron, liver iron and/or non-transferrin bound iron)

c. describe the host defense response in resistant (wild-type) mice

Hepcidin is required for resistance to *V. vulnificus* infection

Iron is thought to be required for rapid growth of *V. vulnificus* and lethality during infections, as previously demonstrated in mice injected with iron-dextran [128, 152]. To examine whether the iron-regulatory hormone hepcidin affects the response to infection, we compared the severity of *V. vulnificus* infection in wild-type (WT) and hepcidin knock-out (*Hamp1*$^{-/-}$) mice. Mice were iron-depleted or iron-loaded by dietary manipulations, and infected subcutaneously with a low (10^3 CFU) or moderate (10^5 CFU) inoculum of *V. vulnificus*. In both iron-depleted (Figure 1A) and iron-loaded (Figure 1B) conditions *Hamp1*$^{-/-}$ mice were significantly more susceptible than WT mice: iron-loaded *Hamp1*$^{-/-}$ died within one day after infection, iron-depleted *Hamp1*$^{-/-}$ within next several days, whereas WT mice survived the infection. WT mice were susceptible to *V. vulnificus* infection only when iron-loaded (Figure 2 and Table 1) and infected with a large inoculum of *V. vulnificus* (10^6 CFU). Under those conditions, iron-loaded mice died within 2 days after infection while most of the iron-depleted mice still survived (Figure 2A), confirming that iron has a striking effect on *V. vulnificus* lethality. The differential susceptibility of WT and *Hamp1*$^{-/-}$ to *V. vulnificus* infection was not attributable to their baseline liver iron differences because iron-depleted *Hamp1*$^{-/-}$ mice were much more susceptible to infection even though they had lower liver iron stores than iron-loaded WT mice, as measured in a parallel set of mice maintained under the same conditions as the mice used for the survival experiments (Figure 1C). As *V. vulnificus* is an extracellular pathogen [153], intracellular hepatocyte iron is not likely to play a direct role in the growth of these bacteria.

To examine whether extracellular iron concentrations alter the growth rate of *V. vulnificus*, we assessed bacterial growth *ex vivo* in sera collected from uninfected iron-loaded or iron-depleted WT animals. *V. vulnificus* growth was greatly enhanced in serum derived from iron-loaded compared to iron-depleted mice (Figure 2B). Supplementing iron-depleted serum with ferric ammonium citrate (FAC) also enhanced bacterial growth. Conversely, addition of the synthetic iron chelator deferiprone to iron-rich serum prevented bacterial growth.

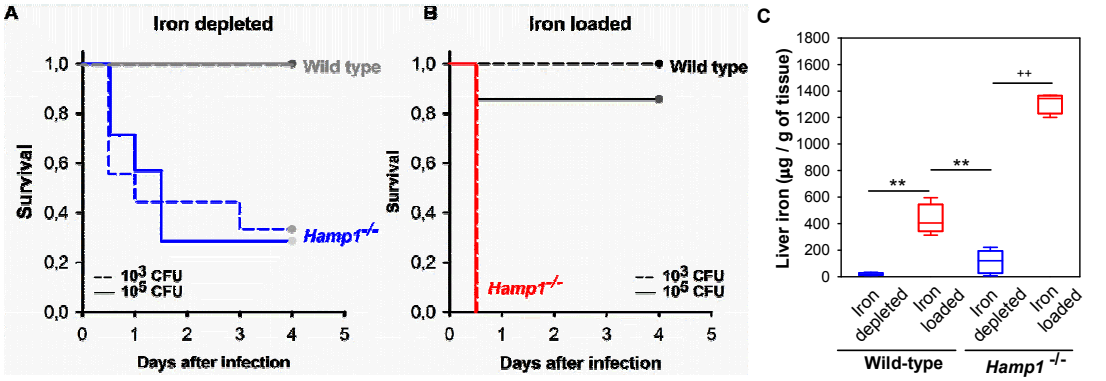

Figure 1. *Vibrio vulnificus* infection is highly lethal in hepcidin-deficient mice. Kaplan-Meier survival curves for iron depleted **(A)** and iron loaded **(B)** mice, after infection with $1x10^3$ (dashed lines) or $1x10^5$ (solid lines) CFU of V. vulnificus (n=4-11 in each group). WT and *Hamp1*$^{-/-}$ mice were iron-depleted or iron-loaded by dietary modification (WT: 4 ppm or 10,000 ppm Fe diet for 2 weeks; *Hamp1*$^{-/-}$: 4 ppm or standard diet for 4-6 weeks, see Chapter II). By multifactorial Kaplan-Meier log-rank analysis, differences in survival between WT and *Hamp1*$^{-/-}$ mice were significant in both iron depleted (combined CFU, $p<0.05$), and iron-loaded conditions (combined CFU, $p<0.001$). **(C)** Liver iron stores were measured in a parallel set of mice and confirmed the effective modulation of iron stores by dietary iron manipulation (n=5-10 per group). For liver iron measurements, statistical significance was assessed using student's t test if data were normally distributed (**$p<0.01$) or Mann-Whitney U test if they were not normally distributed (++$p<0.01$).

Interestingly, growth in low-iron serum was similar to the growth in standard LB-N broth. This indicates that *V. vulnificus* can grow adequately even with limited iron availability but excess iron greatly increases the growth rate. In iron-rich serum, bacteria underwent ~18 divisions within 3 hours, or one division every 10 min, an astoundingly rapid growth rate.

Human infections with *V. vulnificus* and their laboratory models often terminate in septic shock [154]. To verify that this mechanism contributed to rapid death of iron-loaded mice, we inspected hematoxylin and eosin (H&E) stained skin (site of injection) and liver sections of *Hamp1*$^{-/-}$ mice injected with $1x10^3$ CFU of *V. vulnificus* or saline. The venules in the skin and hepatic circulation of infected mice were greatly dilated compared with saline-treated mice (Figure 3). The vasodilatation was accompanied by erythrocyte sludging characteristic of circulatory shock. In the skin, massive aggregates of bacteria were visible in the perivascular space (Figure 3 E-H). In the liver, no bacteria were seen but there was neutrophilic infiltration in perivenular spaces (Figure 3 I-N). These findings are consistent with endotoxemic shock.

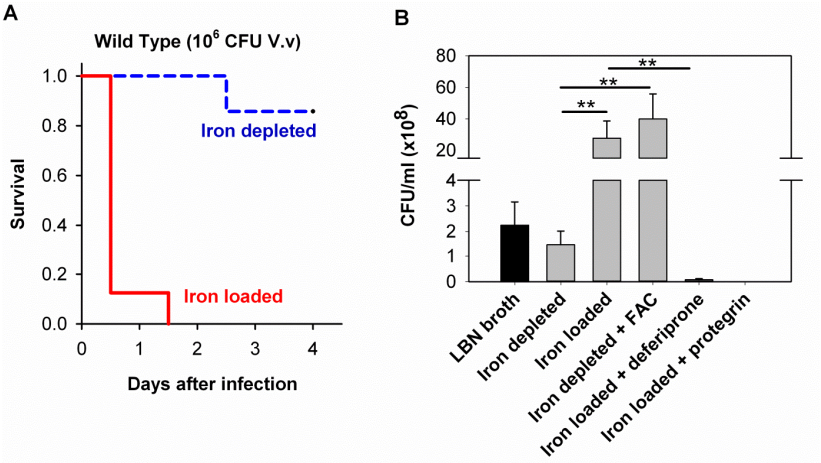

Figure 2. *V. vulnificus* pathogenicity and growth are greatly enhanced by high iron concentrations. (A) Kaplan-Meier survival curves for 8-10 week-old WT mice, after s.c. infection with $1x10^6$ CFU of *V. vulnificus.* Iron-loaded mice (red line) died very rapidly, whereas iron-depleted mice (blue line) survived the infection, with the difference significant at $p<0.001$ by log-rank survival analysis. **(B)** Serum was collected from iron-depleted and iron-loaded WT mice. *V. vulnificus* ($1x10^4$ CFU/ml) was incubated for 3 h at 37 °C with shaking (300 rpm) in LB-N broth (black fill), or in different sera (gray fill) as indicated. Bacterial growth in LB-N broth and low-iron serum (26 µM Fe) was similar, but it was greatly increased in high-iron serum (60 µM Fe) and in iron-depleted serum supplemented with FAC (added to a final concentration of 100 µM Fe). Bacterial growth was impaired in high iron serum treated with the iron chelator deferiprone (150 µM). Addition of the bactericide protegrin (0.4 mg/ml) to high-iron serum killed all the bacteria. Bars represent mean + standard deviation (n=7 per group). Statistical significance was assessed using student's *t* test (**$p<0.01$).

To determine whether the susceptibility of *Hamp1*$^{-/-}$ mice to severe *V. vulnificus* infection was due to greater bacteremia and bacterial dissemination, we assayed bacterial CFU counts in blood and liver of iron-depleted and iron-loaded WT and *Hamp1*$^{-/-}$ mice 16 h after infection. Liver CFU counts likely represent extracellular bacteria as *V. vulnificus* does not appear to invade cells [153]. To allow *Hamp1*$^{-/-}$ mice to survive long enough to undergo analysis at the 16 h time point, we injected all groups with a small inoculum of bacteria (300 CFU). After infection with this low inoculum, only iron-loaded *Hamp1*$^{-/-}$ mice, but not iron-depleted *Hamp1*$^{-/-}$ or either of the WT groups, had CFU in blood and liver (Figure 4A). For the WT groups, the iron-dependent difference in CFUs was observed at a higher inoculum (10^5 CFU, Figure 4B). These data indicate that in both *Hamp1*$^{-/-}$ and WT mice, bacterial replication and dissemination is highly dependent on the host's iron status.

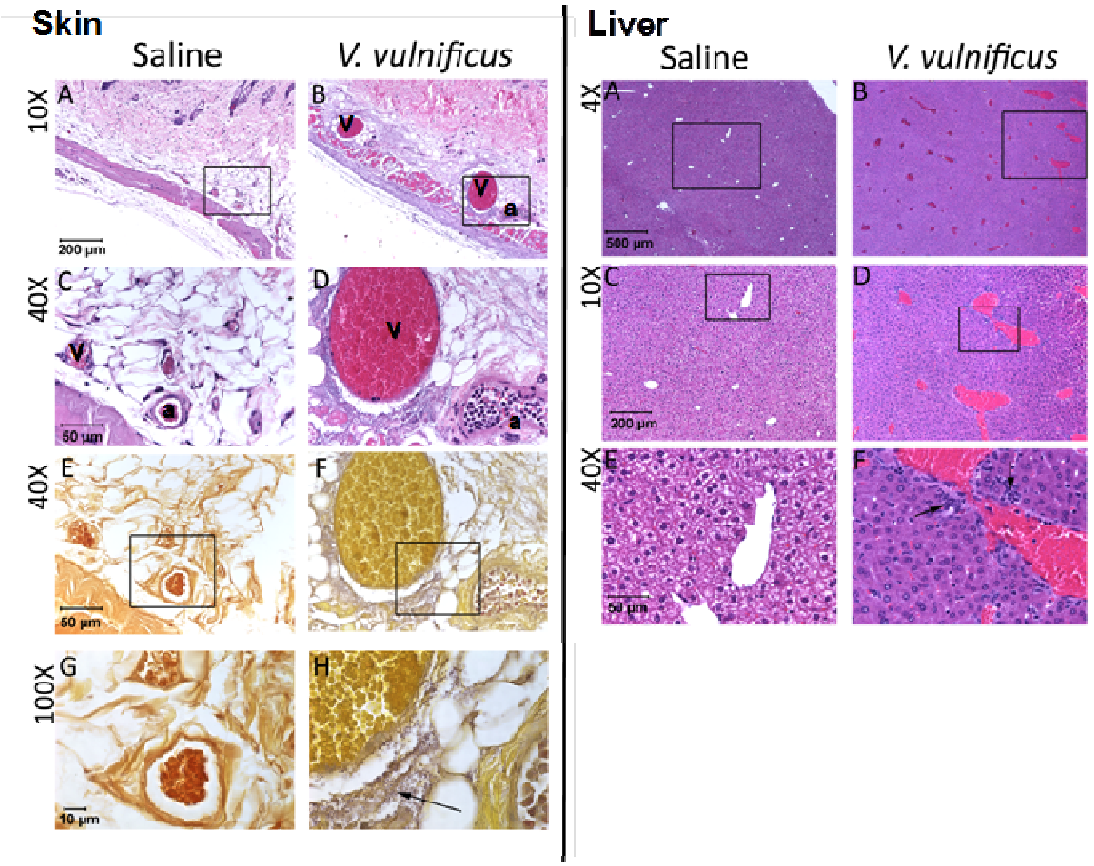

Figure 3. *V. vulnificus* infection induces vasodilation, leukostasis and erythrocyte sludging. Skin (site of injection) and liver sections of *Hamp1*$^{-/-}$ mice injected with saline (A, C, E, G, I, K and M) or 1 x 10^3 CFU of *V. vulnificus* (B, D, F, H, J, L and N). Sections were stained with hematoxylin and eosin (A-D and I-N) or Gram stain and tartrazine (E-H). **Panels A-B** and magnified in **C-D:** dilated venules (v) and arterioles (a), leukostasis and erythrocyte sludging are seen in the skin of *V. vulnificus*-infected mice compared with saline-injected controls**. Panels E-F** and magnified in **G-H:** numerous bacteria (purple) are seen in perivascular spaces of infected mice (arrow). **Panels I-L** Veins and venules in infected mice are dilated and congested with aggregated erythrocytes (J, L), unlike the saline controls (I, K). **(E-F)** Perivascular neutrophil infiltration (arrows) in infected mice (N) but not in saline controls (M).

As shown in Figure 1, mortality from *V. vulnificus* infection did not correlate with baseline liver iron concentrations, therefore we hypothesized that the difference in baseline serum iron concentrations, baseline non-transferrin bound iron (NTBI) and/or the ability to generate hypoferremia may explain the disparate susceptibility of *Hamp1*$^{-/-}$ and WT mice and the iron dependence of bacterial growth *in vivo*.

Indeed, WT mice lowered their serum iron concentrations in response to infection (Figure 4C, mean of 26 µM in iron-depleted and 30 µM in iron-loaded infected mice), whereas *Hamp1*$^{-/-}$ mice had a much smaller decrease in serum iron (mean

of 63 μM in iron-depleted and 52 μM in iron-loaded infected mice), insufficient to affect the replication of *V. vulnificus*. The slight decrease in *Hamp1*$^{-/-}$ serum iron may be a consequence of decreased food intake, a common trait in sick mice, or due to direct effects of inflammatory cytokines on ferroportin mRNA [155, 156].

Among *Hamp1*$^{-/-}$ mice, despite similar serum iron concentrations in iron-loaded and iron-depleted groups, the iron-loaded group had higher CFU counts in the blood and liver (Figure 4A). This difference in bacterial burden may be related to the difference in the serum concentrations of NTBI, a known source of iron for *V. vulnificus* [140]. NTBI was only detected in iron-loaded mice (1.28± 0.60 LPI units), but not in the iron-depleted group (Figure 4D), correlating with the bacterial burden. WT mice had low NTBI levels, similar to those in iron-depleted *Hamp1*$^{-/-}$ mice, suggesting that NTBI did not contribute significantly to bacterial growth in WT mice. Among WT mice infected with the high inoculum (10^5 CFU), the iron-loaded group had higher CFU counts in the blood and liver than the iron-depleted group (Figure 4B), despite the similar degree of hypoferremia 16 h after infection (Figure 4C). As NTBI levels were not significantly different between these two groups, it is likely that serum iron concentrations during the early stages of infection (prior to the hepcidin increase and hypoferremia) also contribute to susceptibility to *V. vulnificus* infection. Thus, our data suggest that baseline concentrations of transferrin-bound and non-transferrin bound iron as well as reactive hypoferremia, all of which are controlled by hepcidin, determine the replication and dissemination of *V. vulnificus in vivo*.

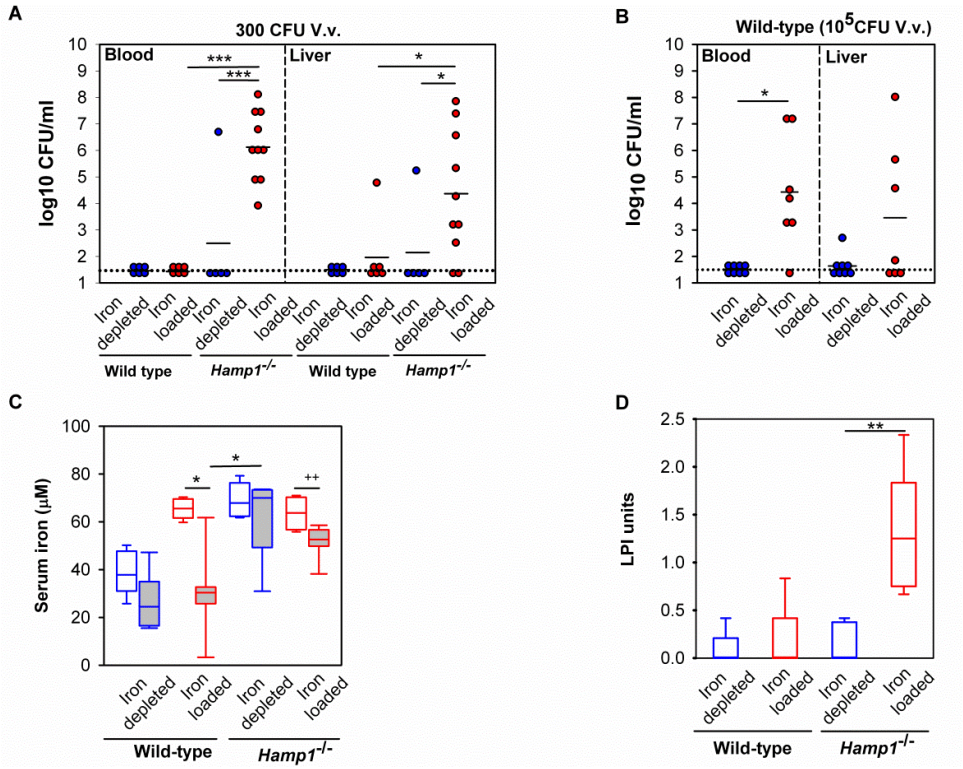

Figure 4. Iron-dependent dissemination of *V. vulnificus* in blood and liver. Wild-type and *Hamp1*$^{-/-}$ mice were iron-depleted or iron-loaded by dietary modification (WT: 4 ppm or 10,000 ppm Fe diet for 2 weeks; *Hamp1*$^{-/-}$: 4 ppm or standard diet for 4-6 weeks, see Chapter II), and infected with *V. vulnificus* (n=5-10 per group). **(A)** and **(B)** Bacterial counts in blood and liver 16 h after infection with 300 CFU (A) and 1x10^5 CFU (B). Each symbol represents one mouse (iron depleted in blue and iron loaded in red); black solid lines represent the mean of CFU counts; black dotted line represents the lower limit of detection of CFU counts (calculated as half of the minimum detectable CFU counts). **(C)** Serum iron levels of WT (1x10^5 CFU) and *Hamp1*$^{-/-}$ (300 CFU) mice (white fill = saline groups, grey fill = *V. vulnificus* groups). Unlike WT mice which decreased their serum iron to the mean of ~30 µM, *Hamp1*$^{-/-}$ mice did not develop marked hypoferremia after infection. **(D)** Measurement of non-transferrin bound iron (as labile plasma iron, LPI) in serum of iron-depleted and iron-loaded WT and *Hamp1*$^{-/-}$ mice prior to infection (n=4-6 per group). Statistical significance was assessed using student's *t* test if data were normally distributed (*p<0.05; **p<0.01; ***p<0.001) or Mann-Whitney *U* test if they were not ($^{+}$p<0.05; $^{++}$p<0.01).

Hepcidin levels increase early after *V. vulnificus* infection

Only WT but not *Hamp1*$^{-/-}$ animals were able to generate significant hypoferremia, suggesting that hepcidin mediates inflammatory hypoferremia during infection. To confirm this hypothesis we analyzed hepatic hepcidin mRNA and serum hepcidin protein at 3, 6 and 10 hours after infection with 10^5 *V. vulnificus* in iron-loaded and iron-depleted WT mice. As expected, iron-loaded mice had higher levels of hepcidin mRNA and protein compared to iron-depleted mice at all time points, due to the iron stimulus on hepcidin expression (Figure 5A and B). By 6 h after infection, both iron-depleted and iron-loaded mice acutely increased their hepatic hepcidin mRNA (Figure 5A) as well as serum hepcidin concentration (Figure 5B) compared to uninfected mice. At 10 h after infection, serum hepcidin increased further in iron-depleted mice and stabilized at very high levels in iron-loaded mice (Figure 5B). These increases in hepcidin concentrations were accompanied by a significant decrease in serum iron at 6 h and 10 h in iron-depleted mice (Figure 5C), and a trend toward decreased serum iron in iron-loaded mice. The latter may not have decreased serum iron as efficiently because iron–loaded hepatocytes, macrophages and enterocytes express more ferroportin [157-159].

IL-6 is thought to be the predominant stimulus for hepcidin synthesis during inflammation [66, 160]. We found dramatically increased serum concentrations of this pro-inflammatory cytokine in infected mice starting at 3 h after infection (Figure 5D), with no differences between iron-depleted and iron-loaded mice. A similar increase was also observed for the inflammatory cytokines KC-GRO, IL-12p70, IL-1β, TNF-α, IL-10 and IL-2, while IFN-γ, IL-4 and IL-5 remained unchanged (Figure 6C). We also observed early increases in hepatic *Saa1* (an inflammatory marker) and *Inhbb* mRNA, which codes for the β_B-subunit of activin B, a protein involved in an alternative pathway for hepcidin regulation by inflammation, (Figure 6A and B).

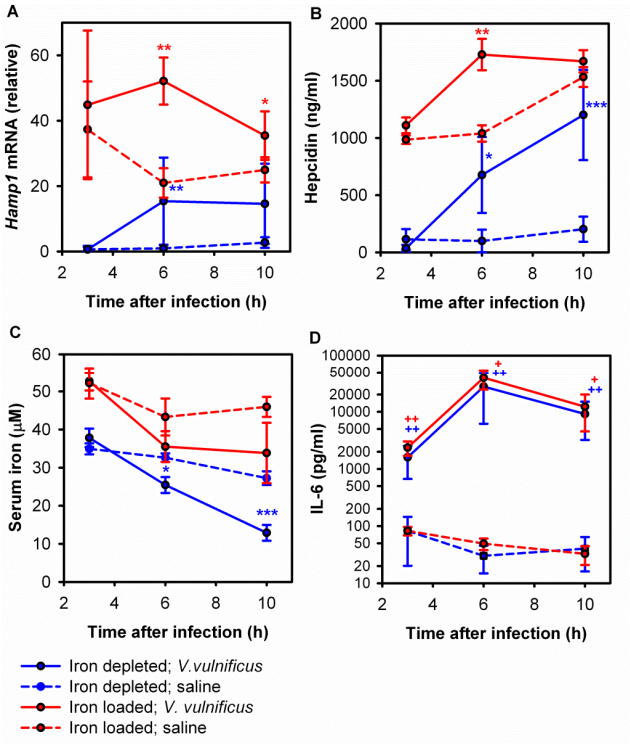

Figure 5. WT mice respond to *V. vulnificus* infection by rapidly increasing plasma hepcidin concentration. WT mice, either iron-depleted (blue) or iron-loaded (red), were injected with $1x10^5$ CFU of *V. vulnificus* (solid lines) or saline (dashed lines) and euthanized at 3, 6 or 10 hours after infection. **(A)** Hepatic *Hamp1* mRNA expression. **(B)** Serum hepcidin concentration. **(C)** Serum iron concentration. **(D)** The inflammatory response to infection was confirmed by serum IL-6 assay. Each point represents the mean ± standard deviation (n=5 per group). Statistical significance was assessed using student's *t* test if data were normally distributed (*p<0.05; **p<0.01; ***p<0.001) or Mann-Whitney *U* test if they were not ($^{+}$p<0.05; $^{++}$p<0.01).

Interestingly, at 16h after infection, no statistically significant differences in hepcidin were observed between infected and saline-treated WT mice, either at the hepatic mRNA or serum protein levels (Figure 7A and B), despite increased inflammatory markers, including hepatic *Saa1* mRNA (Figure 7C) and proinflammatory cytokines in the serum (Figure 7E). *Inhbb* (Activin B gene) mRNA, was also increased in infected iron-loaded groups (Figure 7D). These data imply that hepcidin production in the liver was rapidly increased early in the course of infection by inflammatory mediators induced by bacterial infection. Elevated hepcidin in turn caused acute hypoferremia. The hypoferremia appears to counterregulate hepcidin so that by 16 h hepcidin levels in infected WT mice were no longer different from uninfected controls.

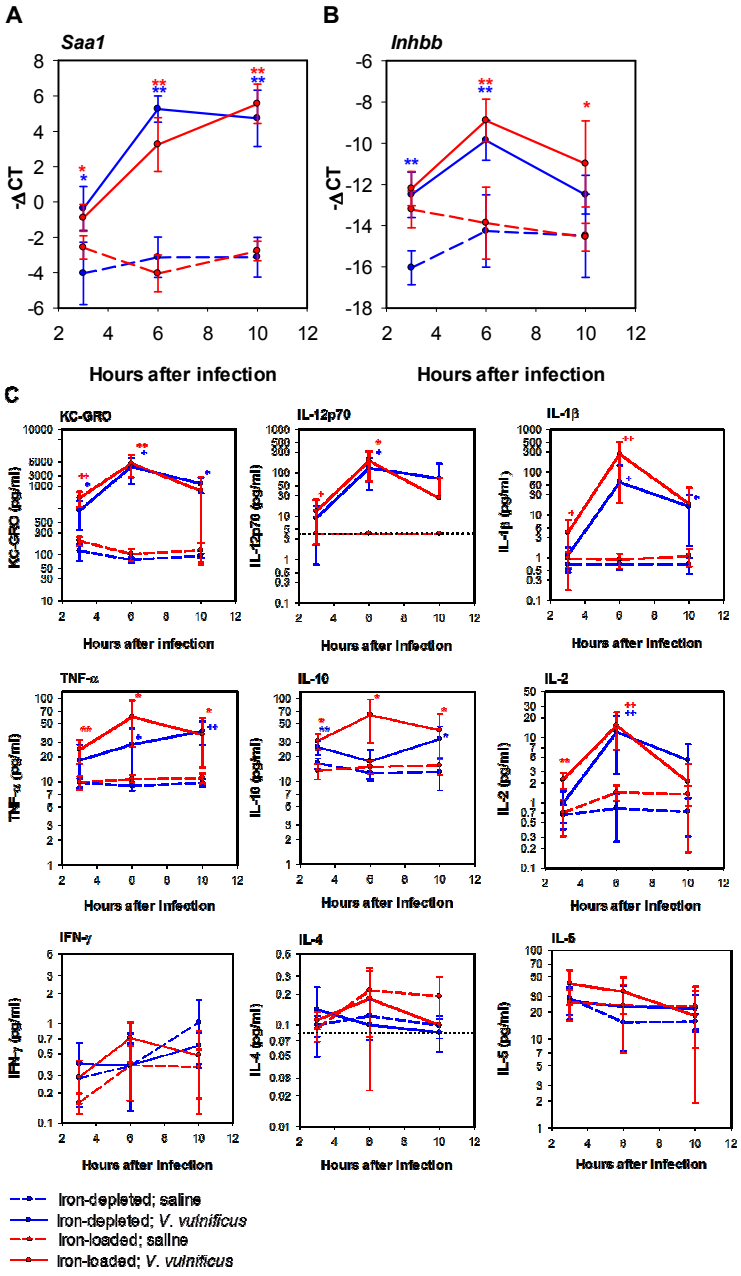

Figure 6. Inflammation is induced early during infection. qRT-PCR from liver samples was performed to analyze the mRNA expression of *Saa1* **(A)** *and Inhbb* **(B)** in iron-depleted (blue) and iron-loaded (red) WT mice, 3, 6 and 10 hours after infection with $1x10^5$ CFU of *V. vulnificus* (solid lines) or saline (dashed lines). All the infected groups increased *Saa1* and *Inhbb* mRNA starting at 3 hours after infection. No differences were observed between iron-loaded and iron-depleted mice. Gene expression results are represented as -ΔCt relative to actin mRNA. Each dot represents the mean, ± standard deviation (n=5). **(C)** A panel of 9 pro-inflammatory cytokines was analyzed in serum from iron-depleted (blue) and iron-loaded (red) WT mice, 3, 6 and 10 hours after *V. vulnificus* infection (solid lines) or saline injection (dashed), n=5 per group. Infected mice presented higher levels of KC-GRO, IL-12p70, IL-1β, TNF-α, IL-10 and IL-2, starting at 3 hours after infection. No changes were observed for IFN-γ, IL-4 and IL-5. The black dotted line represents the lower limit of detection of the assay. Statistical significance was assessed using student's *t* test if data were normally distributed (*p<0.05; **p<0.01***p<0.001) or Mann-Whitney *U* test if they were not ($^{+}$p<0.05; $^{++}$p<0.01).

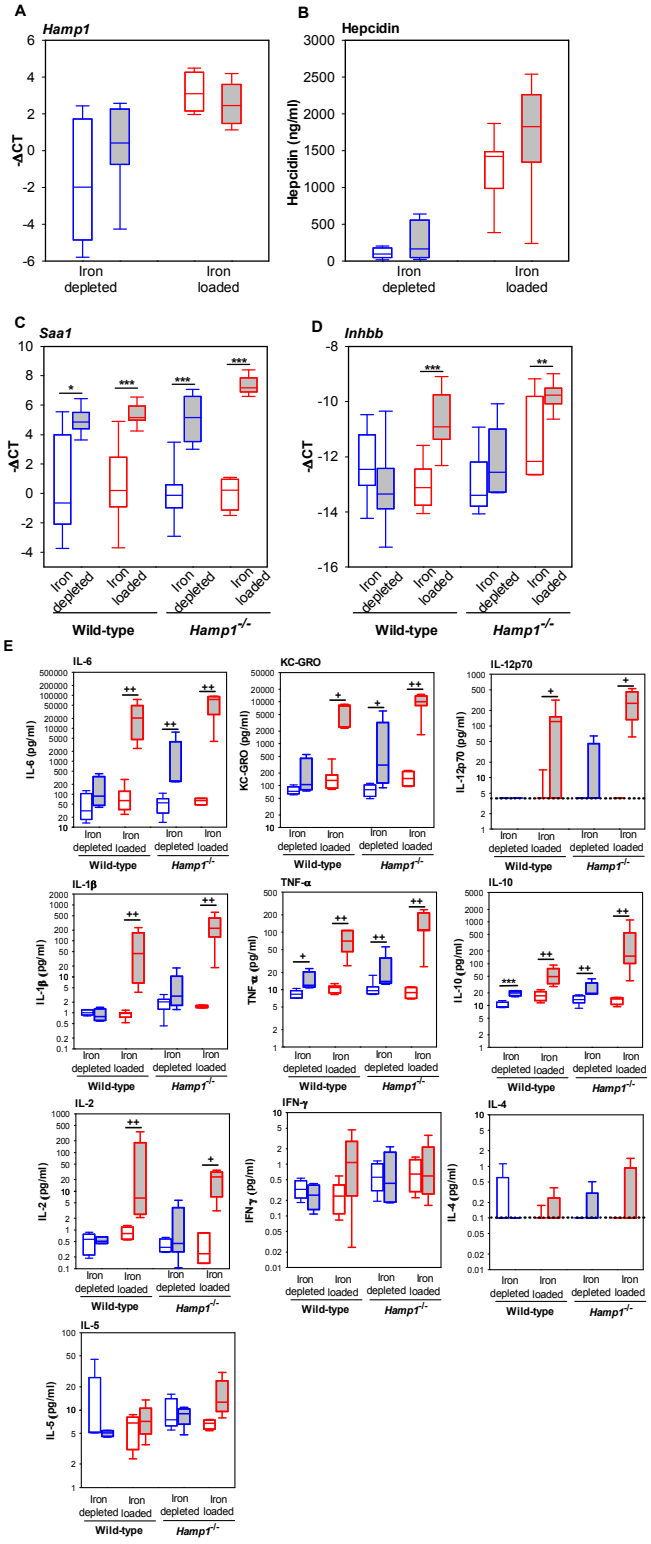

Figure 7 Liver hepcidin mRNA is no longer significantly increased at 16 h after infection, despite evidence of inflammation. Iron-depleted (blue) and iron-loaded (red) WT and *Hamp1*$^{-/-}$ mice were injected with saline (white fill) or with *V. vulnificus* (grey fill, 1x10^5 CFU for WT and 300 CFU for *Hamp1*$^{-/-}$ mice), n=6-8 per group. **(A)** Hepatic *Hamp1* mRNA. **(B)** Serum hepcidin. **(C)** Hepatic *Saa1* mRNA. **(D)** Hepatic *Inhbb* mRNA. Measurements of mRNA concentration are shown as -ΔCt relative to actin mRNA. **(E)** A panel of 10 inflammatory cytokines was analyzed in serum from iron-depleted and iron-loaded WT and *Hamp1*$^{-/-}$ mice 16 hours after *V. vulnificus* infection (grey bars) or saline injection (white bars). Infected mice presented higher levels of IL-6, KC-GRO, IL-12p70, IL-1β, TNF-α, IL-10 and IL-2. No changes were observed for IFN-γ, IL-4 and IL-5. The black dotted line represents the lower limit of detection of the assay. Statistical significance was assessed using student's *t* test if data were normally distributed (*p<0.05; **p<0.01; ***p<0.001) or Mann-Whitney *U* test if they were not ($^+$p<0.05; $^{++}$p<0.01), n=6-8 per group.

Regarding the specific aims of the work presented in this chapter, we demonstrated that: a) hepcidin-deficient mice are highly susceptible to severe *V. vulnificus* infection, while WT mice are resistant; b) serum iron and non-transferrin bound iron are critical for *V. vulnificus* replication during infections, and liver iron stores do not play a significant role during the infection; c) WT mice resist the infection by increasing hepcidin production early in the course of infection, mounting a hypoferremic response triggered by inflammatory stimuli.

Table 1. Serum and liver iron concentrations in WT mice fed an iron-poor (4 ppm Fe) or iron-rich (10000 ppm Fe) diet for 2 weeks (n=8 per group)

	Serum Fe (µM)	**Liver iron (µg/g of wet tissue)**
4 ppm diet	38 ± 9	18 ± 9
10,000 ppm diet	65 ± 4	425 ± 109
p-value	<0.001	<0.001

Means ± SD are shown. Statistical significance assessed using Student's *t* test

CHAPTER IV

Usefulness of minihepcidins to prevent and treat V. vulnificus infections

Specific aims

Based on our findings describing hepcidin-induced hypoferremia as a host defense mechanism against *V. vulnificus* infection (Chapter 3), we sought to develop a therapeutic approach for the prevention and treatment of this infection in hepcidin-deficient conditions. We used hepcidin-deficient (*Hamp1*$^{-/-}$) mice for the proof-of-principle studies, with the objective to correct the hepcidin deficiency through the administration of hepcidin agonists, therefore mimicking the protective response in wild type (WT) mice. The specific aims for this chapter are as follows:

a. test the usefulness of minihepcidins (hepcidin agonists) in the prevention and treatment of *V. vulnificus* infection in *Hamp1*$^{-/-}$ mice

b. describe the mode of action of minihepcidins in this infection (bactericidal versus bacteriostatic effect)

Minihepcidin PR73 protects against mortality from *Vibrio vulnificus* infections

To examine the importance of early hepcidin activity for resistance to *V. vulnificus* infection, we tested the therapeutic effect of minihepcidin PR73 (a synthetic hepcidin agonist, Figure 1) in *Hamp1*$^{-/-}$ mice. Minihepcidins are synthetic hepcidin agonists (7- to 9-amino acid peptides) previously described by our laboratory [161]. These peptides retain the capacity to bind and promote the degradation of ferroportin and were show to possess greater potency and longer lasting effect than full-length hepcidin [144]. Minihepcidins circumvent the various problems associated with the use bioactive hepcidin-25 as a therapeutic, namely the very short half-life [162] due to rapid renal excretion. Furthermore, the synthesis of correctly folded full-length hepcidin is expensive, therefore not ideal for large scale production. For this work, we used the minihepcidin PR73 (Figure 1), a peptide that contains unnatural amino acids to enhance its biological activity and resistance to proteolytic degradation, and also a palmitoyl group to decrease renal clearance through increased binding to albumin [163].

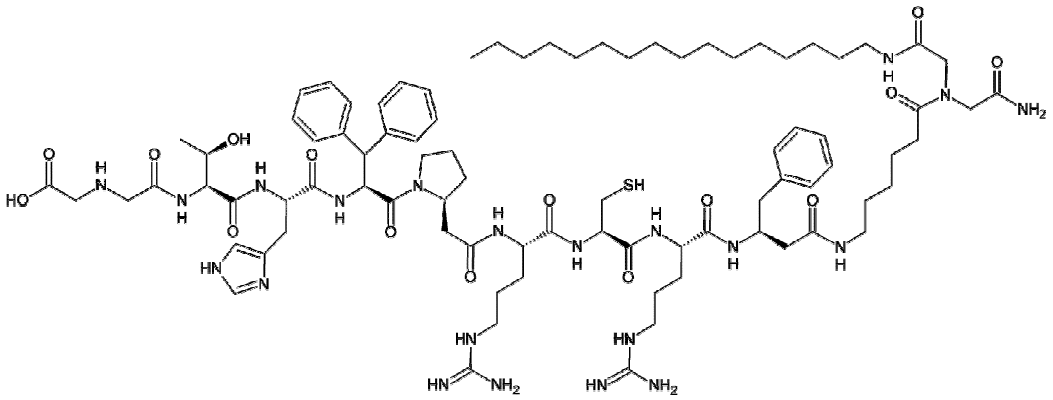

Figure 1. Molecular structure of minihepcidin PR73. From N- to C-terminus the primary sequence of PR73 was: iminodiacetic acid, L-threonine, L-histidine, L-3,3-diphenylalanine, L-β-homoproline, L-arginine, L-cysteine, L-arginine, L-β-homophenylalanine, 6-aminohexanoic acid, iminodiacetic acid palmitylamide (Ida-Thr-His-Dpa-bhPro-Arg-Cys-Arg-bhPhe-Ahx-Ida(NHPal)-CONH2).

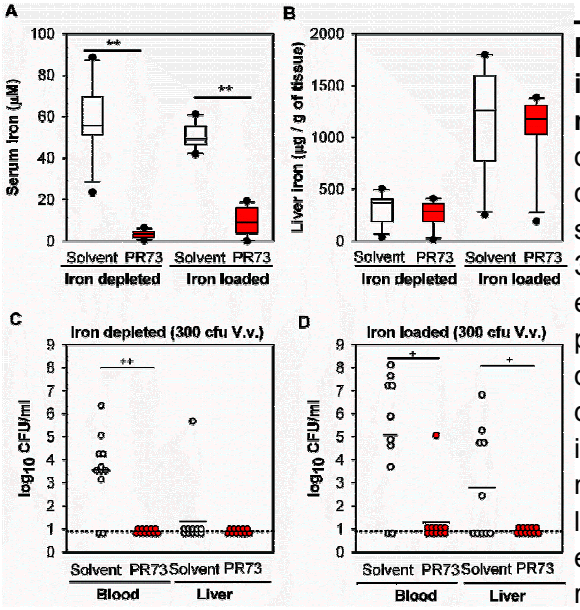

Figure 2. Minihepcidin PR73 mitigates infection by *V. vulnificus* in *Hamp1*$^{-/-}$ mice. *Hamp1*$^{-/-}$ mice (either iron-depleted or iron-loaded) were treated with 100 nmol of PR73 (red symbols) or solvent (white symbols) 24 h and 3 h before infection with 300 CFU of *V. vulnificus*. Mice were euthanized 16 h after infection (n=10-11) per group. **(A)** Serum iron was markedly decreased in PR73-injected mice, with no difference in serum iron between solvent-injected iron-depleted and iron-loaded mice. **(B)** Liver iron was higher in iron-loaded than iron-depleted mice as expected. PR73 administration did not result in significant changes in liver iron stores. **(C)** and **(D)** *V. vulnificus* was undetectable in blood and liver in PR73-treated mice, in contrast to mice treated with saline. Each dot represents one mouse; black solid lines represent the mean of CFU counts. The black dotted line represents the lower limit of detection of CFU counts (calculated as half of the minimum detectable CFU counts). Statistical significance was assessed using student's *t* test if data were normally distributed (**p<0.01) or Mann-Whitney *U* test if they were not ($^{+}$p<0.05; $^{++}$p<0.01).

To test the therapeutic effect of the minihepcidin PR73 in *V. vulnificus* infection, *Hamp1*$^{-/-}$ mice were pretreated with PR73 24h and 3h before infection and were euthanized 16h after subcutaneous (s.c.) infection with 300 CFU of *V. vulnificus*. Administration of minihepcidin caused marked hypoferremia (3 µM in iron-depleted and 9 µM in iron-loaded mice) (Figure 2A). Liver iron stores did not change likely because of the short duration of the experiment (40 h) (Figure 2B). Importantly, minihepcidin treatment resulted in decreased numbers of bacteria in blood and liver of both iron-depleted and iron-loaded mice (Figure 2C and D).

Pretreatment with PR73 also markedly improved survival: while most of the non-treated *Hamp1*$^{-/-}$ mice died within 2 days after infection with 10^3 or 10^5 CFU of *V. vulnificus*, mice treated with minihepcidin survived, regardless of their iron load and regardless of the number of bacteria administered (Figure 3 A and B). To test whether minihepcidins are effective not only for the prevention but also post-exposure treatment of *V. vulnificus* infection, we injected PR73 in iron-loaded *Hamp1*$^{-/-}$ mice 3 h after infection with 10^3 CFU of bacteria. Even delayed injection (post exposure treatment) of PR73 significantly increased the survival of these highly susceptible mice (Figure 3C).

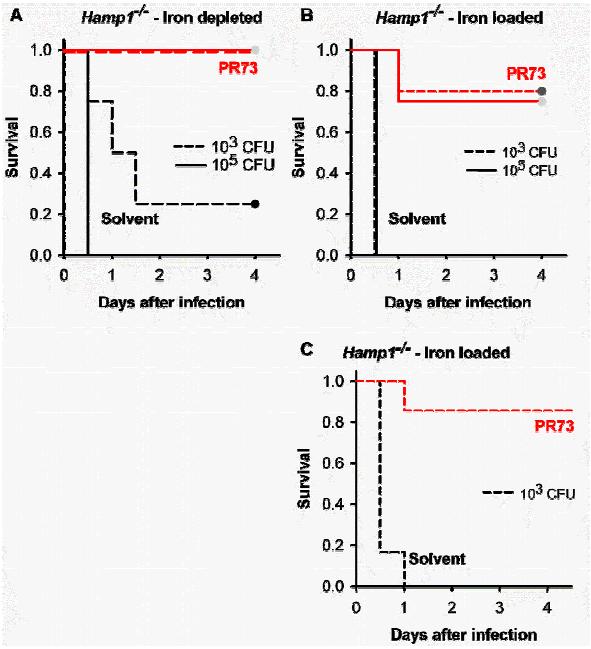

Figure 3. Minihepcidin PR73 prevents death due to *V. vulnificus* infection in *Hamp1*$^{-/-}$ mice. Kaplan-Meier survival curves of 8-10 weeks-old *Hamp1*$^{-/-}$. Both iron-depleted **(A)** and iron-loaded **(B)** *Hamp1*$^{-/-}$ mice survived the infection with 10^3 and 10^5 CFU *V. vulnificus* when treated with 100 nmol PR73 (red) before the infection. **(C)** *Hamp1*$^{-/-}$ mice were resistant to infection even if PR73 was administered 3 h after infection. Statistically significant differences in survival between solvent- and PR73-treated mice were assessed using the log-rank survival analyzes: $p<0.05$ for the iron-depleted group 10^3 CFU group; $p<0.01$ for the other groups (n=4-5 per group).

Like healthy humans, WT mice, which appropriately respond to infection by inducing endogenous hepcidin, are highly resistant to *V. vulnificus* infection. When very large inocula of *V. vulnificus* (10^6 and 10^7 CFU) were administered to WT mice, minihepcidins did not further protect them from lethal infection (Figure 4), showing that endogenous hepcidin is sufficient to protect the host.

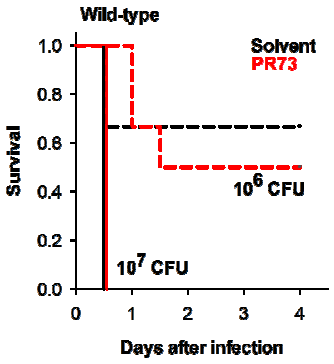

Figure 4. Minihepcidin PR73 does not further protect WT mice from death due to *V. vulnificus* infection. Kaplan-Meier survival curves for 8-10 week-old WT mice (kept on a standard diet, 270 ppm Fe), treated with minihepcidin PR73 (red lines) or solvent (black lines), 24 h and 3 h before infection with $1x10^6$ CFU (dashed lines) or $1x10^7$ CFU (solid lines) *V. vulnificus.* No statistically significant differences were found between solvent and PR73 treated mice for each bacterial inoculum (n=5-6 per group).

Minihepcidin PR73 mitigate the infection through bacteriostatic activity

Hepcidin was firstly described as an antimicrobial peptide, which possessed *in vitro* antimicrobial activity against fungi (*Candida albican, Aspergillus fumigatus, and Aspergillus niger*) and bacteria (*Escherichia coli, Staphylococcus aureus, Staphylococcus epidermidis*, and group B *Streptococcus)* [37]. Therefore, we addressed the possible bactericidal activity of hepcidin-25 and minihepcidin PR73 against *V. vulnificus* (Figure 5). We measured the CFU of *V. vulnificus* growing in LB-N broth containing various concentrations of each peptide, or protegrin (an antimicrobial peptide used as a microbicidal control). We observed an increase in bacterial CFU when low concentrations of hepcidin or minihepcidin peptide were added (0 - 2.7 μM), followed by a dose-dependent decrease in bacterial CFU at higher peptide concentrations, more prominent for PR73 than hepcidin-25. This result suggests that hepcidin and minihepcidin PR73 display bactericidal activity against *V. vulnificus* at high concentrations *in vitro*.

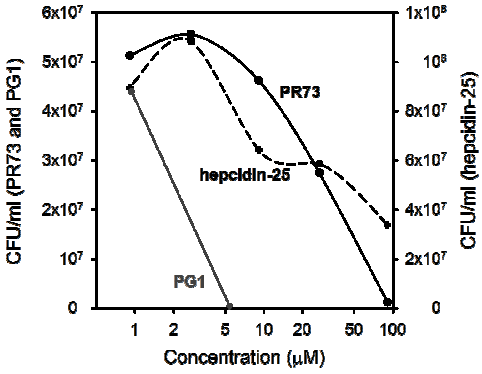

Figure 5. Minihepcidins possess bactericidal activity *in vitro.* *V. vulnificus* ($1x10^3$ CFU/ml) were grown in 12 µl of LB-N broth, supplemented with various concentrations (0, 0.9, 2.7, 9.1, 27 and 91 µM) of murine hepcidin-25 (dashed curved), minihepcidin PR73 (solid black curve), or protegrin (PG1, solid grey curve), for 3 h at 37 ^{o}C with shaking (300 rpm). At 3 h, 5 µl from each condition were collected and used for CFU quantification. At low concentrations (0 - 2.7 µM), bacterial growth was slightly improved by the addition of hepcidin-25 and PR73. At higher concentrations both 25-hepcidin and PR73 show a dose-dependent bactericidal effect, more prominent in PR73 treated samples. The antimicrobial peptide protegrin (control) killed all the bacteria at a very low concentrations. Results represent the average of 2 independent experiments.

To determine if the anti-Vibrio effect of minihepcidin during infections *in vivo* was due to iron restriction of bacterial growth or a direct bactericidal effect of the PR73 peptide, we measured the growth and killing of a *V. vulnificus* strain marked by a chloramphenicol-resistance plasmid, similarly to a published approach (Figure 6) [149]. The marker plasmid only replicates in the presence of arabinose, which is not present in significant amounts in mouse serum. Bacteria were grown *ex vivo* in sera that were obtained from *Hamp1*$^{-/-}$ mice treated with PR73 minihepcidin or with a solvent control. Iron concentrations of these sera are provided in Table 1. After incubating bacteria in the mouse sera for 2 h, CFU counts were determined on plates that allow only plasmid-containing bacteria to grow (supplemented with chloramphenicol and arabinose) or plates that allow all Vibrio bacteria to grow (no chloramphenicol/arabinose). Because the marker plasmid does not replicate in bacteria growing in serum, the reduction in CFU of plasmid-containing Vibrio reflects the killing of the inoculum. The number of total Vibrio CFU reflects both growth and killing of bacteria whereas the ratio of total to plasmid-containing bacteria (T/P) reflects growth only [149] (Figure 6).

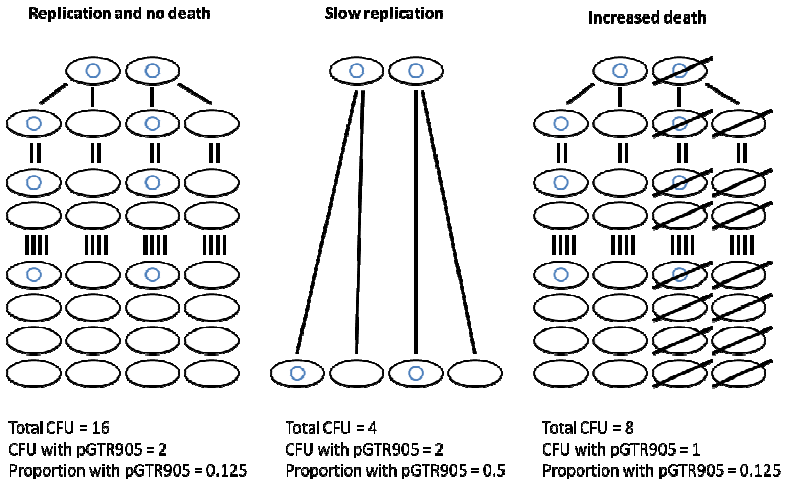

Figure 6. Use of plasmid pGTR905 to differentiate the replication rate from the death rate of *V. vulnificus* in mouse serum. The marker plasmid (blue circle) only replicates in the presence of arabinose, which is not present in significant amounts in mouse serum. **Left panel:** under standard conditions (normal replication and no death), a representative population of 2 plasmid-containing bacteria after three divisions yields 16 bacteria, 2 of which contain the plasmid (proportion of plasmid-containing bacteria = 0.125). **Central panel:** if PR73 decreases the replication rate (e.g. only one division occurs within the same time period), the total number of bacteria will be lower (4 CFU) and the proportion of plasmid-containing bacteria will be higher (0.5). **Right panel:** if PR73 increases killing without affecting the replication rate (e.g. half of the bacteria are killed), the total number of bacteria will be lower (8 CFU), but the proportion of plasmid-containing bacteria will be the same as in standard conditions (0.125). Therefore, the total number of bacteria reflects both growth and killing of bacteria whereas the ratio of total to plasmid-containing bacteria reflects growth only.

After incubation in *ex vivo* sera, total CFU were 15-20-fold lower in sera of minihepcidin-treated *Hamp1*$^{-/-}$ mice compared to the sera of solvent-treated *Hamp1*$^{-/-}$ mice (Figure 7A), regardless whether the donor mice were on low or high iron diet, mirroring the *in vivo* CFU results (Figure 2 C,D). In contrast, CFU of the plasmid-containing bacteria were merely 1.7-1.9-fold lower in minihepcidin-treated sera relative to the solvent sera (Figure 7B), demonstrating that the peptide had only a slight bactericidal effect in serum. T/P ratios (i.e. bacterial growth) were about ten-fold lower for sera from the minihepcidin-treated mice compared with the solvent controls (Table 1), indicating that minihepcidin-triggered hypoferremia significantly decreased bacterial replication. This effect of hypoferremia on *V. vulnificus* growth was also replicated using sera from noninfected WT mice that

were fed low- or high-iron diet (Figure 7 C and D). Moderately hypoferremic sera (because of low-iron diet) slowed down *V. vulnificus* growth compared to iron-rich sera (because of high-iron diet), as shown by a more than 10-fold decreased T/P ratio (Table 1), without affecting the number of plasmid-containing bacteria (Figure 7D). Thus, minihepcidin-induced hypoferremia rather than a direct antimicrobial effect of minihepcidin was responsible for slower *V. vulnificus* replication. The fact that WT mice did not present increased resistance to *V. vulnificus* when treated with minihepcidin (Figure 4) further supports the conclusion that the bactericidal effect of minihepcidins *in vivo* is likely irrelevant.

All the experiments described in this chapter successfully addressed the proposed specific aims for this chapter, as we have shown that: a) minihepcidins efficiently prevent and treat *V. vulnificus* infection in the highly susceptible *Hamp1* $^{-/-}$ mice; b) minihepcidins control infection mostly through a bacteriostatic effect promoted by iron restriction. The protective effect of hepcidin agonists in hepcidin-deficient mice strongly supports the conclusion presented in Chapter III, placing hepcidin as a critical component in the host defense against *V. vulnificus.*

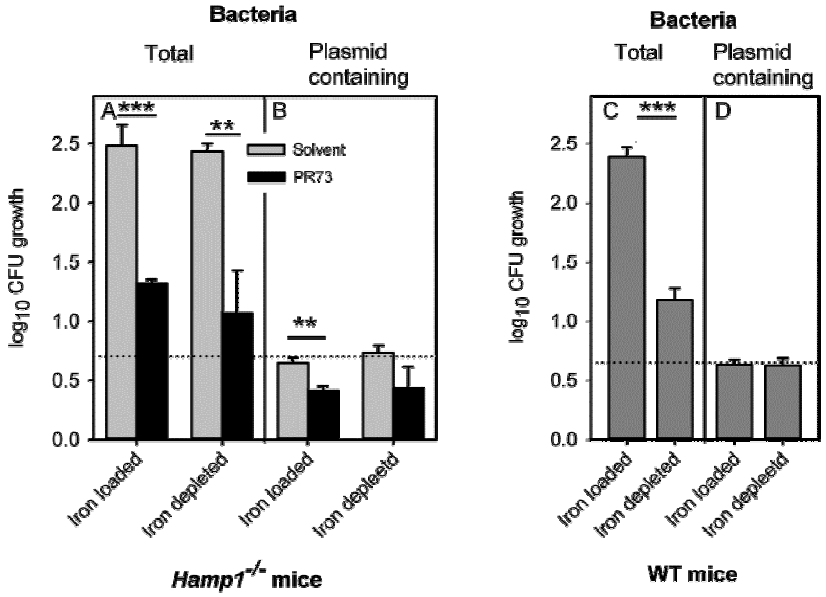

Figure 7. Minihepcidin PR73 acts in serum by slowing bacterial growth. Serum was collected from iron-depleted or iron-loaded 8-10 weeks-old *Hamp1*$^{-/-}$ mice that were injected with PR73 or solvent, and from iron-depleted or iron-loaded WT mice (not treated with PR73). Serum iron concentrations are shown in Table 1. *V. vulnificus* carrying the non-replicating marker plasmid pGTR905 were incubated in these sera *in vitro* for 2 h, and CFU were determined either on plates without chloramphenicol (**total** bacteria) or plates with chloramphenicol and arabinose (allows growth of only **plasmid-containing** bacteria). **(A)** PR73 greatly reduced total bacterial yield, which reflects the sum of bacteriostatic and bactericidal effects. **(B)** PR73 only slightly reduced the yield of plasmid-containing bacteria indicating only a small bactericidal effect. **(C)** The number of total bacteria was much higher in serum from iron-loaded WT mice than in serum from iron-depleted mice, as expected. **(D)** Different serum iron concentrations did not affect the yield of plasmid-containing bacteria indicating that hypoferremia by itself does not have a bactericidal effect. Each vertical bar represents the mean, and error bars represent standard deviation for 3 independent experiments (with 3 replicates in each experiment). The black dotted line represents the number of plasmid-containing bacteria after growth that diluted plasmid copy number to 1 plasmid per bacterium (bacteria in the original inoculum carried 5 plasmids per bacterium). Statistical significance was assessed using student's *t* test (*p<0.05; **p<0.01; ***p<0.001).

Table 1. Serum iron concentrations and bacterial growth in sera *ex vivo*

	Solvent sera		Minihepcidin sera	
	Serum iron	**Log_{10}(T/P)**	**Serum iron**	**Log_{10}(T/P)**
***Hamp1*$^{-/-}$ mice, standard diet**	66 µM	1.84±0.21	13 µM	0.90±0.02**
***Hamp1*$^{-/-}$ mice, low-iron diet**	64 µM	1.70±0.13	4 µM	0.63±0.53*

Means ± SD are shown. *p=0.028, **p=0.0017 compared to solvent sera

	High-iron diet		Low-iron diet	
	Serum iron	**Log_{10}(T/P)**	**Serum iron**	**Log_{10}(T/P)**
WT mice	64 µM	1.75±0.06	37 µM	0.56±0.15*

Means ± SD are shown. *p=0.0002 compared to high-iron sera

CHAPTER V

Molecular mechanism of iron-triggered V. vulnificus virulence

Specific aims

As described in Chapters III and IV, iron is a critical component for the development of severe infection by *V. vulnificus*. For that reason, failure to decrease serum iron during infections leads to increased bacterial virulence and, ultimately, to the death of the host. The present chapter is focused on the bacterial response to iron by addressing the following aims:

a. identify which iron species are relevant to promote rapid bacterial growth

b. address the molecular mechanism by which iron affects *V. vulnificus* virulence

NTBI is required for *V. vulnificus* growth initiation

When circulating iron exceeds the transferrin binding capacity, iron is bound to small molecules, such as citrate, acetate and albumin. This iron species are highly reactive and collectively known as NTBI. NTBI starts appearing in circulation when transferrin saturation exceeds 60%, and therefore is usually found in patients with iron overload disorders and may contribute to the increased susceptibility to bacterial infections. Since this form of iron is not sequestered by tightly binding proteins and is readily available for uptake by invading microbes, we decided to investigate the effect of NTBI on *V. vulnificus* growth. In LB-N broth, bacteria were able to grow at moderate rate even when no Ferric Ammonium Citrate (FAC, a form of NTBI) was added to the medium (Figure 1A), showing that the iron included in the broth composition is sufficient to allow bacterial replication. However, bacterial growth rate was increased as more FAC was made available. By 40 μM of FAC, bacteria reached the maximum growth rate, which remained similar up to 100 μM FAC. Interestingly, after 6h of incubation we observed a dose dependent effect of iron on bacterial survival. Bacteria survived for longer periods as more FAC was added to the broth, and reached a plateau phase when FAC concentrations were higher than 30 μM. To better understand the role of NTBI during infection, we performed the same experiment using inactivated human plasma instead of LB-N. This experimental approach resembles *in vivo* infections, as *V. vulnificus* is mainly present in the blood of infected hosts. *V. vulnificus* did not grow in human plasma without FAC supplementation, despite measurable iron concentrations (38 μM). Addition of at least 20 μM FAC was required to trigger bacterial growth (Figure 1B). Interestingly, the exponential growth phase in plasma started at the same time as in LB-N (3.5 h). The inability to grow in plasma at low FAC concentrations suggests that some factor in the plasma is blocking bacterial growth, and this hindrance is overcome by the presence of NTBI. At 6h we observed a decrease in the optical density (OD), which may imply some bacterial death. However, bacteria rapidly recovered and reached a plateau phase at 8h. These changes may reflect an adaptive response in bacterial behavior that allows for their survival when iron is abundant. As expected, when iron was made inaccessible by adding the synthetic iron chelator deferiprone, bacteria were not able to grow in either LB-N or in human plasma.

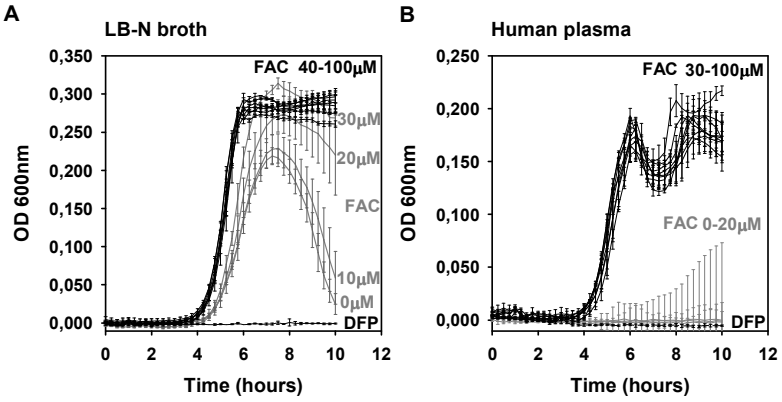

Figure 1. Iron is required for *V. vulnificus* growth in human plasma. *V. vulnificus* ($1x10^3$ CFU/ml) were grown in 250 µl of LB-N broth (**A**) or inactivated human plasma (38 µM of iron) (**B**), supplemented with various concentrations of ferric ammonium citrate (FAC, 0, 10, 20, 30, 40, 50, 60, 70, 80, 90 and 100 µM) or deferiprone (DFP, 150 µM), for 10 h at 37 ^{o}C with shaking (300 rpm). Bacterial growth was measured every 15 min by quantification of the optical density at 600 nm (OD 600nm). **A.** *V. vulnificus* growth rate and survival were enhanced as more FAC was added to LB-N broth, reaching a maximum growth rate at 40-100 µM. **B.** Bacterial growth was abolished in human plasma, unless more than 20 µM of FAC was added. Growth was prevented in both LB-N and human plasma by the addition of deferiprone. Each line represents mean (n=3) ± standard deviation.

The shift in *V. vulnificus* growing capacity in human plasma occurred in a narrow range of FAC concentrations (between 20 and 30 µM). Since the plasma was obtained from a healthy donor, whose transferrin is not fully saturated with iron, we hypothesized that bacteria start to grow when the amount of FAC added is enough to saturate transferrin, and therefore NTBI appears in the plasma. To test this hypothesis, we repeated measurements of bacterial growth in human plasma supplemented with FAC, but using plasma from 6 different donors. We estimated the total amount of iron needed for bacterial replication (baseline plasma iron + minimum amount of FAC added that allowed bacterial growth) and compared it with the total iron binding capacity of transferrin (TIBC) in each sample (Figure 2). We observed that bacteria only grew when the amount of total iron in the plasma is very close to complete transferrin saturation, strongly suggesting that NTBI is the stimulus that enables rapid *V. vulnificus* replication. This fact could also explain why bacteria is able to grow in LB-N medium even without FAC supplementation, since in this medium iron is not bound to transferrin and therefore is readily available to be taken up by the bacteria.

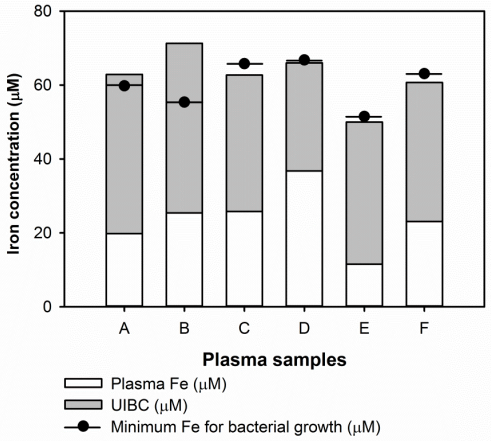

Figure 2. *V. vulnificus* growth in human plasma occurs when iron concentrations exceed the iron-binding capacity of transferrin. Plasma iron (white) and unsaturated iron binding capacity (UIBC, grey) were measured in 6 human plasma samples (A-F) to calculate the total iron binding capacity (TIBC = plasma iron + UIBC). Each plasma sample was then supplemented with increasing concentrations of FAC, and bacterial growth assessed as in Figure 1B. The minimum amount of iron needed to enable *V. vulnificus* growth was calculated as the initial plasma iron + lowest concentration of FAC that allowed bacterial growth in each sample. The minimal amount of iron required for bacterial growth was very close to the transferrin saturation point, which coincides with the presence of NTBI.

To further prove that NTBI is required for *V. vulnificus* growth initiation in human plasma, we compared the growth curves in plasma supplemented with FAC, holo-transferrin (bound to iron), apo-transferrin (not bound to iron), and a combination of FAC with each form of transferrin (Figure 3). As observed in previous experiments, *V. vulnificus* were able to grow when FAC was added to the plasma (Figure 3A). However, bacteria did not reach exponential phase when iron was added as transferrin-bound iron (Figure 3B), which implies that this bacterium at low densities is not able to scavenge iron from transferrin. When bacteria were incubated with a combination of FAC and holotransferrin (Figure 3D), they initiated rapid exponential growth already at 20 μM FAC (rather than 40 μM) suggesting that transferrin-bound iron contributes to the iron pool utilized by the bacterium. A very similar pattern was obtained when bacteria were grown in combination with FAC and apotransferrin (Figure 3E), further strengthening that hypothesis. Interestingly, ferrous ammonium sulfate (FAS) did not trigger bacterial growth, even though iron was not bound to transferrin (Figure 3F). We therefore hypothesize that only iron in the ferric (III) form, and not in the ferrous (II) form is used for bacterial growth. This fact is of importance in the context of an infection since most of the NTBI in humans is circulating as ferric (III) iron. Altogether, these

results show the importance of NTBI as a critical factor for rapid *V. vulnificus* growth leading to severe infections in iron loaded individuals.

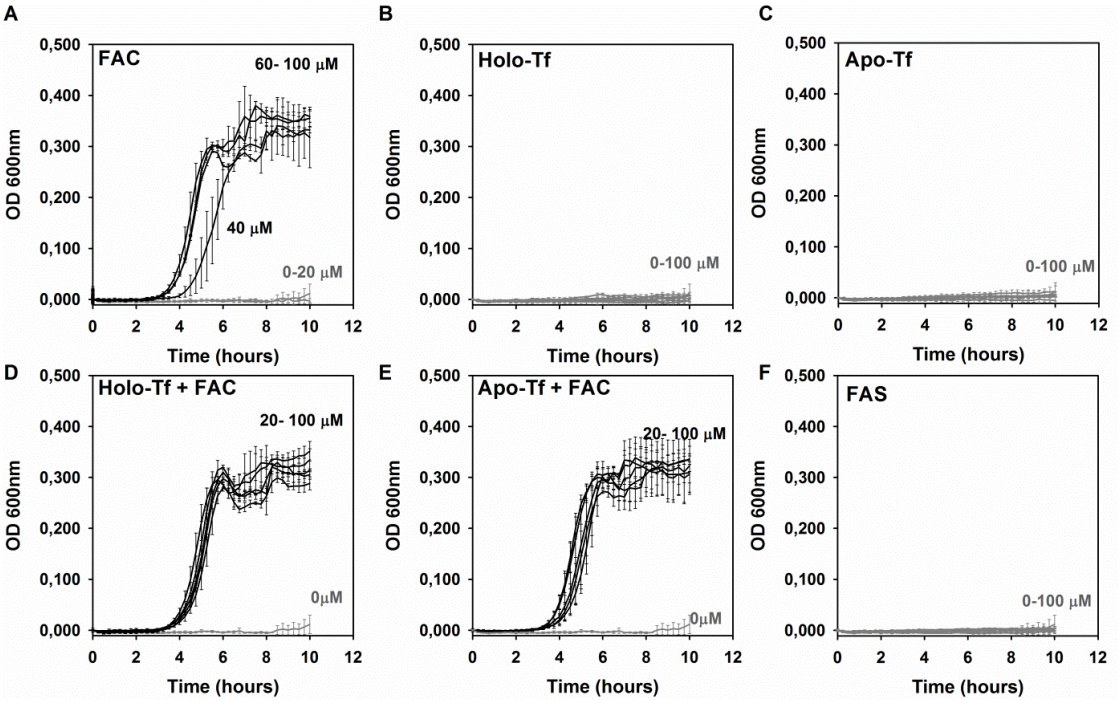

Figure 3. NTBI is required for *V. vulnificus* growth initiation. *V. vulnificus* ($1x10^3$ CFU/ml) were grown in 250 µl of inactivated human plasma (26 µM of iron), supplemented with various concentrations (0, 20, 40, 60, 80, and 100 µM) of **(A)** ferric ammonium citrate (FAC), **(B** and **D)** holo-transferrin (Holo-Tf) alone or in combination with 100 µM of FAC, **(C** and **E)**, apo-transferrin (Apo-Tf) alone or in combination with 100 µM of FAC**, (F)** and Ferrous Ammonium Sulfate (FAS), for 10 h at 37 ^{o}C with shaking (300 rpm). Bacterial growth was measured every 15 min by quantification of the optical density at 600 nm (OD 600nm). *V. vulnificus* growth only started when FAC was added to the plasma at 40-100 µM. Bacteria did not grow in plasma supplemented with Holo-Tf or Apo-Tf, unless excess FAC was added to the plasma. Unlike FAC which contains ferric iron, FAS which contains ferrous iron did not support growth of *V. vulnificus* in plasma. Each line represents mean (n=3) ± standard deviation.

The Ferric Uptake Regulator (Fur) system is dispensable for *V. vulnificus* lethality

The remarkable effect of iron on *V. vulnificus* growth and virulence led us to address the mechanism by which this bacterium uses iron as a signal to trigger its pathogenic behavior. We hypothesized that the Ferric Uptake Regulator (Fur, also known as Ferric Uptake Repressor) system might play a role in the bacterial

response to iron. Fur is a transcription factor ubiquitous in Gram-negative bacteria that uses iron as a co-repressor. It acts by repressing the transcription of genes that contain a Fur binding site, such as genes involved in iron acquisition, synthesis of siderophores, tricarboxylic acid cycle and protection against ROS damage (Figure 4A). In the absence of iron, Fur is not able to bind to DNA, thus target genes are not repressed. Emerging evidence have shown that Fur can also function as a gene activator through indirect pathways that involve small RNAs, recruitment of RNA polymerase holoenzyme, or by functioning as an antirepressor [164]. Since this is a well documented mechanism for iron-dependent genetic control we decided to investigated the ability of a *V. vulnificus* Fur-deletion mutant (ΔFur) to cause lethal infection. We hypothesized that ΔFur strain will have greatly decreased virulence compared to a WT strain. However, after infecting mice with 10^3 or a 10^5 bacteria, we observed that the ΔFur mutants were as lethal as the Fur-expressing native strain in the highly susceptible *Hamp1*$^{-/-}$ mice (Figure 4B and C). As expected, WT mice remained resistant to infection with either bacterial strain. This result strongly suggest that the Fur system is not essential for the increased virulence observed in iron-loaded hosts and prompted us to look for alternative candidates to explain that phenomenon.

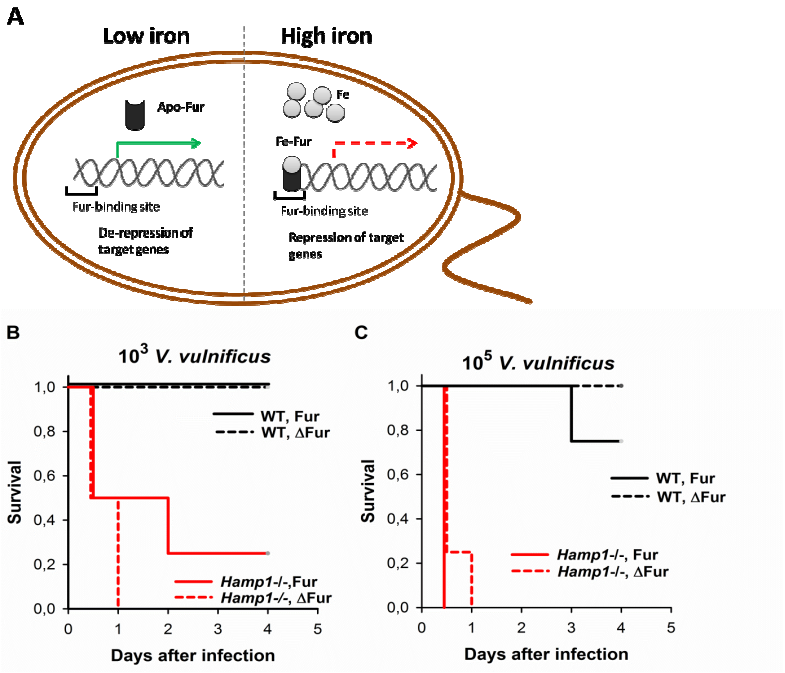

Figure 4. The Ferric Uptake Regulator (Fur) system is dispensable for *V. vulnificus* lethality. (A) Fur is a DNA binding protein that regulates the expression of iron-responsive genes. In low iron conditions, Apo-fur (Fur not bound to iron) is not able to bind to the Fur-binding site and as a consequence the transcription of target genes is not repressed. When iron is abundant, it binds to Fur allowing DNA binding and repression of target genes. (**B** and **C**) Kaplan-Meier survival curves for mice infected with native *V. vulnificus* which expresses Fur, or mutant *V. vulnificus* lacking the Fur regulator (ΔFur). WT mice (black lines) and *Hamp1*$^{-/-}$ mice (red lines) after infection with 10^3 (**B**) or 10^5 CFU (**C**) of Fur-expressing (solid lines) or Fur mutant (dashed lines) strains of *V. vulnificus* (n=8 in 10^3 CFU groups and n=4 in 10^5 CFU groups). By multifactorial Kaplan-Meier log-rank analysis, differences in survival between mice infected with the WT *V. vulnificus* and the Fur mutant were not statistically significant for either mouse genotype at either inoculum.

Iron induces changes in *V. vulnificus* transcriptome

To find molecular pathways involved in iron-induced virulence by *V. vulnificus* we performed RNA sequencing to compare the transcripts of bacteria growing in human plasma supplemented or not with FAC. Since bacteria do not replicate in non-supplemented human plasma (Figure 1B and Figure 2), we first incubated bacteria in the presence of 50 µM of FAC (Figure 5A). At the beginning of the exponential growth phase (T1), bacteria were recovered and divided in 3 groups: one group was harvested for RNA isolation (T1), and the other two groups were further incubated with 50 µM of FAC or without FAC until mid-exponential phase

(T2). This approach is expected to mimic the *in vivo* response, since bacteria either stop growing due to the hepcidin-induced hypoferremia in WT mice (reproduced in the 0 μM group), or continue to grow when NTBI remains in the plasma of *Hamp1*$^{-/-}$ mice (reproduced in the 50 μM group). FAC supplementation resulted in faster growth rate when compared to non-supplemented plasma. In non-supplemented plasma, bacteria were still able to grow, although at a much lower rate. This is probably due to the uptake of NTBI prior to the switch to 0 μM FAC. To compare the genetic changes responsible for different growth rates we recovered RNA at the earliest time point of the exponential phase (T1), and at mid-exponential phase for each group (T2). RNA sequencing analysis revealed several differentially expressed genes among the experimental groups (Figure 5B). We were particularly interested in genes differentially expressed due to the presence versus absence of iron (T2 50 μM vs T2 0 μM) and also due to the different growth phase experienced by the bacteria (T2 0 μM vs T1 and T2 50 μM vs T1). By intersecting the data corresponding to these comparisons we found 117 differentially expressed genes, included in groups II and VI (Figure 5B), and represented as a heat map on Figure 5C, and listed in Table 1 (group II) and Table 2 (group VI).

Group II represents transcripts that were modulated when NTBI was removed (T2 50 μM vs T2 0 μM) and after bacteria triggered exponential growth in the conditions of iron restriction (T2 0 μM vs T1). Only 10 transcripts were found in this analysis, including 5 transfer RNAs (tRNAs) and 4 ribosomal RNAs (rRNAs). These were decreased after iron was removed, pointing to a halt in protein synthesis. We hypothesize that the bacteria adopts a new behavior to conserve energy in response to the sudden nutrient restriction. The UDP-3-O-[3-hydroxymyristoyl] N-acetylglucosamine deacetylase transcript was also decreased in this condition. This enzyme undertakes the first committed step on lipid A biosynthesis (innermost part of the endotoxin lipopolyssacharide). This could partially explain the decrease in *V. vulnificus* virulence in animals able to develop hypoferremia after infection.

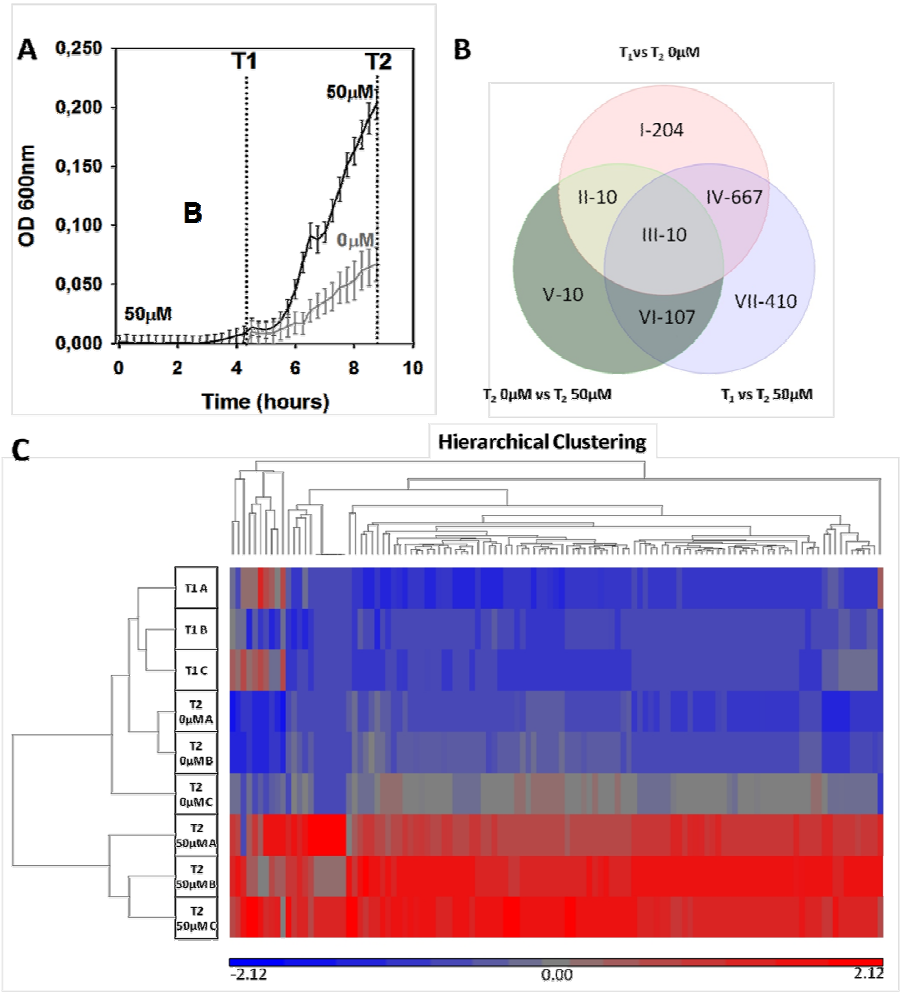

Figure 5. Iron-induced transcriptome changes during *V. vulnificus* growth. (A) *V. vulnificus* (1x10^3 CFU/ml) were incubated in 250 µl of inactivated human plasma (23 µM of iron), supplemented with 50 µM of ferric ammonium citrate, at 37 °C with shaking (300 rpm). At the beginning of the exponential phase (T1) bacteria were recovered for RNA isolation or were additionally incubated with FAC (50 µM, black) or no FAC (0 µM, grey), then harvested at mid-exponential phase (T2) for RNA isolation. Bacterial growth was measured every 15 min by quantification of the optical density at 600 nm. Each data point represents the mean ± standard deviation (n = 192 until T1 and n = 48 from T1 to T2). This experiment is representative of 3 biological replicates. **(B)** Venn diagram representative of differentially expressed genes found by RNA sequencing of the RNA samples represented in Figure 5A (3 biological replicates for each sample). Using ANOVA statistical analysis, genes were considered differentially expressed if the fold change was > 1.5 or < -1.5, and $p < 0.05$. **(C)** Heat map representing the hierarchical clustering of 117 differentially expressed genes found for groups II and VI (Figure 5B). These groups represent genes differentially expressed at different growth phases (T1 vs T2) in response to iron restriction (Group II) or iron abundance (Group VI).

Group VI represents transcripts that were differentially expressed due to the presence of NTBI (T2 50 μM vs T2 0 μM), leading to fast exponential growth (T2 50 μM vs T1). We found a list of 107 transcripts (Table 2) involved in a wide range of bacterial functions, as well as several hypothetical proteins. These functions include membrane transport and sensing (outer membrane protein U, type IV secretory pathway, small conductance mechanosensitive channel, ABC-type transporter, methyl-accepting chemotaxis protein), virulence (vieSAB three-component system, FOG repeats, HipA-like protein, putative oxetanocin A biosynthetic enzyme), stress response (dnaJ-class molecular chaperone and SOS-response transcriptional repressor LexA-like protein), transcription (DNA-binding protein H-NS, DNA-binding protein inhibitor Id-2 related protein, AraC-type DBA-binding domain-containing protein), and mithocondrial respiration (phospholipase D-family protein and Rhs family protein). All these transcripts were increased when compared to bacteria incubated without FAC and to bacteria initiating the exponential growth phase. Together with the massive increase in rRNA transcripts, these changes indicate that bacteria are undergoing an extremely active metabolic state, with dynamic membrane transport, increased protein synthesis, and increased virulence. The concerted increase of *vieS*, *vieA* and *vieB* strongly points that the vieSAB three-component regulatory system may be important for *V. vulnificus* behavior in the presence of iron. Two- and three-component regulatory systems allow bacteria to sense and rapidly respond to environmental changes, based on the stimulus triggering the response. The vieSAB system was described in *V. cholerae* as an important pathway for the production of major virulence factors, such as the cholera toxin, and also in the adaptation to the transition between the environment and the host [165, 166]. We hypothesize that a similar pathway may be responsible for the changes observed in *V. vulnificus* in response to iron, and the role of the vieSAB three-component system will be characterized in future studies.

In this chapter, we achieved our specific aim by identifying NTBI, specifically Fe (III) species, as the critical form of iron that promote rapid bacterial growth and high virulence in *V. vulnificus* (aim a). Even though we could not fully elucidate the molecular mechanism involved in this process (aim b) we excluded the iron

sensitive Fur system, while proposing alternative candidates, namely the three-component system vieSAB.

Table 1. Iron-induced transcriptome changes during *V. vulnificus* growth - Group II. This group represent genes differentially expressed at different growth phases in response to iron restriction. Transcripts were considered differentially expressed if the fold change was > 1.5 or < -1.5, and $p < 0.05$, using ANOVA statistical analysis.

	T2 50 µM vs T2 0µM		**T2 0 µM vs T1**	
Transcript	p-value	Fold change	p-value	Fold change
VV1_tRNAPhe2_tRNA	0.04777	2.98	0.02968	-3.26
VV1_tRNAPhe3_tRNA	0.04777	2.98	0.02968	-3.26
VV1_tRNAMet6_tRNA	0.00210	1.82	0.00996	-1.59
VV1_tRNAMet8_tRNA	0.00210	1.82	0.00996	-1.59
VV1_tRNAMet9_tRNA	0.00210	1.82	0.00996	-1.59
VV1_0571_UDP-3-O-[3-hydroxymyristoyl] N-acetylglucosamine deacetylase	0.00729	1.80	0.01112	-1.72
VV1_r03_rRNA	0.03410	1.71	0.00507	-2.11
VV1_r06_rRNA	0.03410	1.71	0.00507	-2.11
VV1_r09_rRNA	0.03410	1.71	0.00507	-2.11
VV1_r19_rRNA	0.03410	1.71	0.00507	-2.11

Table 2. Iron-induced transcriptome changes during *V. vulnificus* growth - Group VI. This group represent genes differentially expressed at different growth phases in response to iron abundance. Transcripts were considered differentially expressed if the fold change was > 1.5 or < -1.5, and $p < 0.05$, using ANOVA statistical analysis.

	T2 50 µM vs T2 0µM		T2 50 µM vs T1	
Transcript	**p-value**	**Fold change**	**p-value**	**Fold change**
VV1_r01_rRNA	0.00604	67.42	0.00604	67.32
VV1_r04_rRNA	0.00604	67.42	0.00604	67.32
VV1_r10_rRNA	0.00604	67.42	0.00604	67.32
VV1_r15_rRNA	0.00604	67.42	0.00604	67.32
VV1_r18_rRNA	0.00604	67.42	0.00604	67.32
VV1_r21_rRNA	0.00604	67.42	0.00604	67.32
VV1_1686_Outer membrane protein OmpU	0.00265	2.53	0.00875	1.88
VV1_3208_hypothetical protein	0.00024	2.46	0.00011	3.20
VV1_3214_hypothetical protein	0.00132	2.33	0.00145	2.28
VV1_3210_hypothetical protein	0.00026	2.29	0.00017	2.58
VV1_3215_glycosyltransferase	0.00172	2.29	0.00166	2.31
VV1_3213_hypothetical protein	0.00184	2.28	0.00191	2.26
VV1_3207_protein cII	0.00029	2.28	0.00016	2.64
VV1_3209_hypothetical protein	0.00048	2.28	0.00019	2.96
VV1_0381_hypothetical protein	0.00017	2.27	0.00038	1.94
VV1_0395_hypothetical protein	0.00041	2.23	0.00027	2.46
VV2_0746_hypothetical protein	0.00802	2.22	0.00297	3.12
VV1_0399_hypothetical protein	0.00031	2.21	0.00018	2.53
VV1_2044_hypothetical protein	0.00059	2.21	0.00018	3.10
VV1_3216_hypothetical protein	0.00119	2.21	0.00155	2.08
VV1_3212_Heparinase II/III-like protein	0.00137	2.19	0.00169	2.09
VV1_3221_hypothetical protein	0.00045	2.18	0.00014	2.99
VV1_0396_hypothetical protein	0.00031	2.17	0.00017	2.53
VV1_0394_hypothetical protein	0.00062	2.14	0.00028	2.63
VV1_2045_Predicted ATP-binding protein involved in virulence	0.00066	2.12	0.00018	3.04
VV1_0398_ATP-dependent protease HslVU, ATPase subunit	0.00045	2.12	0.00026	2.41
VV1_0393_Ribosomal protein L22	0.00034	2.12	0.00017	2.51
VV1_0392_Predicted HD superfamily hydrolase	0.00033	2.10	0.00017	2.42
VV1_3177_hypothetical protein	0.00127	2.09	0.00034	3.02
VV1_0397_DnaJ-class molecular chaperone with C-terminal Zn finger domain	0.00081	2.08	0.00046	2.37
VV1_0391_Nucleotidyltransferase/DNA polymerase involved in DNA repair	0.00033	2.04	0.00016	2.39
VV1_0389_hypothetical protein	0.00026	2.02	0.00012	2.41
VV1_0383_hypothetical protein	0.00027	2.00	0.00014	2.28
VV1_3217_hypothetical protein	0.00100	1.99	0.00278	1.68

	T2 50 µM vs T2 0µM		T2 50 µM vs T1	
Transcript	**p-value**	**Fold change**	**p-value**	**Fold change**
VV1_0387_hypothetical protein	0.00026	1.99	0.00011	2.38
VV1_0778_Glycosyltransferase	0.00138	1.98	0.00295	1.74
VV1_0386_Putative transposase	0.00027	1.97	0.00015	2.21
VV1_0380_hypothetical protein	0.00037	1.97	0.00091	1.71
VV1_2042_hypothetical protein	0.00082	1.96	0.00019	2.77
VV1_0390_SOS-response transcriptional repressor LexA -like protein	0.00061	1.95	0.00027	2.32
VV1_2041_Predicted transcriptional regulator	0.00023	1.95	0.00006	2.62
VV1_0400_hypothetical protein	0.00064	1.95	0.00031	2.26
VV1_0388_Type IIA topoisomerase, A subunit	0.00036	1.94	0.00014	2.35
VV1_0382_Predicted ATP-dependent endonuclease of the OLD family	0.00032	1.93	0.00014	2.27
VV1_0378_Predicted transcriptional regulator	0.00050	1.92	0.00023	2.23
VV1_0375_Chromosome segregation ATPase	0.00028	1.91	0.00014	2.17
VV1_3201_Response regulator VieB	0.00146	1.90	0.00037	2.59
VV1_0379_hypothetical protein	0.00044	1.90	0.00028	2.07
VV1_3202_Sensory box sensor histidine kinase/response regulator VieS	0.00120	1.90	0.00028	2.63
VV1_0377_FOG: TPR repeat	0.00041	1.88	0.00018	2.21
VV1_0376_Type IV secretory pathway, VirD2 component	0.00051	1.87	0.00022	2.19
VV1_3252_hypothetical protein	0.00046	1.86	0.00010	2.58
VV1_2046_Predicted transcriptional regulator	0.00102	1.85	0.00025	2.48
VV1_0385_Putative transposase	0.00059	1.84	0.00023	2.19
VV1_0373_Predicted phage-specific transcriptional regulator	0.00012	1.84	0.00008	1.97
VV1_2040_ATPase involved in DNA repair	0.00063	1.83	0.00014	2.48
VV1_3200_Transposase and inactivated derivatives	0.00165	1.81	0.00036	2.46
VV1_2038_Predicted transcriptional regulator	0.00027	1.78	0.00006	2.31
VV1_3178_Transposase	0.00177	1.77	0.00034	2.48
VV1_2047_HipA-like protein	0.00243	1.74	0.00055	2.30
VV1_3180_Transposase	0.00071	1.73	0.00012	2.38
VV1_2039_ATPase involved in DNA repair	0.00030	1.73	0.00005	2.35
VV1_0374_DNA-binding protein H-NS	0.00043	1.72	0.00024	1.88
VV1_3199_Transposase and inactivated derivatives	0.00169	1.72	0.00035	2.29
VV2_0665_hypothetical protein	0.00195	1.70	0.00026	2.51
VV1_3183_Predicted transcriptional regulator	0.00267	1.68	0.00068	2.12
VV1_3185_hypothetical protein	0.00406	1.66	0.00130	2.00
VV1_2902_DNA-binding protein inhibitor Id-2-related protein	0.00029	1.66	0.00017	1.78
VV1_0209_Cysteine synthase A(EC:2.5.1.47)	0.01557	1.66	0.00850	1.84
VV2_1224_Rhs family protein	0.00305	1.65	0.00082	2.03

	T2 50 µM vs T2 0µM		T2 50 µM vs T1	
Transcript	**p-value**	**Fold change**	**p-value**	**Fold change**
VV1_2048_Integrase	0.00136	1.63	0.00028	2.08
VV2_0219_hypothetical protein	0.00056	1.62	0.00006	2.38
VV1_3203_Response regulator VieA	0.00254	1.62	0.00053	2.07
VV1_1806_hypothetical protein	0.00317	1.62	0.00093	1.94
VV1_2036_hypothetical protein	0.00049	1.61	0.00011	1.97
VV1_2610_cAMP-binding proteins - catabolite gene activator and regulatory subunit of cAMP-dependent protein kinase	0.00299	1.61	0.00135	1.79
VV1_1807_AraC-type DNA-binding domain-containing protein	0.00160	1.60	0.00056	1.85
VV2_0666_hypothetical protein	0.00319	1.60	0.00036	2.34
VV1_3175_Putative oxetanocin A biosynthetic enzyme	0.00277	1.60	0.00042	2.17
VV2_0667_Integrase	0.00391	1.60	0.00051	2.27
VV1_3187_hypothetical protein	0.00363	1.59	0.00084	1.99
VV2_1692_hypothetical protein	0.00272	1.59	0.00026	2.38
VV2_0664_Cysteinyl-tRNA synthetase	0.00230	1.58	0.00025	2.29
VV1_0008_hypothetical protein	0.00090	1.58	0.00019	1.96
VV1_2037_Type I restriction enzyme EcoEI R protein	0.00072	1.58	0.00014	1.99
VV1_3190_Putative transcriptional regulator	0.00242	1.57	0.00073	1.85
VV1_3186_hypothetical protein	0.00463	1.57	0.00111	1.94
VV1_0007_Small-conductance mechanosensitive channel	0.00294	1.57	0.00065	1.95
VV1_0401_hypothetical protein	0.00104	1.56	0.00121	1.54
VV1_0372_Phage integrase	0.00089	1.55	0.00055	1.64
VV2_1569_DNA-binding HTH domain-containing protein	0.00399	1.55	0.00061	2.05
VV1_1805_Methyl-accepting chemotaxis protein	0.00183	1.54	0.00050	1.82
VV2_0676_hypothetical protein	0.00207	1.54	0.00022	2.16
VV1_2027_hypothetical protein	0.00008	1.54	0.00003	1.73
VV1_3197_Phopholipase D-family protein	0.00241	1.53	0.00041	1.95
VV2_1570_DNA-binding HTH domain-containing protein	0.00276	1.53	0.00030	2.13
VV1_3181_Transposase	0.01179	1.53	0.00198	2.03
VV1_0009_ABC-type transport system, periplasmic component	0.00157	1.53	0.00034	1.86
VV2_0669_hypothetical protein	0.00269	1.51	0.00019	2.26
VV2_0908_Molybdenum cofactor biosynthesis enzyme	0.00750	1.50	0.00088	2.07
VV2_1223_hypothetical protein	0.00599	1.50	0.00144	1.81

CHAPTER VI

Discussion

The growth of pathogens in their hosts is critically dependent on the pathogens' ability to capture and utilize iron. The hosts have evolved several countermeasures to restrict the bioavailability of iron and effectively starve the microbes, while bacteria have become more efficient in scavenging iron from the host [167]. Hepcidin-induced hypoferremia has been proposed as an important host defense mechanism by decreasing iron availability for the pathogen [167, 168]. However, support for its role has been lacking. We hypothesized that this defense mechanism is relevant in the protection against siderophilic bacteria, in which iron is crucial for the development of severe infection. In this study, we demonstrate that hepcidin-induced acute hypoferremia is an important host defense mechanism against the siderophilic bacterial pathogen *V. vulnificus*. We also explore the use of hepcidin agonists to treat susceptible mice, and the mechanism by which this bacterium uses iron to enhance its growth and virulence.

NTBI: a molecular trigger of *V. vulnificus* virulence

As a crucial factor in essential metabolic processes, iron is an essential nutrient for most living creatures, including pathogens. A group of bacteria, designated siderophilic, have developed mechanisms to use iron to increase their growth and virulence, thus making iron an essential element for disease progression [169]. An example is *V. vulnificus*, a deadly pathogen in patients with iron overload disorders such as hereditary hemochromatosis, but also in patients with immunodeficiencies or chronic liver or renal disease. The development of therapies targeting the bacteria requires the understanding of how *V. vulnificus* senses and uses the iron stimulus to trigger their virulence. Despite the evident link between the iron uptake and virulence of *V. vulnificus*, the molecular mechanism by which excess iron reprograms *V. vulnificus* for very rapid growth is still elusive. We speculate that high iron concentrations, or possibly the related presence of one or more non-transferrin bound iron (NTBI) forms in the environment of *V. vulnificus,* activate a genetic program for very rapid growth, leading to septicemia, evidence of septic shock at necropsy and early mortality. We observed that not all forms of iron were able to promote *V. vulnificus* growth in human plasma, as bacteria did not grow when supplemented with Holo-Tf, but grew very efficiently when moderate to high

concentrations of NTBI (in the form of FAC) were added. At low FAC concentrations, iron may be taken up by transferrin in plasma, which is approximately 30% saturated in healthy individuals [25]. If enough FAC is added to exceed the iron-binding capacity of transferrin, iron circulates as NTBI. In some of the plasma samples used for growth experiments, *V. vulnificus* started growing even if transferrin was not fully saturated, which may be explained by the fact that in various conditions NTBI appears in blood even when transferrin is not fully saturated [170, 171]. Additionally, this could explain why not only people with iron overload disorders develop disease. NTBI has been reported in patients with diabetes [172, 173], renal disease [174, 175], and liver disease [25], all conditions that lead to an increased susceptibility to *V. vulnificus* infections. The hypothesis of NTBI as the stimulus for *V. vulnificus* virulence has been previously explored by Kim *et al* [140]. The authors analyzed bacterial growth in cirrhotic ascites and observed that bacteria required NTBI for growth initiation and subsequent siderophore synthesis. This conclusion is strengthened by our results using human plasma, which likely represents the milieu of bacterial replication during human infection. The production of siderophores is a metabolically expensive mechanism for bacteria, but beneficial for the population since siderophores can be taken up by bacteria in the vicinity [176]. Therefore, we can speculate that bacteria only invest energy in siderophore production in iron-replete condition that allow for bacterial replication, in a mechanism controlled by iron and quorum sensing. Additionally, we observed that *V. vulnificus* specifically requires iron as Fe (III), which constitutes the main form of iron circulating as NTBI [177], mainly bound to citrate, acetate, or albumin [171, 178]. This suggests the presence of an iron transporter that specifically transports Fe (III), although such protein has never been reported.

Iron induces changes in *V. vulnificus* transcriptome

The control of iron homeostasis in prokaryotes is controlled by the transcriptional regulator Fur (Ferric uptake regulator) [138]. This protein was first described in *E. coli* [179] and later found to be conserved among Gram-negative and Gram-positive bacteria [180], including *V. vulnificus* [181]. Fur acts as a transcriptional

repressor that uses iron as a co-repressor, and regulates the transcription of genes involved in iron metabolism and/or virulence. We addressed the role of Fur in the development of *V. vulnificus* infection by comparing the lethality of a Fur-deletion mutant (ΔFur) to the WT strain and observed no differences in mouse survival, arguing against a significant role of this system in the context of human or animal infection. Therefore, we used RNA sequencing to look for alternative candidate pathways that could explain the virulence program initiated by *V. vulnificus* in the presence of iron. Previous studies have analyzed the transcriptome of *V. vulnificus* during infections by comparing clinical vs environmental strains [182], or clinical strains exposed to seawater vs human serum [183]. These approaches are not suitable to fully answer our question, as they analyze different bacterial strains (and therefore look for intrinsic differences between strains) or differences relative to the environment independently of the iron levels. Therefore, we decided to develop a different approach, in which we mimicked the conditions experienced by the bacteria during infections. According to our data in animal models of *V. vulnificus*, bacteria encounter iron in the blood, where iron concentration is either decreased through an hypoferremic response in WT mice or is maintained at a high level in hepcidin-deficient animals. We started the analysis by incubating *V. vulnificus* in human serum containing iron (as FAC) to allow bacterial growth and at the beginning of exponential growth we either removed iron or re-incubated bacteria with iron. Comparison of the transcriptome in the beginning of log phase with mid-log phase (with or without iron) allows us to look for genetic changes that lead to differential bacterial growth in response to iron. We found 117 differentially expressed genes of interest involved in several metabolic pathways such as membrane transport and sensing, virulence, stress response, transcription, and mitochondrial respiration, as well as several transcripts corresponding to hypothetical proteins. This indicates that bacteria exposed to iron may adopt a "virulence program", characterized by an extremely active metabolic state, enhanced membrane transport and virulence. By examining the expression of genes that are involved in common signaling pathways, we found a concerted increase in *vieS*, *vieA* and *vieB*, components of the vieSAB system. This is a three-component system found in *V. cholerae* responsible for the production of virulence factors and involved in the transition between the environment and the host [165, 166]. This system acts as a stimulus-

response coupling mechanism that allow bacteria to sense and respond to changes in the environmental conditions. Based on our findings we can speculate that NTBI could be the stimulus that triggers this response. Even though the relevance of the genetic targets found in our analysis is not yet validated, our results clearly demonstrates that iron has a significant impact in *V. vulnificus* virulence during infections, and therefore removal of iron is critical for host defense.

Hypoferremia and host protection

The critical role of iron in the severity of *V. vulnificus* infection suggests that iron levels in the host are highly relevant for the outcome of infection. In fact, Starks *et al* have previously reported that WT mice injected i.p. with iron dextran required a 10^5-fold lower inoculum to develop systemic disease when compared with non-iron dextran-treated mice [152]. Although this is a useful model to study *V. vulnificus* infection, it does not represent the development of the disease in humans, who develop iron overload as a result of faulty iron homeostasis and consequently increased dietary absorption. Therefore, in this study we used two animal models of iron overload obtained through dietary (10000 ppm Fe diet) or genetic (*Hamp1*$^{-/-}$ *)* manipulation, as well as iron-depleted animals (4 ppm Fe diet). In our mouse models, the order of susceptibility to rapid mortality from *V. vulnificus* was *Hamp1*$^{-/-}$ iron-loaded > *Hamp1*$^{-/-}$ iron-depleted > WT iron-loaded > WT iron-depleted. This together with studies of the effect of serum iron on *V. vulnificus* growth *ex vivo* indicated that plasma iron concentrations during the course of infection determined the growth of *V. vulnificus* and host mortality. *Hamp1*$^{-/-}$ mice were more susceptible to lethal infection, even when they had the same baseline serum iron and lower liver iron stores than iron loaded WT mice. However, serum iron 16 h after infection was acutely decreased in WT mice, while *Hamp1*$^{-/-}$ were not able to mount the same response. This suggests that acute hypoferremia after infection is a major iron-related determinant of resistance to *V. vulnificus*. This hypoferremic response is essential to remove NTBI from circulation, and therefore prevent the initiation of rapid bacterial growth followed by sepsis.

WT mice developed hypoferremia within hours after infection with *V. vulnificus*, and this response was dependent on early induction of hepcidin, preceded by a rise in inflammatory cytokines such as IL-6 and activin B. IL-6 acts as an inflammatory signal that triggers hepcidin expression in the liver through the JAK/STAT3 pathway [66, 184, 185]. Activin B, through SMAD1/5/8 signaling [67], is also a stimulus for hepcidin production in response to inflammation. We found that expression of *Inhbb,* encoding the activin β_B-subunit, is increased prior to the hepcidin response, suggesting that the two pathways may cooperate in the induction of hepcidin during infection. A recent study proposed that hepcidin-independent hypoferremia may take place during inflammation, as ferroportin expression is decreased through TLR-2 and TLR-6 signaling [155]. Although we cannot exclude that this mechanism is effective in our model, the very small decrease in serum iron concentrations after infection and the rapid death of *Hamp1*$^{-/-}$ mice argues against its physiological relevance in *V. vulnificus* infections.

Minihepcidins are an effective treatment against *V. vulnificus*

To further examine if hepcidin-induced hypoferremia is an effective component in the innate immune response against *V. vulnificus*, we analyzed the therapeutic effects of minihepcidins in *Hamp1*$^{-/-}$ mice. Minihepcidins are synthetic hepcidin agonists previously shown to bind ferroportin and induce its endocytosis and proteolysis, thus preventing iron overload in hepcidin-deficient mice [144, 145]. In the current study, the short-term minihepcidin treatment robustly decreased serum iron without altering liver iron stores. Both pretreatment with minihepcidin and administration 3 h after the infection protected the highly susceptible *Hamp1*$^{-/-}$ mice from dying after infection, even with a large inoculum of *V. vulnificus*. Minihepcidin-treated mice had much lower concentrations of bacterial CFU in the blood and liver, presumably because of a lower bacterial growth rate due to decreased plasma iron. WT mice with their intact endogenous hepcidin response to infection were not further protected by minihepcidins injections. This limitation is not clinically important because healthy humans do not develop severe *V. vulnificus* infections. Another study [186] showed that treatment with tilapia hepcidin TH(2-3) did increase survival rate in Balb/C mice infected with *V.*

vulnificus, and that TH(2-3) had both antimicrobial and immunomodulatory effects. However, effects on iron metabolism were not investigated and it is not known if TH(2-3) interacts with murine ferroportin.

Since hepcidin and its fragments have microbicidal effects *in vitro* [37], we tested if the minihepcidin had a bactericidal effect on *V. vulnificus*. First, we analyzed the bactericidal effect of native hepcidin and minihepcidins in LB-N broth and observed a decrease in bacterial numbers as the concentrations of peptides was increased. However, as in the study describing the microbicidal effects of hepcidin [37], these were only observed when the peptides were added to very high concentrations, not possible to reach under physiological conditions. To approach this question in a way that resembles infection in mice, we used a *V. vulnificus* strain containing a marker plasmid, pGTR905, that functions as a replicon only in the presence of arabinose (a sugar not found in relevant concentrations in animal tissues). We demonstrated that the minihepcidin-containing serum had only a slight bactericidal effect that was not sufficient to explain the dramatically lower number of total bacterial CFU. Rather, the slower growth of bacteria in sera from minihepcidin-treated mice was caused by the low iron concentrations in those sera. The dependence of *V. vulnificus* growth in *ex vivo* sera on the serum iron concentrations was confirmed in WT mice where serum iron was manipulated not by the administration of minihepcidin but by changing the dietary iron content. The composition of sera is also not favorable for the direct microbicidal activity of hepcidin which is dependent on acidic pH that is not physiologic in serum [187].

Immune response to *V. vulnificus* infection

We cannot exclude the possibility that immunological differences exist between *Hamp1*$^{-/-}$ and WT mice, even when *Hamp1*$^{-/-}$ mice are kept on a low iron diet. Hepcidin deficiency results in altered tissue iron distribution and iron-depleted macrophages, and this could potentially affect innate immune signaling [188, 189]. Also, NTBI has been proposed as a modifier in the generation of T lymphocyte subsets, which can also influence the immune response [190]. In this study we focused on the events that happen during the first 12-16 hours, during which susceptible mice die. This early response suggests that leukocyte subsets do not play a significant role, and neutrophils are rapidly recruited but overmatched by

bacteria as we observed in the liver of infected mice. We measured a panel of 10 pro-inflammatory-cytokines in infected WT and *Hamp1*$^{-/-}$ (either iron-depleted or iron-loaded) and we found no significant differences in the levels of circulating cytokines between the genotypes, suggesting that the immune response is not significantly altered in *Hamp1*$^{-/-}$ mice. Besides, the ability of minihepcidins to rapidly alleviate the mortality of *Hamp1*$^{-/-}$ mice from *V. vulnificus* infection would argue that any immunological differences between *Hamp1*$^{-/-}$ and WT mice are minor or acutely reversible by hepcidin or its analogs. We can therefore speculate that, even though *Hamp1*$^{-/-}$ mice present a functional immune response, the host cannot cope with the extremely rapid bacterial growth when iron is abundant and therefore is not able to clear the infection before sepsis develops. This may partially explain why patients with hereditary hemochromatosis are more susceptible to pathogens that thrive in the presence of iron but not to infections by other pathogens. We therefore conclude that the deficiency of the hormone hepcidin constitutes a new form of innate immune deficit.

Considerations on the proposed mechanism in human patients

Human hereditary hemochromatosis (HH) is described as risk factor for lethal infection with *V. vulnificus.* This infection is, however, extremely rare in spite of the very high frequency of the disease, suggesting that not all patients exhibit the same susceptibility. It is well known that the severity of hepcidin deficiency and iron overload in HH is highly variable. Rare forms of HH with absolute hepcidin deficiency are clinically very severe, but the most common form caused by the pC282Y HFE mutation [191] is extremely heterogeneous, varying from a simple biochemical abnormality to very severe forms of chronic liver disease. This variability can be attributable to both genetic modifiers (e.g. gender and the GNPAT gene [72]) and environmental factors (e.g. alcohol intake) [192]. Therefore, patients with mild or intermediate phenotypes will likely not be at increased risk of siderophilic infections. Indeed, studies in HFE knockout mice showed appropriate decrease in serum iron in response to LPS [193]. Only when a second hemochromatosis gene TfR2 is ablated is the hypoferremic response to LPS lost [193]. It is plausible to assume that, like the HFE mouse model, in the

absence of additional genetic or comorbid factors, most patients with HFE mutations may appropriately respond to infections by increasing hepcidin and developing hypoferremia. In contrast, the loss of hepcidin in *Hamp1*$^{-/-}$ mice generates a particularly severe form of the disease and it nearly completely ablates the hypoferremia of infection. We hypothesize HH patients with very low baseline hepcidin and impaired hepcidin response to infection, either because of the pattern of causative mutations and/or the presence of comorbid factors, will be the ones with increased susceptibility to infections with siderophilic bacteria.

Future perspectives and concluding remarks

After being discovered and described as a component of the innate immunity through its bactericidal activity, the position of hepcidin in homeostasis has shifted to a central role in the orchestration of mammalian iron metabolism. Although recent developments in iron research unveiled additional molecular mediators of iron homeostasis, most of these directly or indirectly converge on hepcidin. The importance of this peptide hormone in iron metabolism is also supported by the pathogenic role of hepcidin deficiency in iron overload diseases (hereditary hemochromatosis and thalassemia) and hepcidin excess in some forms of anemia. The discovery that hepcidin expression was enhanced by inflammation revealed a potential involvement in the immune response. In this study we demonstrate that hepcidin has come full circle as a component of the innate immunity, although not as antimicrobial peptide but rather as a means for the host to keep iron out of the pathogen's reach (Figure 1).

Hepcidin plays an important role in host defense against siderophilic bacteria such as *V. vulnificus* by controlling baseline plasma iron concentrations (specifically NTBI) and mediating hypoferremia in response to infection. These effects prevent the rapid growth of *V. vulnificus* so that other innate immune mechanisms are sufficient to control the infection. However, we still do not know how relevant this mechanism is in the context of other infections. Experiments using additional siderophilic as well as non-siderophilic bacteria are currently being undertaken to address this issue.

Pointing to potential therapeutic applications, pre- or post-infection administration of hepcidin agonists to hepcidin-deficient mice increased their resistance to *V. vulnificus* infection and protected them from consequent mortality. *Hamp1*$^{-/-}$ mice were efficiently rescued through an acute treatment with 3 doses of minihepcidins (3, 24 and 48h after infection). This effective short-term treatment is clinically relevant, as it decreases the chances of side effects that could arise from long-term administrations, such as anemia or increased susceptibility to infections by intracellular pathogens, as iron is retained in macrophages. By fighting the bacteria in two fronts: directly killing the pathogens (using antibiotics) while preventing their rapid growth (using hepcidin agonists), we hope that minihepcidins may prove to be useful as a coadjuvant therapy in the treatment of such a deadly disease. Nevertheless, its application in human patients still requires a series of experiments beyond our mouse models before we can safely guarantee that this treatment fulfills its potential.

Although this thesis elucidates some aspects regarding the relevance of iron for *V. vulnificus* to cause severe infection in susceptible patients, the exact mechanism involved in that process is still not understood. We propose some candidate genes and pathways that require further validation and functional testing. We believe that the discovery of this mechanism may be important not only for *V. vulnificus* infection but may also be shared with other siderophilic pathogens and therefore become a molecular target in this type of infections.

In summary, this thesis for the first time demonstrates the critical role of hepcidin in innate immunity, and represents a significant advance in clarification of the molecular pathobiology of host resistance to *V. vulnificus*, in which hepcidin was shown to play a key role, as well as in the perspective of developing novel therapies to treat this infection (through minihepcidins) and pointing the way for bacteria-targeted approaches to prevent the development of lethal infection.

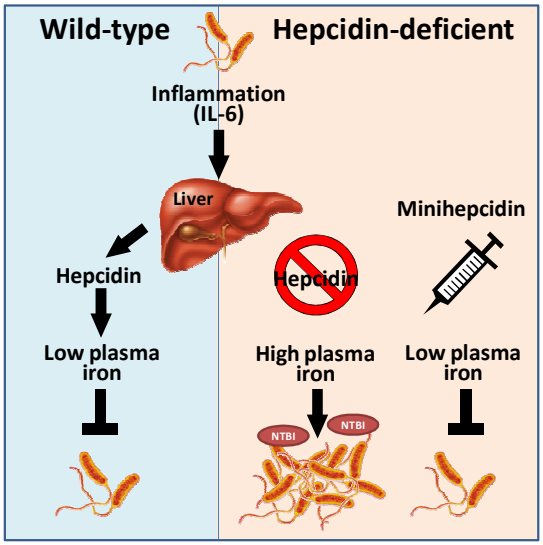

Figure 1. Hepcidin-induced hypoferremia restricts pathogen growth. The multiplication of pathogenic microbes is dependent on an adequate supply of bioavailable iron. In response to infection, the host releases cytokines, such as IL-6, which stimulate hepcidin production in the liver: Early in infection, increased hepcidin lowers plasma iron, restricting its availability to invading V. vulnificus, slowing its growth and decreasing its pathogenic effects. *Hamp1*$^{-/-}$ mice lack hepcidin, leading to high plasma iron concentration and appearance of NTBI that persists even during infection with *V. vulnificus*, causing rapid multiplication of the pathogen and fulminant disease. Treatment of *Hamp1*$^{-/-}$ mice with minihepcidin induces acute hypoferremia, slowing pathogen growth and allowing the host to control the infection.

REFERENCES

1. Geissler, C. and M. Singh, 2011, *Iron, Meat and Health.* Nutrients. **3**(3): p. 283-316.
2. Papanikolaou, G. and K. Pantopoulos, 2005, *Iron metabolism and toxicity.* Toxicology and Applied Pharmacology. **202**(2): p. 199-211.
3. Green, R., R. Charlton, H. Seftel, T. Bothwell, F. Mayet, B. Adams, C. Finch, and M. Layrisse, 1968, *Body Iron Excretion in Man - a Collaborative Study.* American Journal of Medicine. **45**(3): p. 336-&.
4. Ganz, T., 2012, *Macrophages and Systemic Iron Homeostasis.* Journal of Innate Immunity. **4**(5-6): p. 446-453.
5. Graham, R.M., A.C.G. Chua, C.E. Herbison, J.K. Olynyk, and D. Trinder, 2007, *Liver iron transport.* World Journal of Gastroenterology. **13**(35): p. 4725-4736.
6. McKie, A.T., D. Barrow, G.O. Latunde-Dada, A. Rolfs, G. Sager, E. Mudaly, M. Mudaly, C. Richardson, et al., 2001, *An iron-regulated ferric reductase associated with the absorption of dietary iron.* Science. **291**(5509): p. 1755-9.
7. Gunshin, H., C.N. Starr, C. Direnzo, M.D. Fleming, J. Jin, E.L. Greer, V.M. Sellers, S.M. Galica, et al., 2005, *Cybrd1 (duodenal cytochrome b) is not necessary for dietary iron absorption in mice.* Blood. **106**(8): p. 2879-83.
8. Choi, J., P. Masaratana, G.O. Latunde-Dada, M. Arno, R.J. Simpson, and A.T. McKie, 2012, *Duodenal reductase activity and spleen iron stores are reduced and erythropoiesis is abnormal in Dcytb knockout mice exposed to hypoxic conditions.* J Nutr. **142**(11): p. 1929-34.
9. Gunshin, H., B. Mackenzie, U.V. Berger, Y. Gunshin, M.F. Romero, W.F. Boron, S. Nussberger, J.L. Gollan, et al., 1997, *Cloning and characterization of a mammalian proton-coupled metal-ion transporter.* Nature. **388**(6641): p. 482-8.
10. Gunshin, H., Y. Fujiwara, A.O. Custodio, C. Direnzo, S. Robine, and N.C. Andrews, 2005, *Slc11a2 is required for intestinal iron absorption and erythropoiesis but dispensable in placenta and liver.* J Clin Invest. **115**(5): p. 1258-66.
11. Donovan, A., A. Brownlie, Y. Zhou, J. Shepard, S.J. Pratt, J. Moynihan, B.H. Paw, A. Drejer, et al., 2000, *Positional cloning of zebrafish ferroportin1 identifies a conserved vertebrate iron exporter.* Nature. **403**(6771): p. 776-81.
12. McKie, A.T., P. Marciani, A. Rolfs, K. Brennan, K. Wehr, D. Barrow, S. Miret, A. Bomford, et al., 2000, *A novel duodenal iron-regulated transporter, IREG1, implicated in the basolateral transfer of iron to the circulation.* Mol Cell. **5**(2): p. 299-309.
13. Vulpe, C.D., Y.M. Kuo, T.L. Murphy, L. Cowley, C. Askwith, N. Libina, J. Gitschier, and G.J. Anderson, 1999, *Hephaestin, a ceruloplasmin homologue implicated in intestinal iron transport, is defective in the sla mouse.* Nat Genet. **21**(2): p. 195-9.
14. Schade, A.L. and L. Caroline, 1946, *An iron-binding component in human blood plasma.* Science. **104**(2702): p. 340.
15. Dautry-Varsat, A., A. Ciechanover, and H.F. Lodish, 1983, *pH and the recycling of transferrin during receptor-mediated endocytosis.* Proc Natl Acad Sci U S A. **80**(8): p. 2258-62.
16. Harding, C., J. Heuser, and P. Stahl, 1983, *Receptor-mediated endocytosis of transferrin and recycling of the transferrin receptor in rat reticulocytes.* J Cell Biol. **97**(2): p. 329-39.
17. Ohgami, R.S., D.R. Campagna, E.L. Greer, B. Antiochos, A. McDonald, J. Chen, J.J. Sharp, Y. Fujiwara, et al., 2005, *Identification of a ferrireductase required for efficient transferrin-dependent iron uptake in erythroid cells.* Nat Genet. **37**(11): p. 1264-9.
18. Fleming, M.D., M.A. Romano, M.A. Su, L.M. Garrick, M.D. Garrick, and N.C. Andrews, 1998, *Nramp2 is mutated in the anemic Belgrade (b) rat: evidence of a role for Nramp2 in endosomal iron transport.* Proc Natl Acad Sci U S A. **95**(3): p. 1148-53.
19. Jacobs, A., 1976, *An intracellular transit iron pool.* Ciba Found Symp. (51): p. 91-106.
20. Kakhlon, O. and Z.I. Cabantchik, 2002, *The labile iron pool: characterization, measurement, and participation in cellular processes(1).* Free Radic Biol Med. **33**(8): p. 1037-46.

21. Arosio, P. and S. Levi, 2010, *Cytosolic and mitochondrial ferritins in the regulation of cellular iron homeostasis and oxidative damage.* Biochim Biophys Acta. **1800**(8): p. 783-92.
22. Shi, H.F., K.Z. Bencze, T.L. Stemmler, and C.C. Philpott, 2008, *A cytosolic iron chaperone that delivers iron to ferritin.* Science. **320**(5880): p. 1207-1210.
23. Cook, J.D., C.H. Flowers, and B.S. Skikne, 2003, *The quantitative assessment of body iron.* Blood. **101**(9): p. 3359-3364.
24. Hershko, C., G. Graham, G.W. Bates, and E.A. Rachmilewitz, 1978, *Non-specific serum iron in thalassaemia: an abnormal serum iron fraction of potential toxicity.* Br J Haematol. **40**(2): p. 255-63.
25. Brissot, P., M. Ropert, C. Le Lan, and O. Loreal, 2012, *Non-transferrin bound iron: a key role in iron overload and iron toxicity.* Biochim Biophys Acta. **1820**(3): p. 403-10.
26. Le Lan, C., O. Loreal, T. Cohen, M. Ropert, H. Glickstein, F. Laine, M. Pouchard, Y. Deugnier, et al., 2005, *Redox active plasma iron in C282Y/C282Y hemochromatosis.* Blood. **105**(11): p. 4527-31.
27. Piga, A., F. Longo, L. Duca, S. Roggero, T. Vinciguerra, R. Calabrese, C. Hershko, and M.D. Cappellini, 2009, *High nontransferrin bound iron levels and heart disease in thalassemia major.* Am J Hematol. **84**(1): p. 29-33.
28. Liuzzi, J.P., F. Aydemir, H. Nam, M.D. Knutson, and R.J. Cousins, 2006, *Zip14 (Slc39a14) mediates non-transferrin-bound iron uptake into cells.* Proc Natl Acad Sci U S A. **103**(37): p. 13612-7.
29. Hentze, M.W., S.W. Caughman, T.A. Rouault, J.G. Barriocanal, A. Dancis, J.B. Harford, and R.D. Klausner, 1987, *Identification of the iron-responsive element for the translational regulation of human ferritin mRNA.* Science. **238**(4833): p. 1570-3.
30. Casey, J.L., M.W. Hentze, D.M. Koeller, S.W. Caughman, T.A. Rouault, R.D. Klausner, and J.B. Harford, 1988, *Iron-Responsive Elements - Regulatory Rna Sequences That Control Messenger-Rna Levels and Translation.* Science. **240**(4854): p. 924-928.
31. Wilkinson, N. and K. Pantopoulos, 2014, *The IRP/IRE system in vivo: insights from mouse models.* Front Pharmacol. **5**: p. 176.
32. Smith, S.R., M.C. Ghosh, H. Ollivierre-Wilson, W. Hang Tong, and T.A. Rouault, 2006, *Complete loss of iron regulatory proteins 1 and 2 prevents viability of murine zygotes beyond the blastocyst stage of embryonic development.* Blood Cells Mol Dis. **36**(2): p. 283-7.
33. Ghosh, M.C., D.L. Zhang, S.Y. Jeong, G. Kovtunovych, H. Ollivierre-Wilson, A. Noguchi, T. Tu, T. Senecal, et al., 2013, *Deletion of iron regulatory protein 1 causes polycythemia and pulmonary hypertension in mice through translational derepression of HIF2alpha.* Cell Metab. **17**(2): p. 271-81.
34. LaVaute, T., S. Smith, S. Cooperman, K. Iwai, W. Land, E. Meyron-Holtz, S.K. Drake, G. Miller, et al., 2001, *Targeted deletion of the gene encoding iron regulatory protein-2 causes misregulation of iron metabolism and neurodegenerative disease in mice.* Nat Genet. **27**(2): p. 209-14.
35. Ganz, T. and E. Nemeth, 2012, *Hepcidin and iron homeostasis.* Biochim Biophys Acta. **1823**(9): p. 1434-43.
36. Krause, A., S. Neitz, H.J. Magert, A. Schulz, W.G. Forssmann, P. Schulz-Knappe, and K. Adermann, 2000, *LEAP-1, a novel highly disulfide-bonded human peptide, exhibits antimicrobial activity.* FEBS Lett. **480**(2-3): p. 147-50.
37. Park, C.H., E.V. Valore, A.J. Waring, and T. Ganz, 2001, *Hepcidin, a urinary antimicrobial peptide synthesized in the liver.* J Biol Chem. **276**(11): p. 7806-10.
38. Sow, F.B., W.C. Florence, A.R. Satoskar, L.S. Schlesinger, B.S. Zwilling, and W.P. Lafuse, 2007, *Expression and localization of hepcidin in macrophages: a role in host defense against tuberculosis.* J Leukoc Biol. **82**(4): p. 934-45.

39. Pinto, J.P., V. Dias, H. Zoller, G. Porto, H. Carmo, F. Carvalho, and M. de Sousa, 2010, *Hepcidin messenger RNA expression in human lymphocytes.* Immunology. **130**(2): p. 217-30.
40. Bekri, S., P. Gual, R. Anty, N. Luciani, M. Dahman, B. Ramesh, A. Iannelli, A. Staccini-Myx, et al., 2006, *Increased adipose tissue expression of hepcidin in severe obesity is independent from diabetes and NASH.* Gastroenterology. **131**(3): p. 788-96.
41. Nemeth, E., M.S. Tuttle, J. Powelson, M.B. Vaughn, A. Donovan, D.M. Ward, T. Ganz, and J. Kaplan, 2004, *Hepcidin regulates cellular iron efflux by binding to ferroportin and inducing its internalization.* Science. **306**(5704): p. 2090-3.
42. Lakhal-Littleton, S., M. Wolna, C.A. Carr, J.J. Miller, H.C. Christian, V. Ball, A. Santos, R. Diaz, et al., 2015, *Cardiac ferroportin regulates cellular iron homeostasis and is important for cardiac function.* Proc Natl Acad Sci U S A. **112**(10): p. 3164-9.
43. Zhang, D.L., R.I. Hughes, H. Ollivierre-Wilson, M.C. Ghosh, and T.A. Rouault, 2009, *A Ferroportin Transcript that Lacks an Iron-Responsive Element Enables Duodenal and Erythroid Precursor Cells to Evade Translational Repression.* Cell Metabolism. **9**(5): p. 461-473.
44. Yang, F.M., X.C. Wang, D.J. Haile, C.A. Piantadosi, and A.J. Ghio, 2002, *Iron increases expression of iron-export protein MTP1 in lung cells.* American Journal of Physiology-Lung Cellular and Molecular Physiology. **283**(5): p. L932-L939.
45. Qiao, B., P. Sugianto, E. Fung, A. Del-Castillo-Rueda, M.J. Moran-Jimenez, T. Ganz, and E. Nemeth, 2012, *Hepcidin-induced endocytosis of ferroportin is dependent on ferroportin ubiquitination.* Cell Metab. **15**(6): p. 918-24.
46. Ganz, T. and E. Nemeth, 2011, *Hepcidin and Disorders of Iron Metabolism.* Annual Review of Medicine, Vol 62, 2011. **62**: p. 347-360.
47. Ramos, E., L. Kautz, R. Rodriguez, M. Hansen, V. Gabayan, Y. Ginzburg, M.P. Roth, E. Nemeth, et al., 2011, *Evidence for distinct pathways of hepcidin regulation by acute and chronic iron loading in mice.* Hepatology. **53**(4): p. 1333-41.
48. Goswami, T. and N.C. Andrews, 2006, *Hereditary hemochromatosis protein, HFE, interaction with transferrin receptor 2 suggests a molecular mechanism for mammalian iron sensing.* Journal of Biological Chemistry. **281**(39): p. 28494-28498.
49. Ramey, G., J.C. Deschemin, and S. Vaulont, 2009, *Cross-talk between the mitogen activated protein kinase and bone morphogenetic protein/hemojuvelin pathways is required for the induction of hepcidin by holotransferrin in primary mouse hepatocytes.* Haematologica-the Hematology Journal. **94**(6): p. 765-772.
50. Meynard, D., L. Kautz, V. Darnaud, F. Canonne-Hergaux, H. Coppin, and M.P. Roth, 2009, *Lack of the bone morphogenetic protein BMP6 induces massive iron overload.* Nature Genetics. **41**(4): p. 478-481.
51. Andriopoulos, B., E. Corradini, Y. Xia, S.A. Faasse, S.Z. Chen, L. Grgurevic, M.D. Knutson, A. Pietrangelo, et al., 2009, *BMP6 is a key endogenous regulator of hepcidin expression and iron metabolism.* Nature Genetics. **41**(4): p. 482-487.
52. Wang, R.H., C.L. Li, X.L. Xu, Y. Zheng, C.Y. Xiao, P. Zerfas, S. Cooperman, M. Eckhaus, et al., 2005, *A role of SMAD4 in iron metabolism through the positive regulation of hepicidin expression.* Cell Metabolism. **2**(6): p. 399-409.
53. Kautz, L., D. Meynard, A. Monnier, V. Darnaud, R. Bouvet, R.H. Wang, C. Deng, S. Vaulont, et al., 2008, *Iron regulates phosphorylation of Smad1/5/8 and gene expression of Bmp6, Smad7, Id1, and Atoh8 in the mouse liver.* Blood. **112**(4): p. 1503-1509.
54. Babitt, J.L., F.W. Huang, D.M. Wrighting, Y. Xia, Y. Sidis, T.A. Samad, J.A. Campagna, R.T. Chung, et al., 2006, *Bone morphogenetic protein signaling by hemojuvelin regulates hepcidin expression.* Nature Genetics. **38**(5): p. 531-539.
55. Lin, L., Y.P. Goldberg, and T. Ganz, 2005, *Competitive regulation of hepcidin mRNA by soluble and cell-associated hemojuvelin.* Blood. **106**(8): p. 2884-2889.

56. Silvestri, L., A. Pagani, A. Nai, I. De Domenico, J. Kaplan, and C. Camaschella, 2008, *The Serine Protease Matriptase-2 (TMPRSS6) Inhibits Hepcidin Activation by Cleaving Membrane Hemojuvelin.* Cell Metabolism. **8**(6): p. 502-511.
57. Zhang, A.S., A.P. West, Jr., A.E. Wyman, P.J. Bjorkman, and C.A. Enns, 2005, *Interaction of hemojuvelin with neogenin results in iron accumulation in human embryonic kidney 293 cells.* J Biol Chem. **280**(40): p. 33885-94.
58. Enns, C.A., R. Ahmed, and A.S. Zhang, 2012, *Neogenin interacts with matriptase-2 to facilitate hemojuvelin cleavage.* J Biol Chem. **287**(42): p. 35104-17.
59. Ramos, E., L. Kautz, R. Rodriguez, M. Hansen, V. Gabayan, Y. Ginzburg, M.P. Roth, E. Nemeth, et al., 2011, *Evidence for Distinct Pathways of Hepcidin Regulation by Acute and Chronic Iron Loading in Mice.* Hepatology. **53**(4): p. 1333-1341.
60. Kautz, L., G. Jung, E.V. Valore, S. Rivella, E. Nemeth, and T. Ganz, 2014, *Identification of erythroferrone as an erythroid regulator of iron metabolism.* Nature Genetics. **46**(7): p. 678-684.
61. Tanno, T., N.V. Bhanu, P.A. Oneal, S.H. Goh, P. Staker, Y.T. Lee, J.W. Moroney, C.H. Reed, et al., 2007, *High levels of GDF15 in thalassemia suppress expression of the iron regulatory protein hepcidin.* Nat Med. **13**(9): p. 1096-101.
62. Tanno, T., P. Porayette, O. Sripichai, S.J. Noh, C. Byrnes, A. Bhupatiraju, Y.T. Lee, J.B. Goodnough, et al., 2009, *Identification of TWSG1 as a second novel erythroid regulator of hepcidin expression in murine and human cells.* Blood. **114**(1): p. 181-6.
63. Ganz, T., 2009, *Iron in innate immunity: starve the invaders.* Current Opinion in Immunology. **21**(1): p. 63-67.
64. Nicolas, G., C. Chauvet, L. Viatte, J.L. Danan, X. Bigard, I. Devaux, C. Beaumont, A. Kahn, et al., 2002, *The gene encoding the iron regulatory peptide hepcidin is regulated by anemia, hypoxia, and inflammation.* J Clin Invest. **110**(7): p. 1037-44.
65. Khan, F.A., M.A. Fisher, and R.A. Khakoo, 2007, *Association of hemochromatosis with infectious diseases: expanding spectrum.* International Journal of Infectious Diseases. **11**(6): p. 482-487.
66. Nemeth, E., S. Rivera, V. Gabayan, C. Keller, S. Taudorf, B.K. Pedersen, and T. Ganz, 2004, *IL-6 mediates hypoferremia of inflammation by inducing the synthesis of the iron regulatory hormone hepcidin.* J Clin Invest. **113**(9): p. 1271-6.
67. Besson-Fournier, C., C. Latour, L. Kautz, J. Bertrand, T. Ganz, M.P. Roth, and H. Coppin, 2012, *Induction of activin B by inflammatory stimuli up-regulates expression of the iron-regulatory peptide hepcidin through Smad1/5/8 signaling.* Blood. **120**(2): p. 431-9.
68. Verga Falzacappa, M.V., M.V. Spasic, R. Kessler, J. Stolte, M.W. Hentze, and M.U. Muckenthaler, 2007, *Stat3 mediates hepatic hepcidin expression and its inflammatory stimulation.* American Journal of Hematology. **82**(6): p. 590-590.
69. Ganz, T. and E. Nemeth, 2009, *Iron Sequestration and Anemia of Inflammation.* Seminars in Hematology. **46**(4): p. 387-393.
70. Pietrangelo, A., 2010, *Hereditary Hemochromatosis: Pathogenesis, Diagnosis, and Treatment.* Gastroenterology. **139**(2): p. 393-408.
71. Fletcher, L.M., J.L. Dixon, D.M. Purdie, L.W. Powell, and D.H.G. Crawford, 2002, *Excess alcohol greatly increases the prevalence of cirrhosis in hereditary hemochromatosis.* Gastroenterology. **122**(2): p. 281-289.
72. McLaren, C.E., M.J. Emond, V.N. Subramaniam, P.D. Phatak, J.C. Barton, P.C. Adams, J.B. Goh, C.J. McDonald, et al., 2015, *Exome sequencing in HFE C282Y homozygous men with extreme phenotypes identifies a GNPAT variant associated with severe iron overload.* Hepatology.
73. Sham, R.L., P.D. Phatak, E. Nemeth, and T. Ganz, 2009, *Hereditary hemochromatosis due to resistance to hepcidin: high hepcidin concentrations in a family with C326S ferroportin mutation.* Blood. **114**(2): p. 493-4.

74. Origa, R., R. Galanello, T. Ganz, N. Giagu, L. Maccioni, G. Faa, and E. Nemeth, 2007, *Liver iron concentrations and urinary hepcidin in beta-thalassemia.* Haematologica-the Hematology Journal. **92**(5): p. 583-588.
75. Guo, S., C. Casu, S. Gardenghi, S. Booten, M. Aghajan, R. Peralta, A. Watt, S. Freier, et al., 2013, *Reducing TMPRSS6 ameliorates hemochromatosis and beta-thalassemia in mice.* J Clin Invest. **123**(4): p. 1531-41.
76. Gardenghi, S., P. Ramos, M.F. Marongiu, L. Melchiori, L. Breda, E. Guy, K. Muirhead, N. Rao, et al., 2010, *Hepcidin as a therapeutic tool to limit iron overload and improve anemia in beta-thalassemic mice.* J Clin Invest. **120**(12): p. 4466-77.
77. Nemeth, E. and T. Ganz, 2014, *Anemia of Inflammation.* Hematology-Oncology Clinics of North America. **28**(4): p. 671-+.
78. Finberg, K.E., M.M. Heeney, D.R. Campagna, Y. Aydinok, H.A. Pearson, K.R. Hartman, M.M. Mayo, S.M. Samuel, et al., 2008, *Mutations in TMPRSS6 cause iron-refractory iron deficiency anemia (IRIDA).* Nature Genetics. **40**(5): p. 569-571.
79. Kim, A., E. Fung, S.G. Parikh, E.V. Valore, V. Gabayan, E. Nemeth, and T. Ganz, 2014, *A mouse model of anemia of inflammation: complex pathogenesis with partial dependence on hepcidin.* Blood. **123**(8): p. 1129-1136.
80. Zaritsky, J., B. Young, H. Wang, E. Nemeth, T. Ganz, S. Rivera, A. Nissenson, and I. Salusky, 2009, *Hepcidin- a Potential Novel Biomarker for Iron Status and Erythropoietin Resistance in Pediatric Chronic Kidney Disease.* Journal of Investigative Medicine. **57**(1): p. 180-180.
81. Hohaus, S., B. Vannata, M. Giachelia, M.I. Roselli, G. Massini, A. Cuccaro, M.C. Tisi, M. Criscuolo, et al., 2009, *Anemia in Hodgkin Lymphoma: The Role of Interleukin-6 and Hepcidin.* Blood. **114**(22): p. 1410-1410.
82. den Elzen, W.P., A.J. de Craen, E.T. Wiegerinck, R.G. Westendorp, D.W. Swinkels, and J. Gussekloo, 2013, *Plasma hepcidin levels and anemia in old age. The Leiden 85-Plus Study.* Haematologica. **98**(3): p. 448-54.
83. Oliver, J.D., 2013, *Vibrio vulnificus: death on the half shell. A personal journey with the pathogen and its ecology.* Microb Ecol. **65**(4): p. 793-9.
84. Cook, D.W., P. Oleary, J.C. Hunsucker, E.M. Sloan, J.C. Bowers, R.J. Blodgett, and A. Depaola, 2002, *Vibrio vulnificus and Vibrio parahaemolyticus in U.S. retail shell oysters: a national survey from June 1998 to July 1999.* J Food Prot. **65**(1): p. 79-87.
85. Baker-Austin, C., J.A. Trinanes, N.G.H. Taylor, R. Hartnell, A. Siitonen, and J. Martinez-Urtaza, 2013, *Emerging Vibrio risk at high latitudes in response to ocean warming.* Nature Climate Change. **3**(1): p. 73-77.
86. Barton, J.C. and R.T. Acton, 2009, *Hemochromatosis and Vibrio vulnificus wound infections.* J Clin Gastroenterol. **43**(9): p. 890-3.
87. Feldhusen, F., 2000, *The role of seafood in bacterial foodborne diseases.* Microbes Infect. **2**(13): p. 1651-60.
88. Hlady, W.G. and K.C. Klontz, 1996, *The epidemiology of Vibrio infections in Florida, 1981-1993.* J Infect Dis. **173**(5): p. 1176-83.
89. Tison, D.L., M. Nishibuchi, J.D. Greenwood, and R.J. Seidler, 1982, *Vibrio vulnificus biogroup 2: new biogroup pathogenic for eels.* Appl Environ Microbiol. **44**(3): p. 640-6.
90. Rosche, T.M., Y. Yano, and J.D. Oliver, 2005, *A rapid and simple PCR analysis indicates there are two subgroups of Vibrio vulnificus which correlate with clinical or environmental isolation.* Microbiol Immunol. **49**(4): p. 381-9.
91. Amaro, C. and E.G. Biosca, 1996, *Vibrio vulnificus biotype 2, pathogenic for eels, is also an opportunistic pathogen for humans.* Appl Environ Microbiol. **62**(4): p. 1454-7.
92. Bisharat, N., V. Agmon, R. Finkelstein, R. Raz, G. Ben-Dror, L. Lerner, S. Soboh, R. Colodner, et al., 1999, *Clinical, epidemiological, and microbiological features of Vibrio vulnificus biogroup 3 causing outbreaks of wound infection and bacteraemia in Israel. Israel Vibrio Study Group.* Lancet. **354**(9188): p. 1421-4.

93. Blake, P.A., M.H. Merson, R.E. Weaver, D.G. Hollis, and P.C. Heublein, 1979, *Disease caused by a marine Vibrio. Clinical characteristics and epidemiology.* N Engl J Med. **300**(1): p. 1-5.
94. Haq, S.M. and H.H. Dayal, 2005, *Chronic liver disease and consumption of raw oysters: a potentially lethal combination--a review of Vibrio vulnificus septicemia.* Am J Gastroenterol. **100**(5): p. 1195-9.
95. Merkel, S.M., S. Alexander, E. Zufall, J.D. Oliver, and Y.M. Huet-Hudson, 2001, *Essential role for estrogen in protection against Vibrio vulnificus-induced endotoxic shock.* Infect Immun. **69**(10): p. 6119-22.
96. Jones, M.K. and J.D. Oliver, 2009, *Vibrio vulnificus: disease and pathogenesis.* Infect Immun. **77**(5): p. 1723-33.
97. Klontz, K.C., S. Lieb, M. Schreiber, H.T. Janowski, L.M. Baldy, and R.A. Gunn, 1988, *Syndromes of Vibrio vulnificus infections. Clinical and epidemiologic features in Florida cases, 1981-1987.* Ann Intern Med. **109**(4): p. 318-23.
98. Jang, H.C., S.M. Choi, H.K. Kim, S.E. Kim, S.J. Kang, K.H. Park, P.Y. Ryu, T.H. Lee, et al., 2014, *In vivo efficacy of the combination of ciprofloxacin and cefotaxime against Vibrio vulnificus sepsis.* PLoS One. **9**(6): p. e101118.
99. Rhee, J.E., J.H. Rhee, P.Y. Ryu, and S.H. Choi, 2002, *Identification of the cadBA operon from Vibrio vulnificus and its influence on survival to acid stress.* FEMS Microbiol Lett. **208**(2): p. 245-51.
100. Yoshida, S., M. Ogawa, and Y. Mizuguchi, 1985, *Relation of capsular materials and colony opacity to virulence of Vibrio vulnificus.* Infect Immun. **47**(2): p. 446-51.
101. Wright, A.C., L.M. Simpson, J.D. Oliver, and J.G. Morris, Jr., 1990, *Phenotypic evaluation of acapsular transposon mutants of Vibrio vulnificus.* Infect Immun. **58**(6): p. 1769-73.
102. Hilton, T., T. Rosche, B. Froelich, B. Smith, and J. Oliver, 2006, *Capsular polysaccharide phase variation in Vibrio vulnificus.* Appl Environ Microbiol. **72**(11): p. 6986-93.
103. Gray, L.D. and A.S. Kreger, 1987, *Mouse skin damage caused by cytolysin from Vibrio vulnificus and by V. vulnificus infection.* J Infect Dis. **155**(2): p. 236-41.
104. Kang, M.K., E.C. Jhee, B.S. Koo, J.Y. Yang, B.H. Park, J.S. Kim, H.W. Rho, H.R. Kim, et al., 2002, *Induction of nitric oxide synthase expression by Vibrio vulnificus cytolysin.* Biochem Biophys Res Commun. **290**(3): p. 1090-5.
105. Park, J.W., S.N. Ma, E.S. Song, C.H. Song, M.R. Chae, B.H. Park, R.W. Rho, S.D. Park, et al., 1996, *Pulmonary damage by Vibrio vulnificus cytolysin.* Infect Immun. **64**(7): p. 2873-6.
106. Wright, A.C. and J.G. Morris, Jr., 1991, *The extracellular cytolysin of Vibrio vulnificus: inactivation and relationship to virulence in mice.* Infect Immun. **59**(1): p. 192-7.
107. Kothary, M.H. and A.S. Kreger, 1987, *Purification and characterization of an elastolytic protease of Vibrio vulnificus.* J Gen Microbiol. **133**(7): p. 1783-91.
108. Shao, C.P. and L.I. Hor, 2000, *Metalloprotease is not essential for Vibrio vulnificus virulence in mice.* Infect Immun. **68**(6): p. 3569-73.
109. Jeong, K.C., H.S. Jeong, J.H. Rhee, S.E. Lee, S.S. Chung, A.M. Starks, G.M. Escudero, P.A. Gulig, et al., 2000, *Construction and phenotypic evaluation of a Vibrio vulnificus vvpE mutant for elastolytic protease.* Infect Immun. **68**(9): p. 5096-106.
110. Fan, J.J., C.P. Shao, Y.C. Ho, C.K. Yu, and L.I. Hor, 2001, *Isolation and characterization of a Vibrio vulnificus mutant deficient in both extracellular metalloprotease and cytolysin.* Infect Immun. **69**(9): p. 5943-8.
111. Lee, J.H., M.W. Kim, B.S. Kim, S.M. Kim, B.C. Lee, T.S. Kim, and S.H. Choi, 2007, *Identification and characterization of the Vibrio vulnificus rtxA essential for cytotoxicity in vitro and virulence in mice.* J Microbiol. **45**(2): p. 146-52.
112. Kim, Y.R., S.E. Lee, H. Kook, J.A. Yeom, H.S. Na, S.Y. Kim, S.S. Chung, H.E. Choy, et al., 2008, *Vibrio vulnificus RTX toxin kills host cells only after contact of the bacteria with host cells.* Cell Microbiol. **10**(4): p. 848-62.

113. Lee, T.H., M.H. Kim, C.S. Lee, J.H. Lee, J.H. Rhee, and K.M. Chung, 2014, *Protection against Vibrio vulnificus infection by active and passive immunization with the C-terminal region of the RtxA1/MARTXVv protein.* Vaccine. **32**(2): p. 271-6.
114. Shin, S.H., D.H. Shin, P.Y. Ryu, S.S. Chung, and J.H. Rhee, 2002, *Proinflammatory cytokine profile in Vibrio vulnificus septicemic patients' sera.* FEMS Immunol Med Microbiol. **33**(2): p. 133-8.
115. Goo, S.Y., Y.S. Han, W.H. Kim, K.H. Lee, and S.J. Park, 2007, *Vibrio vulnificus IlpA-induced cytokine production is mediated by Toll-like receptor 2.* J Biol Chem. **282**(38): p. 27647-58.
116. Stamm, L.V. and R.L. Drapp, 2014, *TLR2 and TLR4 mediate the TNFalpha response to Vibrio vulnificus biotype 1.* Pathog Dis. **71**(3): p. 357-61.
117. Lee, S.E., S.Y. Kim, B.C. Jeong, Y.R. Kim, S.J. Bae, O.S. Ahn, J.J. Lee, H.C. Song, et al., 2006, *A bacterial flagellin, Vibrio vulnificus FlaB, has a strong mucosal adjuvant activity to induce protective immunity.* Infect Immun. **74**(1): p. 694-702.
118. Bang, Y.B., S.E. Lee, J.H. Rhee, and S.H. Choi, 1999, *Evidence that expression of the Vibrio vulnificus hemolysin gene is dependent on cyclic AMP and cyclic AMP receptor protein.* Journal of Bacteriology. **181**(24): p. 7639-7642.
119. Choi, M.H., H.Y. Sun, R.Y. Park, C.M. Kim, Y.H. Bai, Y.R. Kim, J.H. Rhee, and S.H. Shin, 2006, *Effect of the crp mutation on the utilization of transferrin-bound iron by Vibrio vulnificus.* Fems Microbiology Letters. **257**(2): p. 285-292.
120. Jeong, H.S., K.C. Jeong, H.K. Choi, K.J. Park, K.H. Lee, J.H. Rhee, and S.H. Choi, 2001, *Differential expression of Vibrio vulnificus elastase gene in a growth phase-dependent manner by two different types of promoters.* Journal of Biological Chemistry. **276**(17): p. 13875-13880.
121. Kim, Y.R., S.Y. Kim, C.M. Kim, S.E. Lee, and J.H. Rhee, 2005, *Essential role of an adenylate cyclase in regulating Vibrio vulnificus virulence.* Fems Microbiology Letters. **243**(2): p. 497-503.
122. Kovacikova, G. and K. Skorupski, 1999, *A Vibrio cholerae LysR homolog, AphB, cooperates with AphA at the tcpPH promoter to activate expression of the ToxR virulence cascade.* Journal of Bacteriology. **181**(14): p. 4250-4256.
123. Jeong, H.G. and S.H. Choi, 2008, *Evidence that AphB, essential for the virulence of Vibrio vulnificus, is a global regulator.* Journal of Bacteriology. **190**(10): p. 3768-3773.
124. Liu, M., A.F. Alice, H. Naka, and J.H. Crosa, 2007, *The HlyU protein is a positive regulator of rtxA1, a gene responsible for cytotoxicity and virulence in the human pathogen Vibrio vulnificus.* Infect Immun. **75**(7): p. 3282-9.
125. Hor, L.I., Y.K. Chang, C.C. Chang, H.Y. Lei, and J.T. Ou, 2000, *Mechanism of high susceptibility of iron-overloaded mouse to Vibrio vulnificus infection.* Microbiol Immunol. **44**(11): p. 871-8.
126. Bullen, J.J., P.B. Spalding, C.G. Ward, and J.M. Gutteridge, 1991, *Hemochromatosis, iron and septicemia caused by Vibrio vulnificus.* Arch Intern Med. **151**(8): p. 1606-9.
127. Dechet, A.M., P.A. Yu, N. Koram, and J. Painter, 2008, *Nonfoodborne Vibrio infections: an important cause of morbidity and mortality in the United States, 1997-2006.* Clin Infect Dis. **46**(7): p. 970-6.
128. Wright, A.C., L.M. Simpson, and J.D. Oliver, 1981, *Role of iron in the pathogenesis of Vibrio vulnificus infections.* Infect Immun. **34**(2): p. 503-7.
129. Simpson, L.M. and J.D. Oliver, 1983, *Siderophore Production by Vibrio-Vulnificus.* Infection and Immunity. **41**(2): p. 644-649.
130. Kim, C.M., R.Y. Park, J.H. Park, H.Y. Sun, Y.H. Bai, P.Y. Ryu, S.Y. Kim, J.H. Rhee, et al., 2006, *Vibrio vulnificus vulnibactin, but not metalloprotease VvpE, is essentially required for iron-uptake from human holotransferrin.* Biological & Pharmaceutical Bulletin. **29**(5): p. 911-918.

131. Kim, I.H., J.I. Shim, K.E. Lee, W. Hwang, I.J. Kim, S.H. Choi, and K.S. Kim, 2008, *Nonribosomal peptide synthase is responsible for the biosynthesis of siderophore in Vibrio vulnificus MO6-24/O.* J Microbiol Biotechnol. **18**(1): p. 35-42.
132. Litwin, C.M., T.W. Rayback, and J. Skinner, 1996, *Role of catechol siderophore synthesis in Vibrio vulnificus virulence.* Infect Immun. **64**(7): p. 2834-8.
133. Webster, A.C. and C.M. Litwin, 2000, *Cloning and characterization of vuuA, a gene encoding the Vibrio vulnificus ferric vulnibactin receptor.* Infect Immun. **68**(2): p. 526-34.
134. Kim, C.M., Y.J. Park, and S.H. Shin, 2007, *A widespread deferoxamine-mediated iron-uptake system in Vibrio vulnificus.* J Infect Dis. **196**(10): p. 1537-45.
135. Tanabe, T., A. Naka, H. Aso, H. Nakao, S. Narimatsu, Y. Inoue, T. Ono, and S. Yamamoto, 2005, *A novel aerobactin utilization cluster in Vibrio vulnificus with a gene involved in the transcription regulation of the iutA homologue.* Microbiol Immunol. **49**(9): p. 823-34.
136. Litwin, C.M. and B.L. Byrne, 1998, *Cloning and characterization of an outer membrane protein of Vibrio vulnificus required for heme utilization: regulation of expression and determination of the gene sequence.* Infect Immun. **66**(7): p. 3134-41.
137. !!! INVALID CITATION !!!
138. Fillat, M.F., 2014, *The FUR (ferric uptake regulator) superfamily: diversity and versatility of key transcriptional regulators.* Arch Biochem Biophys. **546**: p. 41-52.
139. Lee, H.J., J.A. Kim, M.A. Lee, S.J. Park, and K.H. Lee, 2013, *Regulation of haemolysin (VvhA) production by ferric uptake regulator (Fur) in Vibrio vulnificus: repression of vvhA transcription by Fur and proteolysis of VvhA by Fur-repressive exoproteases.* Mol Microbiol. **88**(4): p. 813-26.
140. Kim, C.M., R.Y. Park, M.H. Choi, H.Y. Sun, and S.H. Shin, 2007, *Ferrophilic characteristics of Vibrio vulnificus and potential usefulness of iron chelation therapy.* J Infect Dis. **195**(1): p. 90-8.
141. Pigeon, C., G. Ilyin, B. Courselaud, P. Leroyer, B. Turlin, P. Brissot, and O. Loreal, 2001, *A new mouse liver-specific gene, encoding a protein homologous to human antimicrobial peptide hepcidin, is overexpressed during iron overload.* J Biol Chem. **276**(11): p. 7811-9.
142. Nemeth, E., E.V. Valore, M. Territo, G. Schiller, A. Lichtenstein, and T. Ganz, 2003, *Hepcidin, a putative mediator of anemia of inflammation, is a type II acute-phase protein.* Blood. **101**(7): p. 2461-3.
143. Lesbordes-Brion, J.C., L. Viatte, M. Bennoun, D.Q. Lou, G. Ramey, C. Houbron, G. Hamard, A. Kahn, et al., 2006, *Targeted disruption of the hepcidin 1 gene results in severe hemochromatosis.* Blood. **108**(4): p. 1402-5.
144. Ramos, E., P. Ruchala, J.B. Goodnough, L. Kautz, G.C. Preza, E. Nemeth, and T. Ganz, 2012, *Minihepcidins prevent iron overload in a hepcidin-deficient mouse model of severe hemochromatosis.* Blood. **120**(18): p. 3829-36.
145. Preza, G.C., P. Ruchala, R. Pinon, E. Ramos, B. Qiao, M.A. Peralta, S. Sharma, A. Waring, et al., 2011, *Minihepcidins are rationally designed small peptides that mimic hepcidin activity in mice and may be useful for the treatment of iron overload.* Journal of Clinical Investigation. **121**(12): p. 4880-4888.
146. Esposito, B.P., W. Breuer, P. Sirankapracha, P. Pootrakul, C. Hershko, and Z.I. Cabantchik, 2003, *Labile plasma iron in iron overload: redox activity and susceptibility to chelation.* Blood. **102**(7): p. 2670-7.
147. Kim, A., E. Fung, S.G. Parikh, E.V. Valore, V. Gabayan, E. Nemeth, and T. Ganz, 2014, *A mouse model of anemia of inflammation: complex pathogenesis with partial dependence on hepcidin.* Blood. **123**(8): p. 1129-36.
148. Starks, A.M., K.L. Bourdage, P.C. Thiaville, and P.A. Gulig, 2006, *Use of a marker plasmid to examine differential rates of growth and death between clinical and environmental strains of Vibrio vulnificus in experimentally infected mice.* Mol Microbiol. **61**(2): p. 310-23.
149. Gulig, P.A., T.J. Doyle, M.J. Clare-Salzler, R.L. Maiese, and H. Matsui, 1997, *Systemic infection of mice by wild-type but not Spv- Salmonella typhimurium is enhanced by*

neutralization of gamma interferon and tumor necrosis factor alpha. Infect Immun. **65**(12): p. 5191-7.
150. Langmead, B. and S.L. Salzberg, 2012, *Fast gapped-read alignment with Bowtie 2.* Nat Methods. **9**(4): p. 357-9.
151. Anders, S. and W. Huber, 2010, *Differential expression analysis for sequence count data.* Genome Biol. **11**(10): p. R106.
152. Starks, A.M., T.R. Schoeb, M.L. Tamplin, S. Parveen, T.J. Doyle, P.E. Bomeisl, G.M. Escudero, and P.A. Gulig, 2000, *Pathogenesis of infection by clinical and environmental strains of Vibrio vulnificus in iron-dextran-treated mice.* Infect Immun. **68**(10): p. 5785-93.
153. Gulig, P.A., K.L. Bourdage, and A.M. Starks, 2005, *Molecular Pathogenesis of Vibrio vulnificus.* J Microbiol. **43 Spec No**: p. 118-31.
154. Shan, J., J. Shen, L. Liu, F. Xia, C. Xu, G. Duan, Y. Xu, Q. Ma, et al., 2012, *Nanog regulates self-renewal of cancer stem cells through the insulin-like growth factor pathway in human hepatocellular carcinoma.* Hepatology. **56**(3): p. 1004-14.
155. Guida, C., S. Altamura, F.A. Klein, B. Galy, M. Boutros, A.J. Ulmer, M.W. Hentze, and M.U. Muckenthaler, 2015, *A novel inflammatory pathway mediating rapid hepcidin-independent hypoferremia.* Blood. **125**(14): p. 2265-75.
156. Ludwiczek, S., E. Aigner, I. Theurl, and G. Weiss, 2003, *Cytokine-mediated regulation of iron transport in human monocytic cells.* Blood. **101**(10): p. 4148-54.
157. Zoller, H., I. Theurl, R. Koch, A. Kaser, and G. Weiss, 2002, *Mechanisms of iron mediated regulation of the duodenal iron transporters divalent metal transporter 1 and ferroportin 1.* Blood Cells Mol Dis. **29**(3): p. 488-97.
158. Delaby, C., N. Pilard, A.S. Goncalves, C. Beaumont, and F. Canonne-Hergaux, 2005, *Presence of the iron exporter ferroportin at the plasma membrane of macrophages is enhanced by iron loading and down-regulated by hepcidin.* Blood. **106**(12): p. 3979-84.
159. Chua, A.C., S.F. Drake, C.E. Herbison, J.K. Olynyk, P.J. Leedman, and D. Trinder, 2006, *Limited iron export by hepatocytes contributes to hepatic iron-loading in the Hfe knockout mouse.* J Hepatol. **44**(1): p. 176-82.
160. Rodriguez, R., C.L. Jung, V. Gabayan, J.C. Deng, T. Ganz, E. Nemeth, Y. Bulut, and C.R. Roy, 2014, *Hepcidin induction by pathogens and pathogen-derived molecules is strongly dependent on interleukin-6.* Infect Immun. **82**(2): p. 745-52.
161. Preza, G.C., P. Ruchala, R. Pinon, E. Ramos, B. Qiao, M.A. Peralta, S. Sharma, A. Waring, et al., 2011, *Minihepcidins are rationally designed small peptides that mimic hepcidin activity in mice and may be useful for the treatment of iron overload.* J Clin Invest. **121**(12): p. 4880-8.
162. Xiao, J.J., W. Krzyzanski, Y.M. Wang, H. Li, M.J. Rose, M. Ma, Y. Wu, B. Hinkle, et al., 2010, *Pharmacokinetics of anti-hepcidin monoclonal antibody Ab 12B9m and hepcidin in cynomolgus monkeys.* AAPS J. **12**(4): p. 646-57.
163. Resh, M.D., 2006, *Palmitoylation of ligands, receptors, and intracellular signaling molecules.* Sci STKE. **2006**(359): p. re14.
164. Troxell, B. and H.M. Hassan, 2013, *Transcriptional regulation by Ferric Uptake Regulator (Fur) in pathogenic bacteria.* Front Cell Infect Microbiol. **3**: p. 59.
165. Tischler, A.D., S.H. Lee, and A. Camilli, 2002, *The Vibrio cholerae vieSAB locus encodes a pathway contributing to cholera toxin production.* J Bacteriol. **184**(15): p. 4104-13.
166. Tischler, A.D. and A. Camilli, 2005, *Cyclic diguanylate regulates Vibrio cholerae virulence gene expression.* Infect Immun. **73**(9): p. 5873-82.
167. Ganz, T., 2009, *Iron in innate immunity: starve the invaders.* Curr Opin Immunol. **21**(1): p. 63-7.
168. Drakesmith, H. and A.M. Prentice, 2012, *Hepcidin and the iron-infection axis.* Science. **338**(6108): p. 768-72.

169. Dauros-Singorenko, P. and S. Swift, 2014, *The transition from iron starvation to iron sufficiency as an important step in the progression of infection.* Sci Prog. **97**(Pt 4): p. 371-82.
170. Breuer, W., C. Hershko, and Z.I. Cabantchik, 2000, *The importance of non-transferrin bound iron in disorders of iron metabolism.* Transfus Sci. **23**(3): p. 185-92.
171. van der Heul, C., H.G. van Eijk, W.F. Wiltink, and B. Leijnse, 1972, *The binding of iron to transferrin and to other serum components at different degrees of saturation with iron.* Clin Chim Acta. **38**(2): p. 347-53.
172. Sulieman, M., R. Asleh, Z.I. Cabantchik, W. Breuer, D. Aronson, A. Suleiman, R. Miller-Lotan, H. Hammerman, et al., 2004, *Serum chelatable redox-active iron is an independent predictor of mortality after myocardial infarction in individuals with diabetes.* Diabetes Care. **27**(11): p. 2730-2.
173. Lee, D.H., D.Y. Liu, D.R. Jacobs, Jr., H.R. Shin, K. Song, I.K. Lee, B. Kim, and R.C. Hider, 2006, *Common presence of non-transferrin-bound iron among patients with type 2 diabetes.* Diabetes Care. **29**(5): p. 1090-5.
174. Sengoelge, G., V. Rainer, J. Kletzmayr, M. Jansen, K. Derfler, M. Fodinger, W.H. Horl, and G. Sunder-Plassmann, 2004, *Dose-dependent effect of parenteral iron therapy on bleomycin-detectable iron in immune apheresis patients.* Kidney Int. **66**(1): p. 295-302.
175. Prakash, M., S. Upadhya, and R. Prabhu, 2005, *Serum non-transferrin bound iron in hemodialysis patients not receiving intravenous iron.* Clin Chim Acta. **360**(1-2): p. 194-8.
176. Griffin, A.S., S.A. West, and A. Buckling, 2004, *Cooperation and competition in pathogenic bacteria.* Nature. **430**(7003): p. 1024-7.
177. May, P.M. and D.R. Williams, 1977, *Computer simulation of chelation therapy. Plasma mobilizing index as a replacement for effective stability constant.* FEBS Lett. **78**(1): p. 134-8.
178. Grootveld, M., J.D. Bell, B. Halliwell, O.I. Aruoma, A. Bomford, and P.J. Sadler, 1989, *Non-transferrin-bound iron in plasma or serum from patients with idiopathic hemochromatosis. Characterization by high performance liquid chromatography and nuclear magnetic resonance spectroscopy.* J Biol Chem. **264**(8): p. 4417-22.
179. Hantke, K., 1981, *Regulation of ferric iron transport in Escherichia coli K12: isolation of a constitutive mutant.* Mol Gen Genet. **182**(2): p. 288-92.
180. Andrews, S.C., A.K. Robinson, and F. Rodriguez-Quinones, 2003, *Bacterial iron homeostasis.* FEMS Microbiol Rev. **27**(2-3): p. 215-37.
181. Litwin, C.M. and S.B. Calderwood, 1993, *Cloning and genetic analysis of the Vibrio vulnificus fur gene and construction of a fur mutant by in vivo marker exchange.* J Bacteriol. **175**(3): p. 706-15.
182. Bisharat, N., M. Bronstein, M. Korner, T. Schnitzer, and Y. Koton, 2013, *Transcriptome profiling analysis of Vibrio vulnificus during human infection.* Microbiology. **159**(Pt 9): p. 1878-87.
183. Williams, T.C., E.R. Blackman, S.S. Morrison, C.J. Gibas, and J.D. Oliver, 2014, *Transcriptome sequencing reveals the virulence and environmental genetic programs of Vibrio vulnificus exposed to host and estuarine conditions.* PLoS One. **9**(12): p. e114376.
184. Wrighting, D.M. and N.C. Andrews, 2006, *Interleukin-6 induces hepcidin expression through STAT3.* Blood. **108**(9): p. 3204-9.
185. Verga Falzacappa, M.V., M. Vujic Spasic, R. Kessler, J. Stolte, M.W. Hentze, and M.U. Muckenthaler, 2007, *STAT3 mediates hepatic hepcidin expression and its inflammatory stimulation.* Blood. **109**(1): p. 353-8.
186. Pan, C.Y., S.C. Lee, V. Rajanbabu, C.H. Lin, and J.Y. Chen, 2012, *Insights into the antibacterial and immunomodulatory functions of tilapia hepcidin (TH)2-3 against Vibrio vulnificus infection in mice.* Dev Comp Immunol. **36**(1): p. 166-73.

187. Maisetta, G., R. Petruzzelli, F.L. Brancatisano, S. Esin, A. Vitali, M. Campa, and G. Batoni, 2010, *Antimicrobial activity of human hepcidin 20 and 25 against clinically relevant bacterial strains: effect of copper and acidic pH.* Peptides. **31**(11): p. 1995-2002.
188. Wang, L., L. Harrington, E. Trebicka, H.N. Shi, J.C. Kagan, C.C. Hong, H.Y. Lin, J.L. Babitt, et al., 2009, *Selective modulation of TLR4-activated inflammatory responses by altered iron homeostasis in mice.* J Clin Invest. **119**(11): p. 3322-8.
189. Oexle, H., A. Kaser, J. Most, R. Bellmann-Weiler, E.R. Werner, G. Werner-Felmayer, and G. Weiss, 2003, *Pathways for the regulation of interferon-gamma-inducible genes by iron in human monocytic cells.* J Leukoc Biol. **74**(2): p. 287-94.
190. Good, M.F., L.W. Powell, and J.W. Halliday, 1987, *The effect of non-transferrin-bound iron on murine T lymphocyte subsets: analysis by clonal techniques.* Clin Exp Immunol. **70**(1): p. 164-72.
191. Waalen, J., V. Felitti, T. Gelbart, N.J. Ho, and E. Beutler, 2002, *Prevalence of hemochromatosis-related symptoms among individuals with mutations in the HFE gene.* Mayo Clin Proc. **77**(6): p. 522-30.
192. Rochette, J., G. Le Gac, K. Lassoued, C. Ferec, and K.J. Robson, 2010, *Factors influencing disease phenotype and penetrance in HFE haemochromatosis.* Hum Genet. **128**(3): p. 233-48.
193. Wallace, D.F., C.J. McDonald, L. Ostini, and V.N. Subramaniam, 2011, *Blunted hepcidin response to inflammation in the absence of Hfe and transferrin receptor 2.* Blood. **117**(10): p. 2960-6.


POPH
QUALIFICAR É CRESCER.

QREN
QUADRO
DE REFERÊNCIA
ESTRATÉGICO
NACIONAL
PORTUGAL 2007.2013

GOVERNO DA REPÚBLICA
PORTUGUESA

UNIÃO EUROPEIA
Fundo Social Europeu